



# WPI

## Fabrication of a Nutrient Perfusion Enhancing Cartilage Tissue Scaffold

---

Major Qualifying Project

April 30, 2015

Submitted by:

Dominick Calvao

Handwritten signature of Dominick Calvao in black ink, written over a horizontal line.

Gaetana D'Alesio-Spina

Handwritten signature of Gaetana D'Alesio-Spina in black ink, written over a horizontal line.

Patrick Thomas

Handwritten signature of Patrick Thomas in black ink, written over a horizontal line.

Advisor: Sakthikumar Ambady

Co-Advisor: Dirk Albrecht

*This report represents the work of WPI undergraduate students submitted to the faculty as evidence of completion of a degree requirement. WPI routinely publishes these reports on its website without editorial or peer review. For more information about the projects program at WPI, please see <http://www.wpi.edu/academics/ugradstudies/project-learning.html>*

# Table of Contents

Authorship Page.....	5
Acknowledgements.....	6
Abstract.....	7
List of Figures.....	8
List of Tables.....	9
Chapter 1 Introduction.....	10
Chapter 2 Literature Review.....	12
2.1 Significance.....	12
2.1.1 Cartilage.....	12
2.1.2 Meniscus.....	13
2.1.3 Meniscus Tears and Treatment.....	15
2.1.4 Project Justification.....	16
2.2 Tissue Engineering Approaches.....	16
2.2.1 Nutrient Perfusion.....	16
2.2.2 Material Choice.....	17
2.2.3 Meniscus Replacement.....	18
2.3 Cartilage Cell Culture.....	18
2.3.1 Chondrocytes.....	19
2.3.2 Culture Conditions.....	19
2.3.3 Histology.....	20
2.4 Three Dimensional Cell Culture.....	20
2.4.1 Hydrogels.....	20
2.4.2 Hydrogel Choice.....	21
2.5 Three Dimensional Printing.....	23
2.5.1 Process.....	23
2.5.2 Biomedical Applications.....	24
2.5.3 Monoprice Dual Extrusion 3D Printer.....	24
2.6 Conclusion.....	26
Chapter 3 Project Strategy.....	27
3.1 Initial Client Statement.....	27
3.2 Objectives and Constraints.....	28

3.2.1 Objectives .....	28
3.2.2 Pairwise Comparison Chart .....	30
3.2.3 Constraints .....	30
3.2.4 Objective Tree .....	32
3.3 Revised Client Statement .....	33
3.4 Project Approach.....	33
3.4.1 Design and Fabrication of Scaffold .....	33
3.4.2 Hydrogel Analysis and Selection .....	34
3.4.3 Scaffold Seeding and Validation .....	34
Chapter 4 Methods and Alternative Designs .....	35
4.1 Needs Analysis.....	35
4.2 Functions (Specifications).....	35
4.2.1 Cell Viability and Distribution .....	35
4.2.2 Cellular Differentiation.....	36
4.2.3 Nutrient Perfusion.....	36
4.3 Design Alternatives .....	36
4.3.1 PLA-PVA Dual Extruded Scaffold .....	37
4.3.2 PLA-only Scaffold.....	37
4.3.3 Threaded PLA Scaffold .....	38
4.4 Feasibility Study/ Experiments .....	39
4.4.1 Scaffold Feasibility.....	39
4.4.2 Hydrogels.....	40
4.4.3 Cell Culture.....	40
4.4.4 Threading Materials.....	40
4.4.5 Calcién Staining.....	41
4.5 Experimental Methods .....	41
4.5.1 ATDC5 Cell Culture Protocol .....	41
4.5.2 Cell Isolation for Hydrogel Seeding.....	42
4.5.3 Cell Differentiation.....	43
4.5.4 Hydrogel Synthesis.....	44
4.5.5 Hydrogel Cell Suspension .....	47
4.5.6 PDMS Fabrication .....	47

4.5.7 Sterilization Technique for Scaffolds .....	48
4.5.8 Lattice Design Seeding .....	48
4.5.9 Threaded PLA Design Seeding .....	49
4.5.10 Cell Viability Testing .....	49
Chapter 5 Experimental Results.....	51
5.1 ATDC5 Cell Culture .....	51
5.2 Cell Differentiation in 2D Culture .....	52
5.3 Calcein AM Live Cell Staining.....	52
5.3 Hydrogels .....	53
5.4 Differentiation in 3D Hydrogel.....	54
5.5 PLA-PVA Dual Extruded Scaffold Results .....	55
5.6 PLA-only Scaffold Results .....	56
5.7 Threaded PLA Scaffold Results.....	57
Chapter 6 Final Design Validation .....	59
6.1 Cell Viability .....	59
6.2 Cell Proliferation.....	60
6.3 Cell Differentiation .....	60
Chapter 7 Discussion .....	61
7.1 Objectives Tree Assessment.....	61
7.2 Safe.....	62
7.3 Similar to Physiological Structure.....	62
7.4 Reproducible .....	62
7.5 Customizable.....	63
7.6 Economic Impact.....	63
7.7 Environmental Impact.....	63
7.8 Societal Influence.....	64
7.9 Political Ramifications .....	64
7.10 Ethical Concerns .....	64
7.11 Health and Safety Issues .....	64
7.12 Manufacturability .....	65
7.13 Sustainability.....	65
Chapter 8 Conclusion and Recommendations .....	66

8.1 Conclusions .....	66
8.2 Recommendations .....	67
8.2.1 Biomorphic .....	67
8.2.2 Mechanical Attributes.....	67
8.2.3 Cell Selection.....	68
8.2.4 Clinical Application.....	68
Bibliography .....	70
Appendix A: ReplicatorG Print Settings for the Final Design .....	72
Appendix B: PVA Swelling Study .....	73
Appendix C: Project Budget .....	74
Appendix D: Project Gantt Chart.....	75
Appendix E: G-code of Final Design.....	83
Appendix F: BME Learning Outcomes .....	142

## **Authorship Page**

All members of the design team contributed equally to this project.

## **Acknowledgements**

The authors of this study would like to thank the following individuals for their contributions:

- Our advisor, Prof. Sakthikumar Ambady (BME) for his knowledge and guidance through the completion of this project.
- Our co-advisor, Prof. Dirk Albrecht (BME).
- Lisa Wall, Lab Director, for her assistance in the laboratory.
- Dr. Robert Meislin of New York University Medical School for his advice and support throughout the project.
- Dr. Thomas Spina of Milford Regional Medical Center for providing the suture materials used in the final design.

## **Abstract**

The main challenge associated with engineering avascular tissue such as cartilage is overcoming the physiological nutrient perfusion limit of 100  $\mu\text{m}$ . Using a 3D printer, a PLA tissue scaffold with a diameter of 6.2 mm was fabricated. The scaffold was threaded with degradable collagen sutures and filled with a chondrogenic cell line suspended in a 4% alginate hydrogel. The scaffold system successfully supported cell proliferation and differentiation for 1 week, indicating efficient nutrient perfusion to the center of the scaffold.



## List of Figures

Figure 1: Diagram of Menisci in the Knee	13
Figure 2: Diagram of a Meniscus with Labeled Dimensions	14
Figure 3: Current Treatment Methods	15
Figure 4: The Menaflex Collagen Meniscus Implant	18
Figure 5: The Monoprice Dual Extrusion 3D Printer	25
Figure 6: Objectives Tree	32
Figure 7: PLA-PVA Dual Extruded Scaffold SolidWorks Design	37
Figure 8: PLA-only Scaffold SolidWorks Design	38
Figure 9: Threaded PLA Scaffold SolidWorks Design	39
Figure 10: Graph of PDL Study of ATDC5 Cells	51
Figure 11: 2D Alizarin Red Staining at 4 Weeks	52
Figure 12: Calciem AM Feasibility Study Results	53
Figure 13: Alginate Shrinkage Testing	54
Figure 14: Differentiation Comparison of Alginate and Fibrin- PureCol EZ Gel	55
Figure 15: PVA Swelling out of a Scaffold	56
Figure 16: PVA Swelling Study	56
Figure 17: Different Threaded PLA Scaffold Designs	58
Figure 18: Calciem AM Live Staining for Cell Viability	59
Figure 19: Calciem AM Live Staining for Cell Proliferation	60
Figure 20: Alizarin Red Staining for Calcium Deposits	60
Figure 21: Objectives Tree Assessment	61
Figure 22: Concept Diagram of Clinical Application	69

## List of Tables

<i>Table 1: Dimensions of Adult Human Menisci</i>	14
<i>Table 2: Specifications of the Monoprice Dual Extrusion 3D Printer</i>	25
<i>Table 3: Pairwise Comparison Chart</i>	30
<i>Table 4: Proliferation Media Composition</i>	41
<i>Table 5: PDL Study of ATDC5 Cells</i>	51
<i>Table 6: Hydrogel Experimental Results</i>	54
<i>Table 7: PLA Degradation Study</i>	57

## Chapter 1 Introduction

A common sports related injury in the United States is meniscal tearing or damage. The majority of reported ACL injuries also result in damage to the meniscus (Drosos & Pozo, 2004). The meniscus, which is composed entirely of fibrocartilage, cannot regenerate on its own due to its avascular nature. A lack of blood vessels reduces the potential for nutrients to reach the cells, which limits the tissue's ability to heal after a tear. Treatment options are currently limited to physical therapy, either a full or partial meniscectomy, or arthroscopic repair. All of these surgical methods alter the balance in the knee and put the patient at a higher risk of re-tear for the rest of their lives. A full knee replacement is necessary when damage to the meniscus is the result of degenerative bone disease. Between 500,000 and 1,000,000 meniscal repair surgeries occur each year, generating a \$4 billion market (Frizziero *et al*, 2012). The aim of this project was to develop a three-dimensional tissue scaffold, which, when seeded with cells via a hydrogel, supported cell growth and proliferation beyond the natural nutrient perfusion limit of 100  $\mu\text{m}$  in the body (Carmeliet and Jain, 2000).

The team broke the project down into three major components. A three-dimensional tissue scaffold was designed using SolidWorks computer modeling software. The model architecture was a hollow cylinder, through which channels could be created to increase nutrient perfusion. The model was transferred into the 3D printer software, ReplicatorG, where a G-code was generated in python. The scaffold was then manufactured using biodegradable polymers polylactic acid (PLA) and/or polyvinyl alcohol (PVA). The scaffold was printed with a commercially available dual extruder 3D printer (Dual Extrusion ABS/PLA/PVA Monoprice 3D printer). Concurrently, the team researched different hydrogels and how well they mimicked *in vivo* conditions. The hydrogels had to have the appropriate stiffness, support cell life, and have short gelation times to

ensure that the cells experienced an environment as close to physiological conditions as possible and that they did not settle to the bottom of the scaffold before the gel was set. Finally, the team worked with a chondrogenic cell line (ATDC5 cells, Sigma) to demonstrate that proper proliferation and differentiation could be achieved both in two dimensional and three dimensional cell cultures. The team used histological analysis and microscopy to demonstrate robust growth and differentiation of ATDC5 cells to cartilage in the center of a 6.2 mm diameter scaffold indicating efficient nutrient perfusion at those depths. The results demonstrate that a 3D printed PLA scaffold threaded with degradable collagen sutures can form channels to support effective nutrient perfusion for cell growth and differentiation over a 1-week period. This technology may be a viable approach to develop patient specific meniscus implants and could be adapted more broadly to other tissue engineering applications.

## **Chapter 2 Literature Review**

### **2.1 Significance**

Meniscus injuries pose a major treatment challenge to patients and surgeons. The current state of treatment is not effective at reducing the increased risk of re-tear or fully restoring the shock absorption function of the meniscus. Additionally, fibrocartilage is primarily an avascular tissue, creating further challenges in tissue engineering of the material. For these reasons, further research into viable tissue engineering approaches for meniscus replacements is necessary.

#### **2.1.1 Cartilage**

Cartilage is a connective tissue present throughout the body. There are three types of cartilage: articular, elastic, and fibrous. Each type of cartilage has a different role in the body and is present in different areas. Articular cartilage, sometimes referred to as hyaline cartilage, is found in joints, between the bones. The function of articular cartilage is to decrease friction between bones in joints and to distribute loads on joints with a low coefficient of friction (Fox *et al*, 2009). Elastic cartilage is similar to hyaline cartilage based on its composition of collagen II fibers. Elastic cartilage also has a network of branched elastic fibers, making it a more flexible form of cartilage. This cartilage can be found in the ear lobe, epiglottis, and areas of the larynx. Elastic cartilage helps to maintain shape but remains flexible in its support of the area. Fibrous cartilage is the toughest form of cartilage, composed of collagenous bundles that orient based on the stresses the area is experiencing. Fibrous cartilage can be found in vertebral disks, between the pubic bones in the front of the pelvic girdle, and around the edges of articular cavities in joints. This cartilage is a shock absorber that provides support without impeding movement (Buckwalter *et al*, 2000). Fibrous cartilage receives nutrients from synovial fluid via diffusion and mechanical compression (Fox *et al*, 2012).

Cartilage poses some challenges for tissue engineering. Each type of cartilage is avascular, meaning there is no blood supply or nutrients for damage repair. This lack of vasculature makes nutrient perfusion a significant obstacle when generating cartilage *ex vivo*. Additionally, cartilage cells cannot proliferate once they are differentiated because the differentiation is terminal. In other tissues of the body, precursor cells are present to generate replacement tissue for growth or after injury. Due to the physiological limits of cartilage, there is a significant need to engineer the tissue *ex vivo*.

### 2.1.2 Meniscus

The meniscus is a semicircle disk, composed of fibrous cartilage, located in the knee joint. There are two in each knee, a lateral and a medial meniscus. The parts of both menisci towards the center of the knee are partially vascularized with capillaries extending 10% - 30% of the way into the meniscus (Beaufils & Verdonk, 2010).

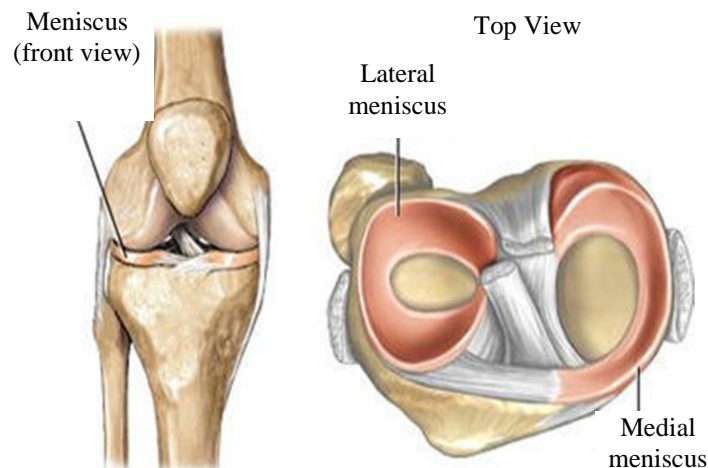


Figure 1: Diagram of Menisci in the Knee

The lateral meniscus is slightly smaller than the medial meniscus. As depicted in Figure 1, the lateral meniscus is located towards the outer portion of the knee and the medial meniscus is towards the center of the body. Figure 2 labels the pertinent dimensions of the meniscus. In Table 1, the mean, standard deviation, and range of each dimension are shown.

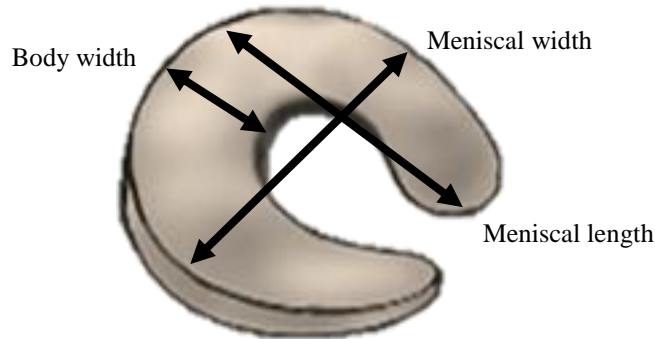


Figure 2: Diagram of a Meniscus with Labeled Dimensions

Table 1: Dimensions of Adult Human Menisci

	Mean (mm)	Standard Deviation	Range
Medial Meniscus Circumference	99.0	9.3	84-119
Medial meniscal body width	9.3	1.3	6.7-12.4
Medial meniscal length	45.7	5.0	30.1-56.1
Medial meniscal width	27.4	2.5	23.3-32.7
Lateral meniscal circumference	91.7	9.6	78-112
Lateral meniscal body width	10.9	1.3	8.3-14.5
Lateral meniscal length	35.7	3.7	29.5-51.2
Lateral meniscal width	29.3	3.0	24.0-36.3

The orientation of fibers in the meniscus, in conjunction with the dimensions listed in Table 1 allow for certain mechanical properties to be exhibited. To support the significant load that the knee experiences, fibers in the menisci are arranged in longitudinal and radial patterns (Beufils & Verdonk, 2010). Because of this composition, the meniscus is ten times stronger in tension than compression, allowing for easy shock absorption. The menisci are responsible for 20% of the shock absorption in the knee with the lateral meniscus supporting 70% of the load and the medial supporting 50% (Frizziero et al, 2012). When the knee is fully extended, the menisci absorb 50%

of the joint compressive forces. When the knee is at 90 degrees of flexion, 85% of the weight is supported by the menisci.

### 2.1.3 Meniscus Tears and Treatment

The second most common injury to the knee is a meniscal tear. In about 80% of ACL tears, the most common knee injury, there is damage to the meniscus as well (Drosos & Pozo, 2004). Meniscus tears occur in approximately 61 in 100,000 people each year (Frizziero *et al*, 2012). The commonality of meniscal damages results in a \$4 billion surgical industry with treatment options including arthroscopic repair and partial or full menisectomy.

Arthroscopic repair involves an orthopedic surgeon suturing a surface tear that is present towards the center of the meniscus. A menisectomy is necessary when there is damage to the outer portions of the meniscus. A menisectomy involves removal of part or the entire meniscus, depending on the percentage of tissue affected by the damage. Both of these procedures can be seen in Figure 3

The current treatment methods each have drawbacks. Arthroscopic repair sutures the damaged

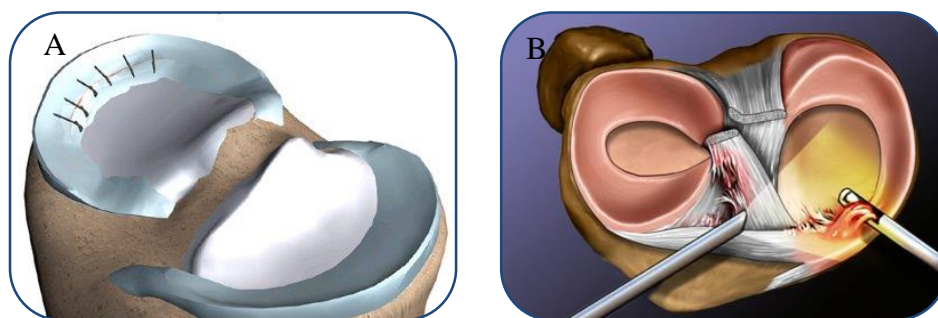


*Figure 3: Current Treatment Methods*

*A. Arthroscopic repair of a central tear in a meniscus. B. A partial menisectomy involving shaving of the outer portion of the meniscus to remove damaged tissue.*

area but the tear rarely heals completely resulting in an imbalance in the knee. A partial or full menisectomy also disrupts the load distribution in the knee, putting the patient at a higher risk of arthritis. Both, arthroscopic repair and menisectomy procedures leave the patient with a very high



risk of re-tearing the meniscus. Osteoarthritis is the most common complication after meniscus surgery (Frizziero *et al*, 2012).

#### **2.1.4 Project Justification**

The goal of this project was to create a scaffold that would overcome the physiological nutrient perfusion limit by creating channels through a hydrogel cell suspension. Overcoming the perfusion limit would allow for the engineering of avascular tissues, such as the meniscus. Ideally, the living meniscus implant will be grown using a human chondrogenic cell line. For the meniscus it is not necessary to use autologous cells as the knee is an immune privileged area. Current methods do not replace damaged meniscus tissue with anything to rebalance the knee. A meniscus transplant made of living tissue is the ideal treatment as it would balance the joint. This balance correction in the knee would reduce the patient's risk of re-injury and the possible need for subsequent procedures.

### **2.2 Tissue Engineering Approaches**

Tissue engineering scaffolds are 3D structures that enable cell growth and tissue formation in various conformations for specific applications. They provide pertinent structural support for the tissue to grow in the proper morphology. When dealing with an avascular tissue, such as cartilage, the scaffold can also provide avenues for vital nutrient perfusion.

#### **2.2.1 Nutrient Perfusion**

A main barrier to tissue engineering is that cells need a continuous supply of oxygen and nutrients to survive. Large cell aggregates form a necrotic core since oxygen and nutrients cannot permeate the tissue and cell waste cannot be excreted (Miller, 2014). The cell aggregates impede the flow of nutrients causing necrosis. A bioreactor can be used to force nutrients throughout a culture system and it has been shown that ventilation could also provide nutrients. These methods were

used with vasculature and were able to properly perfuse nutrients but could not maintain the parenchyma of the tissue (Scarritt *et al*, 2015). Based on previous research it is evident that a need remains for a way to perfuse nutrients throughout an avascular tissue *ex vivo*.

### **2.2.2 Material Choice**

The ideal material choice for any tissue engineering application is the natural extracellular matrix (ECM) of the specific tissue (Chan & Leong, 2008). This is due to the proteins and chemical triggers present in the ECM, which stimulate cells to function properly and create a uniform tissue. Although these are ideal properties for tissue engineering applications, these scaffolds are difficult and expensive to fabricate. They are also limited by the ECM source as allografts (human to human) and xenografts (animal to human) can illicit an immune response. Autografts (self-sourcing) can also be challenging due to the limited quantity of ECM available.

More feasible options for scaffold materials are synthetic or natural polymers. Synthetic polymers have a myriad of advantages and disadvantages. They have highly tunable mechanical properties making them suitable for a wide range of tissue scaffolds. However, biocompatibility is a major concern with synthetic polymers. Because of this, synthetic polymers have to be tested to determine cytotoxicity, degradation by-products, and other undesirable effects they may have on the surrounding cells. Suitable synthetic polymers include nylon, polylactic acid (PLA), polyvinyl alcohol (PVA), polyglycolic acid (PGA), ultrahigh molecular weight polyethylene (UHMWPE), Vicryl, and many others. Commercially available three-dimensional printers are capable of printing some of these synthetic polymers.

Natural polymers tend to be more biocompatible as they are generated by biological systems. However, they can lack in mechanical properties and are not as adaptable to specific applications as synthetic polymers. The sources of natural polymers are also much more limited, making them

less available. Some natural polymers are silk, collagen, chitosan, alginate, and cellulose. Some modified Inkjet printers have been proven capable of printing natural polymers (Baek *et al*, 2014).

### **2.2.3 Meniscus Replacement**

Currently, the gold standard for meniscus treatment is to remove damaged tissue without replacing it. The Menaflex product, made by ReGen, was the leading technology in meniscus replacement before the FDA retracted their approval. The Menaflex, shown in Figure 4, was a collagen meniscus implant derived from bovine Achilles tendons, which were processed and reshaped into a meniscus for human implantation. Some limitations associated with the Menaflex were that it was not composed of living tissue, it degraded in size over time, and that it is no longer available.

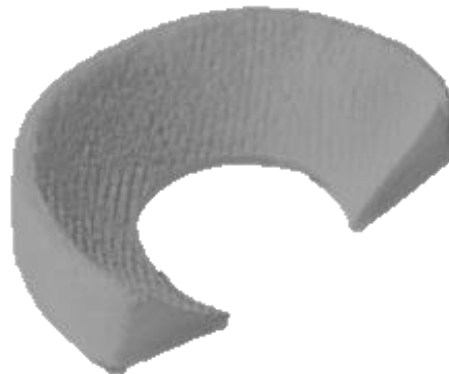


*Figure 4: The Menaflex Collagen Meniscus Implant*

While the product appeared successful, the proper documentation protocols were not followed leading to the retraction of the product by the FDA. Since the approval was overturned, ReGen has filed for bankruptcy and is no longer in business.

### **2.3 Cartilage Cell Culture**

Chondrocytes pose a challenge for cell culture because they do not proliferate. This makes obtaining a proper cell density for treatment more difficult than other tissues. Progenitor cells such as mesenchymal stem cells or induced pluripotent stem cells must be cultured and proliferated to

the appropriate cell density before differentiation is initiated. Throughout the process of proliferation and differentiation, histological and fluorescent staining can be used as assessments.

### **2.3.1 Chondrocytes**

Chondrocytes are terminally differentiated cells which make up cartilage tissue. Chondrocytes generate the cartilaginous matrix composed of collagen and proteoglycans. The progenitor cells of chondrocytes are mesenchymal stem cells (MSCs). These cells have the ability to differentiate into three different types of cells: osteoblasts, adipose, and chondrocytes. In the process of chondrocyte formation, MSCs lose their pluripotency as they proliferate and crowd together as chondroblasts which, in turn, develop into chondrocytes (Chadwick *et al*, 2013). This process can be replicated *ex vivo* using a combination of insulin and ascorbic acid (Negishi *et al*, 2001). For *ex vivo* experimentation, ATDC5 cells offer a good model as they are an immortalized cell line of mouse chondrogenic precursor cells and are accepted as the standard model for cartilage research (Newton *et al*, 2012).

### **2.3.2 Culture Conditions**

The media most commonly used with ATDC5 cells is composed of a 1:1 ratio of Dulbecco's Modified Eagle Medium (DMEM) without L-Glutamine, with phenol red as a pH indicator and 4.5 g/L glucose and sodium pyruvate, and Ham's F12 plus 2 mM L-Glutamine and 5% fetal bovine serum (FBS). Cells can be stored in an incubator at 37°C, 5% CO<sub>2</sub>, and 70% humidity. They can also be cultured effectively in 3D hydrogel systems. There are no known differences in population doubling levels (PDL) or phenotype when cultured in 3D or 2D conditions (Tortelli & Cancedda, 2009).

### **2.3.3 Histology**

Histology is the process of staining cells as a method of assessment to determine viability and differentiation efficiency. Live/dead staining with Hoechst or DAPI and Propidium Iodide (PI) provides a contrast view of all the cells and the dead cells, respectively. In some cases, Propidium Iodide can over stain certain cell types and in some cases Hoechst may not sufficiently stain all live cells. To overcome this problem, Calcein AM can also be used as a live only stain. To determine differentiation of chondrocytes, Alizarin red can be used. This stain denotes the calcium deposits that are generated by differentiated chondrocytes. Alizarin red can be used in conjunction with live/dead staining to show percent differentiation and viability.

## **2.4 Three Dimensional Cell Culture**

Hydrogels provide an environment mimicking physiological conditions to culture cells in. Most cell cultures are currently conducted in two-dimensional environments that are not representative of natural tissue conditions. To generate a functioning three-dimensional tissue, a 3D culture must be utilized. There are many different types of hydrogels that are available for use with this application, each with their own advantages and disadvantages.

### **2.4.1 Hydrogels**

Hydrogels are polymer matrixes characterized by covalent bonds, physical bonds between chain entanglements, and Van der Waal interactions between chains. They are often lightly crosslinked and water swollen. Hydrogels can be tuned to mimic different physiological conditions within the body by varying the polymer composition and ratios. Due to their tunable properties, hydrogels are often used in tissue engineering applications as they provide a three dimensional (3D) environment for cells to grow in as they would in the body, as opposed to a two dimensional culture plate. They can also be controlled to release different growth factors or drugs to help support cell

viability. There are a few mechanical properties that are important to consider when using hydrogels. The gel stiffness should be around 22.4 Pascals to best replicate *in vivo* conditions (Sanz-Ramos *et al*, 2013). The time necessary for gelation also needs to be considered because a long gel time can result in cell settling before the gel is fully crosslinked. If the cells are allowed to settle at the bottom of the well they will not grow in a true 3D environment. For this reason, a gelation time of under 5 minutes is the most desirable. In order to best assess cell viability, histological staining can be used in a 3D environment.

#### **2.4.2 Hydrogel Choice**

Some of the common hydrogels used for chondrogenic applications are alginate, chitosan, collagen, fibrin-polyurethane copolymer, and agarose. These hydrogels each have advantages and disadvantages associated with them and their ability to support chondrocyte proliferation and differentiation.

##### *Alginate*

Chondrocytes cultured in alginate beads were able to maintain their phenotype for more than eight months. The chondrocytes in the 3D environment are still capable of responding to growth factors and cytokines that are known to affect metabolism. Alginate hydrogels are easily fabricated as they will immediately crosslink in the presence of  $\text{CaCl}_2$  and can be removed from the hydrogel when necessary (Deceuninck *et al*, 2004). Despite these advantages, alginate has been shown to suppress proliferation of undifferentiated chondrocytes (Wei *et al*, 2012). To overcome the disadvantages of alginate, the material can be combined with an RGD peptide through carbodiimide chemistry. This will increase cell adhesion and mechanotransduction between integrins forming a functional tissue (Genes *et al*, 2004).

### *Chitosan*

Hydrogels composed of chitosan allow for significant chondrocyte proliferation and a high percent of differentiation. They are also easy to crosslink, which allows them to be tuned to the appropriate stiffness. However, the process of creating a chitosan hydrogel is intensive, complicated and time consuming (Garcia-Giralt *et al*, 2013).

### *Collagen*

Chondrocytes in a 0.8% collagen based hydrogel generate an extracellular matrix with favorable mechanical properties. Although collagen makes up a significant portion of the physiological meniscus, there are some draw backs of collagen based hydrogels. They require a long gelation time of approximately one hour and the gels constrict over time. The constriction of the gel inhibits extracellular matrix extension within the environment, which can slow proliferation and ECM generation (Sanz-Ramos *et al*, 2014). Collagen hydrogels can be modified by adding fibrin to make the hydrogel more mechanically sound and reduce constriction. Another option is a bovine collagen solution in a hyaluronic-based hydrogel. This is commercially available in a kit called Extracel, which has been shown to work particularly well with chondrocytes, as well as a product called PureCol EZ Gel.

### *Fibrin-Polyurethane Copolymer*

Within a fibrin-polyurethane copolymer hydrogel, chondrocytes exhibit an increased percentage of glycosaminoglycan (GAG), a primary protein of the ECM. Mechanical stimulation of this hydrogel can further increase GAG expression. The properties of this hydrogel also enhance expression of collagen II and aggrecan, which are key components of the physiological meniscus (Tortelli & Cancedda, 2009). Although this synthetic hydrogel has been shown to generate a mechanically stable ECM and well oriented fibers, the components are significantly more

expensive than other hydrogel options. Additionally, a biocompatible polyurethane can be challenging to synthesize.

### *Agarose*

Low melting point (LMP) agarose is compatible with cell culture. The agarose promotes chondrocyte cell to cell adhesion because the cells are unable to attach to the hydrogel. This is representative of physiological conditions, allowing for the proper formation of the ECM. This cell to cell adhesion is also advantageous because the ECM will not be disrupted by scaffold degradation. The biggest drawback to using agarose is that cells cannot metabolize the hydrogel, necessitating the use of agarase enzyme to degrade the material. The use of an enzyme significantly increases the cost of the hydrogel system (Buschmann *et al*, 1992).

## **2.5 Three Dimensional Printing**

In biomedical applications, 3D printing provides a method of fabricating a support system for cell growth and eventual tissue formation. The tunable properties of this method allow for precise orientation of materials and geometry of the scaffold, which can lead to accurate mechanical properties of the specific tissue being grown.

### **2.5.1 Process**

Software such as computer aided design (CAD) programs can be used to model different designs. 3D models can be generated using these programs to reflect natural parts of the body. These models can then be converted into layer-by-layer instructions for 3D printers to generate. Parameters can be set to control the print speed, extruder temperature, layer thickness, etc. to increase the precision of the print. Once the printer receives these coded parameters and instructions, it begins the heating process. The extruders, which are loaded with filaments of material, are heated to the predetermined temperature (above the melting point of the filament material). Common filament



materials are acrylonitrile butadiene styrene (ABS) plastic, PLA, and PVA. Some printers contain a heated build platform, to help the printed material stick and form a flat base. Once the printer has fully warmed up, the build begins. The extruders melt the filaments and generate layers of material, which build upon each other into the final product.

### **2.5.2 Biomedical Applications**

3D printing can be applied to many different areas in the biomedical field. Tissue scaffold fabrication is a key technology associated with 3D printing. It allows for very precise, reproducible and customizable generation of scaffolds, which can determine the overall shape and structure of the engineered tissue. A prime example of the utility of 3D printing in this field is the fabrication of electrospun collagen fibers. These fibers can be created on the nano scale which allows them to have a high surface area to volume ratio (SA:V). This SA:V is important in tissue engineering design because it allows for superior cell adhesion to the scaffold material. Electrospun fibers allow for proper cell orientation in the tissue engineered scaffold (Baek *et al*, 2014). Another method of 3D printing in biomedical applications is the use of modified Inkjet printers to fabricate living tissue. These printers are capable of printing cells and scaffold together, layer by layer (Xu *et al*, 2012).

### **2.5.3 Monoprice Dual Extrusion 3D Printer**

The Monoprice is a commercially available dual extrusion 3D printer. Dual extrusion means the printer can be loaded with two different filament materials, allowing it to print objects with a combination of the two materials. The Monoprice is capable of printing ABS, PLA and PVA. ABS is a non-biocompatible plastic and is not used in biological applications for tissue engineering. PLA and PVA, however, are both FDA approved, biocompatible polymers, which can support cell growth in a scaffold system. PLA melts at a temperature of 160-177°C and PVA

melts at a temperature between 170-220°C. The Monoprice printer is able to heat the extruders to a temperature of 250°C, making extrusion of both PLA and PVA possible. Figure 5 is a picture of the 3D printer and Table 2 outlines its specifications.



Figure 5: The Monoprice Dual Extrusion 3D Printer

Table 2: Specifications of the Monoprice Dual Extrusion 3D Printer

<b>Specifications</b>	
Case Color	Black Powder Coated
Extruder	MK-8 Dual Head with upgraded release
Plate	Heated Metal Build Plate
Print Technology	FDM
Build Volume	8.9" x 5.7" x 5.9" (225 x 145 x 150 mm)
Printing Material	ABS/PLA/PVA Filament 1.75mm
Layer Resolution	±0.10mm
Positioning Precision	XY: 11 Microns (0.0004") Z: 2.5 Microns (0.0001")
Layer Thickness	0.1 - 0.5mm
Nozzle Diameter	0.40mm
Printing Speed	24cc/hour
Extruder Temp.	0-250°C
Heating Plate Temp.	0-120°C
Connectivity	USB Cable, SD Card

<b>Specifications</b>	
OS Compatibility	Windows® XP/Vista®/7/8 Linux, Mac® OS X®
Operation	LCD Screen + 5 keys control
AC Input	100~240 VAC, ~2 amps, 50~60 Hz, 350W
Dimensions	18.7" x 12.7" x 15.1" (476 x 322 x 383 mm)
Weight	28.7 lbs. (13kg)
Software	ReplicatorG
File Types	Input:STL/OBJ Output:X3G

## **2.6 Conclusion**

This project is a combination of different novel technologies into a single tissue engineering based approach. Cell culture and differentiation techniques can be used in 2D and 3D to study cell growth in varying media compositions. Biocompatible hydrogels are able to assist in cell proliferation and differentiation while providing realistic culture conditions for cells to grow in. The physiological conditions represented by the hydrogel aid in cell orientation and ECM generation. Tissue engineering scaffolds can be fabricated with the use of a 3D printer and appropriate software. Customizable 3D printed models offer various geometries to effect tissue morphology. Optimizing the porosity of the 3D scaffold allows for proper infiltration of nutrients to support cell life within the scaffold. Cells seeded into a hydrogel mimicking physiological conditions within a 3D printed scaffold may result in the perfusion of nutrients beyond 100  $\mu\text{m}$ .

## **Chapter 3 Project Strategy**

The goal of this project is to design a 3D biomorphic tissue scaffold using a commercially available 3D printer and to seed ATDC5 cells onto the engineered scaffold using a hydrogel to facilitate nutrient diffusion. This chapter serves to outline the steps and methods used to prioritize and create the objectives and constraints of this project, coinciding with our client statement. The project approach also includes the goals of this project and strategy for completing them.

### **3.1 Initial Client Statement**

The project's initial client as presented by the advisor, Professor Sakthikumar Ambady:

*“The knee meniscus is a two-part three-dimensional structure that provides shock absorption, stability and lubricity to the knee. Meniscal tears and ruptures of the knee are very common injuries. The team will engineer a three-dimensional, biomorphic tissue scaffold to research the ability to grow, ex vivo, replacement menisci. This scaffold will be printed with a commodity 3-D printer modified and reengineered as necessary by the team to provide higher resolution.”*

Once this initial project statement was presented to the team, the members developed a list of questions to ask the advisor. The questions were designed to clarify the motivation for the project and the exact design specifications of the client.

The subsequent step to this process was to decide who the stakeholders were for the final product design. Professor Sakthikumar Ambady is the main advisor and client for this design. Dr. Robert Meislin of New York University Medical School is a secondary client who brought the project to Professor Ambady's attention. In addition, other research facilities would benefit from the resulting procedure of printing a scaffold and being able to provide nutrients during cell proliferation and into the depth of a live, avascular tissue. The users of this device would ultimately

be orthopedic researchers and physicians working towards regenerating avascular tissue for wound treatment. The design team consisted of Dominick Calvao, Gaetana D'Alesio-Spina, and Patrick Thomas. All members worked to design a solution that fulfills the needs and requests of the client and potential end users.

### **3.2 Objectives and Constraints**

Working with the advisor, the project team developed a set of objectives and constraints to guide the project to completion. The objectives outlined the necessary attributes that the final design had to meet in order to be successful. The constraints described boundaries and conditions that the project had to abide by and the final product had to meet.

#### **3.2.1 Objectives**

The team's primary objectives were that the product had to be safe, physiologically accurate, customizable, and reproducible. Each objective is described below:

**Safe:** If this product did not meet safety standards it would never be usable *in vivo*. The secondary objectives associated with the safety of the product are as follows:

1. **Biocompatibility:** All materials used, including the 3D printing materials and hydrogel, must support both cell proliferation and differentiation.
2. **Sterilizable:** The product must be fully sterilizable to reduce risk of contamination during the culture period.
3. **Comply with FDA standards:** For potential future use in a clinical setting, the final design of this product must comply with FDA standards.
4. **Autologous cells:** To prevent immunogenic response or the need for immunosuppressant drugs *in vivo*, an autologous cell source should be used.

Physiologically accurate: For the proof of concept nutrient diffusion scaffold, a chondrogenic cell line had to be used in order to best mimic cartilage tissue response to the scaffold. The ranked secondary objectives that had to be fulfilled to achieve this primary objective are as follows:

1. Nutrient perfusion: Nutrients had to be able to penetrate to the center of the scaffold and sustain cell life.
2. Fiber orientation: Within a physiological meniscus fibers are oriented both longitudinally and radially.
3. Mechanical properties: The scaffold had to allow for effective shock absorption and a high surface area to volume ratio for cell adhesion.
4. Morphology: For use *in vivo* the shape of the product had to be consistent with the natural shape of the meniscus.

Reproducible: For the design to be applicable to other areas of the body and to achieve consistent success the product had to be reproducible. The ranked secondary objectives are as follows:

1. Protocol establishment: Protocols had to be established and followed to ensure proper record of experimentation and results that would allow for expansion of the project to further applications.
2. 3D Printing: A commercially available 3D printer had to be used to ensure the scaffold could be generated repeatedly and consistently.

Customizable: Individual menisci have different geometric properties that had to be considered on a case by case basis. The secondary objectives to achieve a customizable product are as follows:

1. Computer aided design model from MRI: The scaffold had to be modeled in CAD software from an individual patient's MRI results.
2. IPSc differentiation: The cell source had to be induced pluripotent stem cells that have been de-differentiated from the patient's own chondrocytes.

### 3.2.2 Pairwise Comparison Chart

*Table 3: Pairwise Comparison Chart*

<b>Goal</b>	<b>Safe</b>	<b>Similar to physiological structure</b>	<b>Reproducible</b>	<b>Customizable</b>	<b>Score</b>
<b>Safe</b>	X	1	1	1	3
<b>Physiologically accurate</b>	0	X	1	1	2
<b>Reproducible</b>	0	0	X	1	1
<b>Customizable</b>	0	0	0	X	0

The objectives were ranked according to Table 3 by the team in conjunction with the advisor. Each objective was compared to the others to determine which of each pair was more important. The outcomes show that safety was the most important objective, because the future plan for the product is human implantation. This is followed by physiological structure, which is essential based on the meniscus' geometric constraints to ensure its mechanical integrity. Reproducibility comes next due to the proof of concept aspect that this project represents. Customizability is last because it is necessary for clinical applications but not for concept purposes.

### 3.2.3 Constraints

There are a number of constraints associated with the design of this product that were considered.

- **Manufacturability:** If the product could not be manufactured in a cost effective and consistent way, the design would not be feasible.
- **Permeability:** Nutrients had to be able to perfuse 3-5 mm into the scaffold to create a clinically applicable tissue.
- **Cell Capabilities:** The seeding procedure had to comply with the observed population doubling level of 0.59 doublings/day. The cells needed the appropriate amount of time to proliferate and then differentiate after seeding into the scaffold.
- **Commercial dual extrusion printer:** The printing resolution of the commercial 3D printer is 0.1 mm. This constraint effected the design of the scaffold features.

**Project Constraints:** There are additional constraints that were imposed due to the nature of the project.

- **Time:** Due to the nature of the MQP the project had to be completed within a timeframe of 28 weeks (the academic year).
- **Cost:** The project had to be completed within the allocated MQP budget of \$468. This excluded department purchased supplies.

Most of the cost constraints were bypassed due to donations and department purchases. Some of the most significant constraints that had to be considered were the structure manufacturability, the permeability of the scaffold and hydrogel, the cell capabilities, and the specifications of the commercial dual extrusion printer. Another constraint that had to be considered was the time that it took to generate the scaffold, culture cells, and perform the appropriate validation tests.



### 3.2.4 Objective Tree

Each of the objectives associated with this project had number of sub-objectives as outlined in

Figure 6 below.

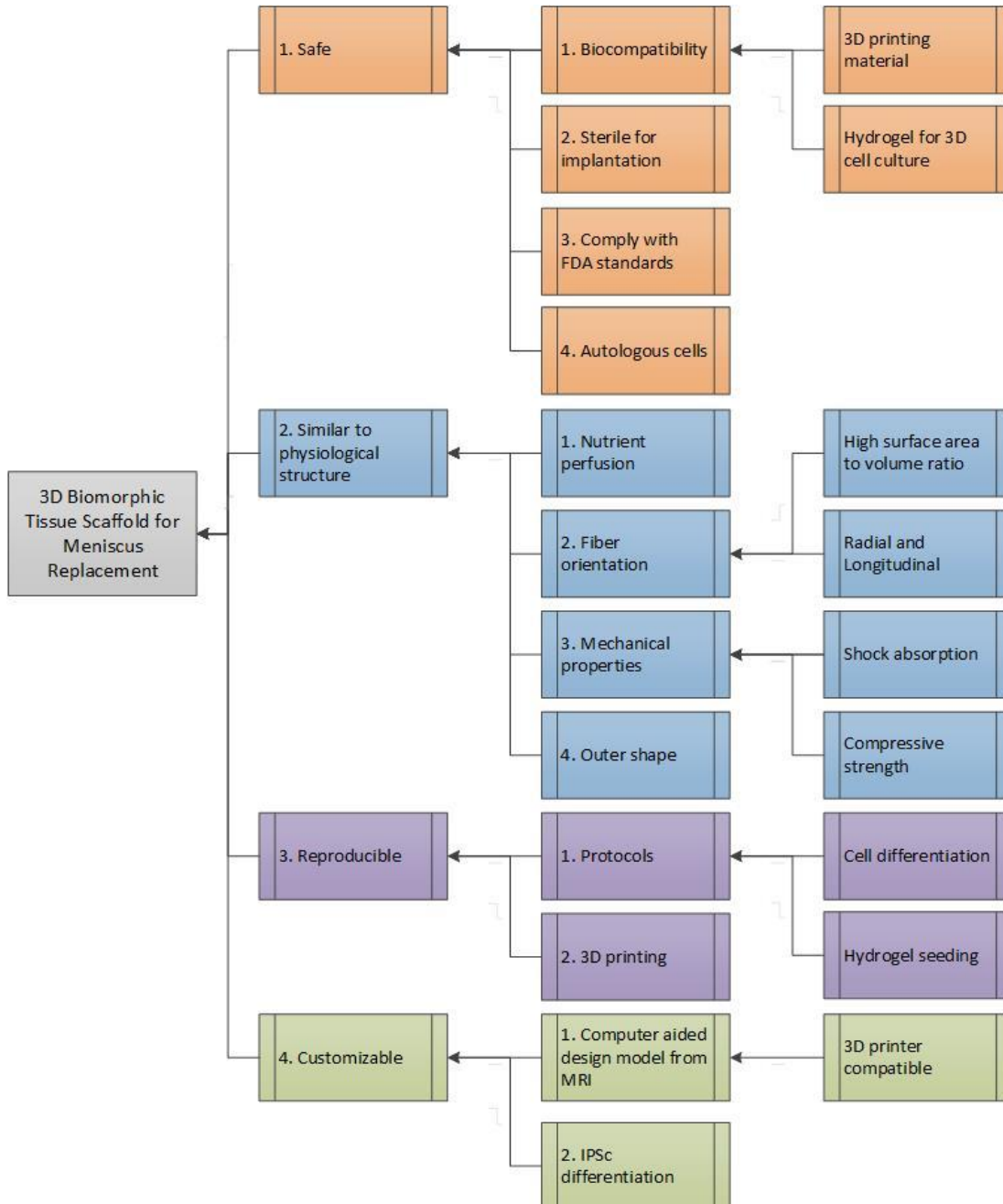


Figure 6: Objectives Tree

### **3.3 Revised Client Statement**

After the designation of objectives and constraints, the initial client statement was revised:

*“Based on the commonality of meniscal injuries the team is tasked with engineering a three-dimensional, biomorphic tissue scaffold. The scaffold will be seeded with cells, ex vivo, in a hydrogel, to overcome the physiological perfusion limit. The scaffold will be printed with a Monoprice dual-extrusion 3D printer for concept reproducibility.”*

This statement is a more accurate representation of the desired ultimate outcome of this project. It contains a more detailed description of what the final product had to contain.

### **3.4 Project Approach**

Effectively overcoming the constraints of this project required the team members to each lead a different aspect of the project. The three main aspects of the project were the design and fabrication of the scaffold, hydrogel analysis and selection, and cell seeding and validation. Based on results from early experiments, the team modified future testing in order to best create a scaffold with channels for nutrient perfusion through a 3D hydrogel cell suspension.

#### **3.4.1 Design and Fabrication of Scaffold**

Designing of the scaffolds began with the concept of creating channels through a hydrogel in order to perfuse nutrients. Channels would allow nutrients to perfuse and would help in orienting the cells into the proper fiber architecture. The initial idea was to use PVA to create a latticework that would degrade in the presence of the hydrogel and leave channels behind. When this method proved inapplicable, PLA was used to create the lattice. PLA did not degrade and shrank slightly as it cooled after printing, creating a lattice that was more closely packed than anticipated and the

gel was unable to be removed for analysis. The final concept used threads to create channels through the hydrogel. This was explored with cotton, silk, Vicryl, and degradable collagen sutures.

### **3.4.2 Hydrogel Analysis and Selection**

The main hydrogel materials analyzed were PureCol EZ Gel, fibrin, and alginate. Different combinations of PureCol EZ Gel and fibrin were tested to shorten the gel time of the PureCol EZ Gel and create a more uniform cell suspension. Alginate was studied because it can be immediately crosslinked with  $\text{CaCl}_2$  and its stiffness can be tuned by altering the concentrations of alginate and  $\text{CaCl}_2$ . Each gel was tested for gel time, cell distribution, cell viability, and gel shrinking. Gel time was important for cell distribution and eventual tissue generation. In order to maintain the proper scaffold dimensions, the ideal gel could not shrink.

### **3.4.3 Scaffold Seeding and Validation**

Each scaffold rendition would require a different seeding method, but the hydrogel cell suspension preparation was the same. The cells were suspended in the hydrogel and thoroughly mixed by pipetting up and down prior to seeding into the scaffold. For the two lattice work scaffolds, a syringe had to be used to push the hydrogel cell suspension into the scaffold during seeding. For the threaded scaffold, a pipette was used to seed the hydrogel cell suspension into the scaffold. Validation was done using Hoechst 33342 and Propidium Iodide live/dead counter staining as well as Calcein AM live staining based on the over staining of Propidium Iodide. Alizarin red staining was done to show the presence of differentiation. The validation stains were used to prove cell viability at a depth greater than 100  $\mu\text{m}$ .

## **Chapter 4 Methods and Alternative Designs**

### **4.1 Needs Analysis**

The most important criteria for success of this project was to develop a 3D tissue scaffold, which prevented the formation of a necrotic core and generated a clinically sized living tissue. In order to best mimic the nutrient delivery system of fibro-cartilage tissue without focusing on mechanical stimulation, the team designed and tested different scaffold geometries and materials that would create channels through a hydrogel system. The channels were designed to aid in nutrient perfusion throughout the depth of the scaffold.

The minimally viable product to satisfy the needs of the client had to accomplish the following (listed in order of importance):

- Prevent the formation of a necrotic core in a 3-5 mm tissue scaffold
- Comply with FDA regulations for safety and biocompatibility
- Manufacturable using a commercially available 3D printer

These main client needs were addressed throughout the project and the final design of the tissue scaffold successfully accounted for each need.

### **4.2 Functions (Specifications)**

The functions and specifications are important parameters to consider throughout the execution of the project. The three functions that the final product had to fulfill were: promote cell viability and distribution, induce cellular differentiation, and allow for proper nutrient perfusion past the natural perfusion limit.

#### **4.2.1 Cell Viability and Distribution**

In order to satisfy the function of proper cell viability and distribution, a proper environment for cell growth was necessary. Hydrogel selection was an important aspect of accomplishing this goal.

A hydrogel with a short gelation time was necessary to ensure cells would be well-dispersed in the 3D environment. Additionally, the selected hydrogel had to be non-cytotoxic and had to maintain its mechanical integrity as the cells proliferated.

#### **4.2.2 Cellular Differentiation**

For the final product to be clinically applicable, cells must be able to differentiate into the proper cell type within the scaffold. As previously stated, cartilage is a terminally differentiated cell type and will not proliferate once differentiation is induced. The design had to be made to allow the cells to differentiate after the cells had reached an appropriate cell density. Additionally, the cells had to successfully differentiate in all layers of the scaffold in a timeframe which could be applied to a clinical setting.

#### **4.2.3 Nutrient Perfusion**

One of the greatest challenges in tissue engineering is generating tissue at sizes and depths which can be clinically applicable for implantation into the body (Costa-Almeida *et al*, 2014). As outlined in Chapter 2, the natural perfusion limit in the body is 100  $\mu\text{m}$ . To overcome this challenge, the design had to mimic the channels which naturally develop in the meniscus (Fox *et al*, 2012). Proper nutrient perfusion was important to keep the cells viable and to transport differentiation factors to the depths of the scaffold.

#### **4.3 Design Alternatives**

Three main scaffold designs were fabricated and tested. All of the designs utilized the concept of creating a network of channels through a 3D hydrogel system. These channels were to maximize the surface area to volume ratio within the scaffold and allow nutrients to perfuse into the depths of the scaffold.

### 4.3.1 PLA-PVA Dual Extruded Scaffold

The first design was a combination of PLA and PVA as seen in Figure 7. This design featured a slowly degrading PLA shell, filled with a network of PVA rods. Once printed, the scaffold would be filled with cells suspended in a non-crosslinked hydrogel. Once the hydrogel crosslinked, cell proliferation media would be added, initiating the degradation of the PVA. The PVA would then degrade away, leaving channels in their place. Utilizing these channels, the cells would receive the nutrients they need to proliferate and, once the appropriate cell density was reached, differentiate.

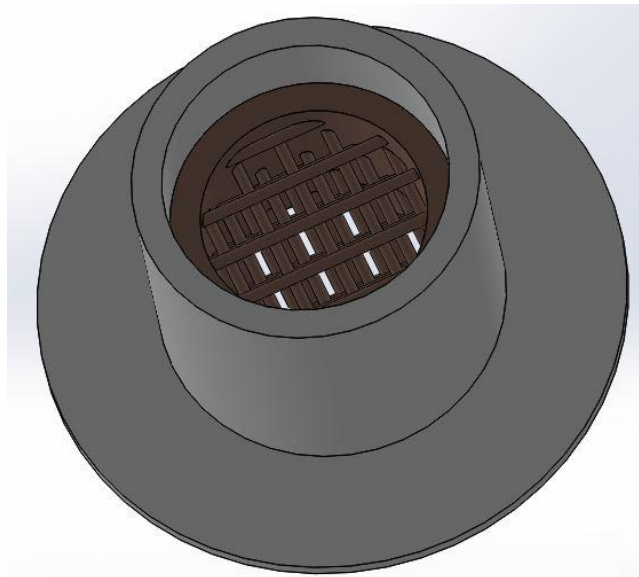


*Figure 7: PLA-PVA Dual Extruded Scaffold SolidWorks Design*

### 4.3.2 PLA-only Scaffold

Based on the results of the initial testing of the PLA-PVA combination scaffold, another design featured a scaffold made entirely of PLA as seen in Figure 8. Similar to the concept of the Dual Extruded Scaffold, this design featured 3D printed rods to create a network of channels within the scaffold. It would be filled with the cells suspended in the non-crosslinked hydrogel, which would then be crosslinked to solidify the cell suspension within the scaffold. Proliferation media would then be added and the PLA rods would begin to degrade away. As the rods would be much thinner

than the PLA shell, they would degrade away, leaving the hydrogel contained within the cylindrical shell. Due to the biocompatible nature of PLA, cells were expected to adhere to the rods, which would aid in the cell orientation throughout the hydrogel system and promote the formation of channels after the PLA had degraded away completely.

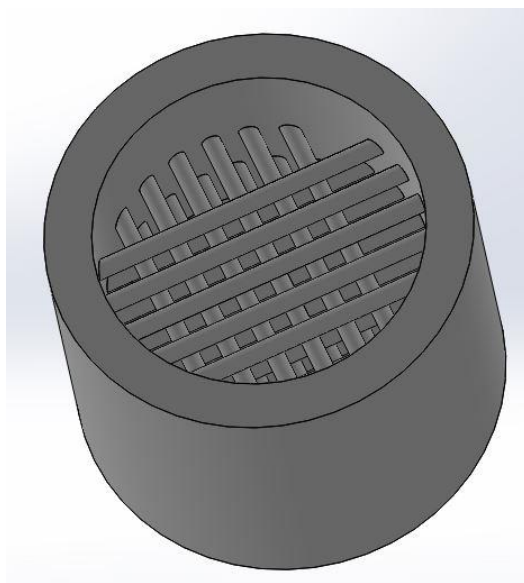


*Figure 8: PLA-only Scaffold SolidWorks Design*

### **4.3.3 Threaded PLA Scaffold**

After extensive testing of these models, a third design shown in Figure 9 utilizing sutures as the channel creation method was created to overcome the limitations associated with the first two designs. A PDMS cap was placed on the top of the scaffold. A suture was then threaded through the cap and through holes in the bottom of the scaffold. The end of the suture was then pulled back through the PDMS cap to secure the suture in place. The scaffold was subsequently filled with a non-crosslinked hydrogel cell suspension which was then crosslinked to solidify the gel. Proliferation media was added to sustain the cells until an appropriate cell density was reached. Differentiation media was then added to induce differentiation. The sutures were expected to wick nutrients into the center of the scaffold mimicking the natural fibers in the meniscus. Some

degradable sutures were also examined and were expected to degrade over time leaving channels for nutrient perfusion. The threaded scaffold design was validated using Calcein AM live cell staining (eBioscience 65-0853-39) and fluorescent microscopy to assess cell viability and Alizarin Red staining to assess cell differentiation.

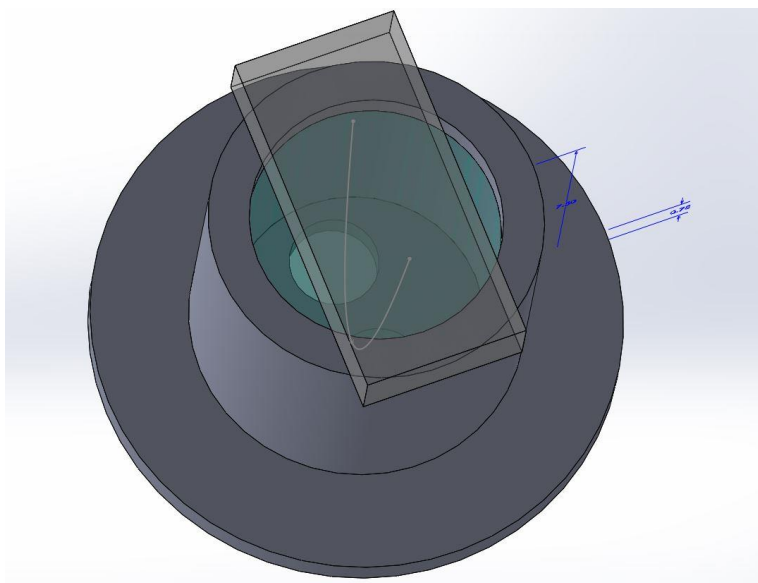


*Figure 9: Threaded PLA Scaffold SolidWorks Design  
Includes the PLA cylinder, PDMS cap, thread, and hydrogel.*

#### **4.4 Feasibility Study/ Experiments**

The different aspects of the project had to be evaluated for feasibility. The scaffold materials had to be evaluated for cytotoxicity and degradation. Additionally, the different scaffold designs were evaluated based on their ability to maintain cell viability throughout the entire depth of the scaffold. The hydrogels were evaluated based on the optimal gelation time, which would result in the best cell distribution at all layers of the scaffold.

##### **4.4.1 Scaffold Feasibility**

Approximately fifty-five different scaffold designs were modeled in SolidWorks throughout the course of the project. Multiple iterations were made of similar designs based on the manufacturability with the 3D printer. The controllable properties of the printer including feed



rate, travel feed rate, extrusion temperature, build plate temperature, infill percent, number of shells, filament diameter, and layer height were tuned based on the desired design.

A degradation study was conducted to determine the degree and speed of degradation of PLA and PVA. This study was necessary to assess the feasibility of these materials as scaffold components. Additionally, due to observed swelling of PVA, a swelling ratio test was conducted.

#### **4.4.2 Hydrogels**

Over one-hundred different hydrogel permutations were evaluated based on gel time, cell distribution, cell viability, and gel shrinking. The primary hydrogel materials analyzed were collagen, fibrin, and alginate based. Different hydrogel concentrations and combinations, and different crosslinking agent concentrations and times were tested to determine the optimal hydrogel.

#### **4.4.3 Cell Culture**

The PDL of the ATDC5 cell line was calculated to aid in the design of experiments. This was an important factor to consider when determining experiment duration and for routine subculturing of the cell line. The appropriate differentiation media was determined using different concentrations of each insulin and ascorbic acid, as well as with combinations of the two. Once the proper differentiation media was selected, a differentiation timeline was developed in 2D and 3D cell culture environments.

#### **4.4.4 Threading Materials**

For the purposes of threading the scaffolds, a variety of degradable and non-degradable sutures were analyzed. The sutures were evaluated based on cell viability in the hydrogel-scaffold system.

The degradable sutures used were violet-dyed Vicryl and plain collagen sutures. The non-degradable sutures used were silk and cotton.

#### 4.4.5 Calciem Staining

To validate the final design successfully support cell life, Calciem AM staining was used to fluoresce the living cells in the scaffold. To ensure that Calciem AM only stained living cells, a plate of living cells and a plate of cells that had been fixed for 10 minutes in ice cold methanol were stained.

### 4.5 Experimental Methods

#### 4.5.1 ATDC5 Cell Culture Protocol

The ATDC5 cell line was cultured in proliferation media as outlined in Table 4, composed of a 50:50 mixture of DMEM (Corning, 15-013-CV), Ham's F12 media (Corning, 10-080-CV), supplemented with 5% FBS (Atlanta Biologics) and Penicillin/Streptomycin (Lonza, TS-17-603-2).

*Table 4: Proliferation Media Composition*

Component	Stock Solution	Volume (mL)	Final Concentration
DMEM basal media	1X	235	47%
Penicillin/Streptomycin	100X	5	1%
Ham's F12		235	47%
FBS		25	5%
Total Volume		500	

ATDC5 cells in 2D were cultured on 100 mm tissue culture plates (Falcon) and incubated at 37°C in a 5% CO<sub>2</sub> environment according to the following protocol:

1. Aspirate media
2. Rinse cells with 5mL DPBS(-)
3. Aspirate DPBS(-)

4. Add 3mL of 0.25% trypsin/EDTA (Corning, 25-053-CI)
5. Incubate for 3 minutes at 37°C
6. Neutralize trypsin/EDTA with 2mL proliferation media (Table 4)
7. Transfer the cell suspension into a 15mL conical tube
8. Remove 10 $\mu$ L of cell suspension and place in a C-chip disposable hemocytometer for counting
9. Centrifuge the cells at 200g for 7 minutes to form a pellet
10. Aspirate the media from the pellet and re-suspend in proliferation media to achieve a final density of 1x10<sup>6</sup> cells/mL
11. Re-plate at the desired cell density, adding the appropriate amount of additional proliferation media to achieve a total volume of 10mL/plate

#### **4.5.2 Cell Isolation for Hydrogel Seeding**

For seeding into the scaffold, counted cells were re-suspended in 6X DMEM proliferation media. This media consisted of the same components as the proliferation media in Table 4 with 6X DMEM instead of 1X DMEM. The 6X DMEM was created using powdered DMEM (Corning, 50-003-PB) at a 6X concentration in diH<sub>2</sub>O and filtered for sterilization using a 0.2  $\mu$ m vacuum filter. ATDC5 cells were isolated for experimentation within the scaffolds using the following protocol:

1. Aspirate media
2. Rinse cells with 5mL DPBS(-)
3. Aspirate DPBS(-)
4. Add 3mL of 0.25% trypsin/EDTA
5. Incubate for 3 minutes at 37°C

6. Neutralize trypsin/EDTA with 2mL proliferation media (Table 4)
7. Transfer the cell suspension into a 15mL conical tube
8. Remove 10 $\mu$ L of cell suspension and place in a C-chip disposable hemocytometer for counting
9. Centrifuge the cells at 200g for 7 minutes to form a pellet
10. Aspirate the media from the pellet and re-suspend in 6X DMEM proliferation media at the desired density for seeding into the scaffold

#### **4.5.3 Cell Differentiation**

ATDC5 cells were differentiated in proliferation media supplemented with ascorbic acid (37  $\mu$ g/mL) and insulin (10  $\mu$ g/mL). For scaffold seeding, the cells were re-suspended in 6X proliferation media. Once suspended in the hydrogel and added to the scaffold, the filled scaffold was submersed in differentiation media. To determine differentiation, Alizarin Red (Lifeline Cell Technology, CM-0058) staining was conducted based on the following protocol from Lifeline Cell Technology:

1. Always wear eye protection and gloves when working with staining reagents.
2. Remove medium completely from well(s).
3. Gently, from the side of the well, add 1.0 mL PBS (CM-0001) (6-well).
4. Aspirate PBS.
5. Add 3 mL of absolute ethanol and fix for 30 minutes.
6. Remove ethanol and allow well(s) to dry completely.
7. Add 1.0 mL of 2% Alizarin Red Stain Solution (CM-0058) and gently tilt side-to-side until solution completely covers well.\*
8. Incubate for 15 minutes at room temperature

9. Remove Alizarin Red from the well(s).

10. Using care, rinse well(s) three times with 1.0 mL dH<sub>2</sub>O and allow to dry. Take extreme care when rinsing well or calcium crystals may be dislodged and rinsed away.

\*For 3D culture, the volume of Alizarin Red in step 7 was modified to 1.5 mL to submerge the gel within the scaffold.

#### **4.5.4 Hydrogel Synthesis**

##### *Fibrin*

Fibrin was synthesized using a 50:50 mixture of fibrinogen (Sigma, F8630) and thrombin (Sigma, T4648). After these two components were mixed, Fibrin crosslinked at room temperature. The fibrinogen and thrombin were synthesized using the following protocol:

HEPES buffered saline (HBS) preparation

1. Definition: HBS contains 20 mM HEPES and 0.9% (w/v) NaCl
2. Add the following reagents to 200 mL:
  - a. 2.25g of NaCl
  - b. 1.1915g of HEPES
3. pH solution to 7.4 using NaOH/HCl.
4. Bring final volume to 250 mL.
5. Store at room temperature.

Fibrinogen aliquots (70 mg/mL)

1. Measure 14.3 mL of HBS into a 50 mL conical tube.
2. Weigh 1.00 gram of fibrinogen and pour into conical tube.
3. Put conical tube on rocker plate, adjusting the position every 30-40 minutes until fibrinogen goes into solution.

**NEVER SHAKE/VORTEX FIBRINOGEN SOLUTION!!!! THIS WILL CAUSE FIBRINOGEN TO FALL OUT OF SOLUTION AND BIND TO ITSELF!!!!**

4. Incubate conical tube at 37 C overnight to ensure fibrinogen is completely dissolved.
5. The next morning, measure 1 mL aliquots in eppendorfs and store at -20 °C.

Thrombin aliquots (40 U/mL)

1. Add 25 mL HBS to bottle of 1KU thrombin, mix well.
2. Aliquot 200 µL into eppendorfs and store at -20 °C (Final concentration: 8U / 200 µL).

Before aliquoting the fibrinogen and thrombin, both components were filtered using 0.2 µm vacuum filter.

*PureCol EZ Gel*

PureCol EZ Gel (5074G, Advanced BioMatrix) was ready to use. During use, the product was kept on ice. To induce crosslinking the gel was incubated at 37° C until fully gelled.

*Alginate*

Alginate gels were synthesized at 2 wt%, 3 wt% and 4 wt% concentrations. Each solution was mixed into PBS and left on a rocker overnight. CaCl<sub>2</sub> was used as the crosslinking agent to crosslink the alginate immediately. A stock solution of 110 mM CaCl<sub>2</sub> was made by mixing powdered CaCl<sub>2</sub> in diH<sub>2</sub>O. This stock solution was diluted to 77 mM, 55 mM, and 33 mM to achieve the optimal gel consistency. The gel was allowed to crosslink for 2 minutes in the presence of CaCl<sub>2</sub>.

*Extracel*

Glycosil, Gelin-S, and Extralink were dissolved in DG Water (Glycosan Biosystems, G5208). The hydrogel was prepared following the Advanced BioMatrix protocol:

1. Allow the Glycosil, Gelin-S, Extralink, and DG Water vials to come to room temperature.
2. Under aseptic conditions, using a syringe and needle, add 1.0 mL of DG Water to the Glycosil vial. Repeat for the Gelin-S vial.
3. Place both vials horizontally on a rocker or shaker. It will take <30 minutes for the solids to fully dissolve. Warming to not more than 37 °C and/or gently vortexing will speed dissolution, Solutions will be clear and slightly viscous.
4. Under aseptic conditions, using a syringe and needle, add 0.5 mL of DG Water to the Extralink vial. Invert several times to dissolve.
5. As soon as possible, but within 2 hours of making the solutions, aseptically mix equal volumes of Glycosil and Gelin-S™. To mix, pipette back and forth slowly to avoid trapping air bubbles.
6. If encapsulating cells, resuspend cell pellet in 2.0 mL of Glycosil + Gelin-S. Pipette back and forth to mix.
7. To form the hydrogel, add Extralink to the Glycosil + Gelin-S mix in a 1:4 volume ratio (0.5 mL Extralink™ to 2.0 mL Glycosil + Gelin-S) and mix by pipette.
8. Gelation will occur within ~20 minutes

#### *Gel Mixtures - Fibrin-PureCol EZ Gel*

Different mixtures of Fibrin and PureCol EZ Gel were synthesized by mixing different proportions of the two materials. Because thrombin is the crosslinking agent in fibrin, thrombin was added last to ensure that crosslinking did not occur during the mixing process. The different ratios tested were 40% fibrin with 60% PureCol EZ Gel, a 50%/50% mixture of the two, and 60% fibrin with 40%

PureCol EZ Gel. These mixtures were tested to achieve optimal gel time and cell distribution throughout the suspension.

#### *Gel Mixtures - Fibrin-2% Alginate*

Fibrin and 2% alginate at a 50%/50% concentration were analyzed in order to find a hydrogel that best supported cell viability. The fibrin and 2% alginate were mixed and CaCl<sub>2</sub> was added immediately, at 2 minutes, or, at 4 minutes to allow the fibrin to crosslink prior to the immediate crosslinking of the 2% alginate. The hydrogel mixture was exposed to all four concentrations of CaCl<sub>2</sub> for 2 minutes regardless of when it was added.

#### *Gel Mixtures - Fibrin-PureCol EZ Gel-2% Alginate*

Based on the promising results seen with the fibrin-PureCol EZ Gel mixture as well as the positive aspects of the 2% alginate hydrogel, a mixture was created with all three materials. The solution used a 60% fibrin, 40% PureCol EZ Gel mixture that made up 50% of the final mixture, with 2% alginate accounting for the other 50%. This hydrogel was exposed to all four concentrations of CaCl<sub>2</sub> for 2 minutes.

### **4.5.5 Hydrogel Cell Suspension**

In a 96-well plate, preliminary tests used 16.8 μL of cells at a density of 120,000 cells/well. This was added to 53.2 μL of hydrogel to result in a 70 μL cell suspension. A second experiment was conducted using 183.2 μL of hydrogel to yield a 200 μL suspension. The suspension was mixed by pipetting up and down several times to achieve a uniform cell distribution prior to seeding into the well. After gelation was completed, gels were examined for uniform cell distribution and shrinkage.

### **4.5.6 PDMS Fabrication**

PDMS was fabricated using a Sylgard 184 Silicone kit (Dow Corning) following these steps:



1. Pour 3g of the silicone elastomer base into a medium sized octagonal weigh boat. It will coat the bottom
2. Add 0.3g of the silicone elastomer crosslinking agent
3. Mix well using a tongue depressor
4. Place weigh boat in vacuum chamber for ~20 minutes to remove all bubbles in liquid PDMS
5. Transfer weigh boat to oven and bake at 65° C for eight hours

#### **4.5.7 Sterilization Technique for Scaffolds**

1. Place the scaffold in a fresh plate\*
2. Submerge the scaffold in ethanol 200 for 10 minutes under UV exposure
3. Using sterile forceps, remove the scaffold and aspirate excess ethanol clinging to the scaffold
4. Transfer the scaffold to a fresh plate\*
5. Expose to UV light for 10 minutes
6. Remove from UV exposure

\*Depending on the size and quantity of scaffolds being sterilized, plates of different quantities may be used.

#### **4.5.8 Lattice Design Seeding**

PVA-PLA combination scaffolds and PLA-only scaffolds were placed in 24-well plates and sterilized following the protocol in 4.5.7 Sterilization Technique for Scaffolds. Scaffolds were then seeded with a hydrogel suspension following the hydrogel suspension protocol for the 200  $\mu$ L hydrogel suspension.

#### **4.5.9 Threaded PLA Design Seeding**

The threaded PLA scaffolds were placed in 24-well plates and sterilized following the protocol in 4.5.7 Sterilization Technique for Scaffolds. PDMS cured previously was also sterilized. Small PDMS caps were cut and threaded with collagen, vicryl, and silk sutures. The sutures were sewn through the holes in the bottom of the scaffolds and back up through the PDMS cap to hold the sutures in place. The scaffolds were then filled with a 650  $\mu$ L hydrogel cell suspension with a cell density of 700,000 cells/scaffold for preliminary testing due to cell sourcing. Final testing and validation was conducted at a cell density of  $4.5 \times 10^6$  cells/scaffold.

#### **4.5.10 Cell Viability Testing**

Hoechst 33342 and Propidium Iodide live/dead staining was done to determine cell viability within the hydrogels in the scaffold design using the following protocol:

1. Aspirate media
2. Wash 3x with DPBS(+)
3. Add 1.5 mL proliferation media
4. Add 1.2  $\mu$ L Hoechst 33342 at 2 mg/mL
5. Incubate for 30 min
6. Wash 3x with DPBS (+)
7. Add 1.5 mL proliferation media
8. Add 1.2  $\mu$ L Propidium Iodide at 375  $\mu$ M/mL
9. Incubate for 3 minutes
10. Wash 3x with DPBS (+)
11. Image with fluorescent microscope

Calcein AM live staining was conducted on the 4% alginate crosslinked with 77 mM CaCl<sub>2</sub> to show cell viability using the following protocol based on the following Novamatrix 3-D alginate live stain protocol:

1. Aspirate media
2. Wash 3x with DPBS(+)
3. Add 1.5 mL DPBS(+)
4. Add 3  $\mu$ L Calcein at 2  $\mu$ M concentration
5. Incubate for 30 minutes in a dark area at room temperature
6. Wash 3x with DPBS(+)
7. Image with fluorescent microscope

## Chapter 5 Experimental Results

### 5.1 ATDC5 Cell Culture

The population doubling level was determined to be 0.59 doublings/day as shown in Table 5 and Figure 10.

Table 5: PDL Study of ATDC5 Cells

Date	Day Started	Days after Sub	Initial Counts	Final Counts	PDL
21-Sep	0		500000	4200000	3.069
25-Sep	0	4	500000	4087500	0.757
25-Sep	0	4	500000	2637500	0.599
30-Sep	0	5	1000000	8112500	0.604
30-Sep	0	5	1000000	7400000	0.577
30-Sep	0	5	1000000	8800000	0.627
30-Sep	0	5	1000000	8000000	0.600
5-Oct	0	5	500000	3825000	0.587
5-Oct	0	5	500000	3950000	0.596
5-Oct	0	5	500000	2637500	0.480
5-Oct	0	5	500000	2987500	0.515
		<b>Average:</b>	<b>681818</b>	<b>5148864</b>	<b>0.594227</b>

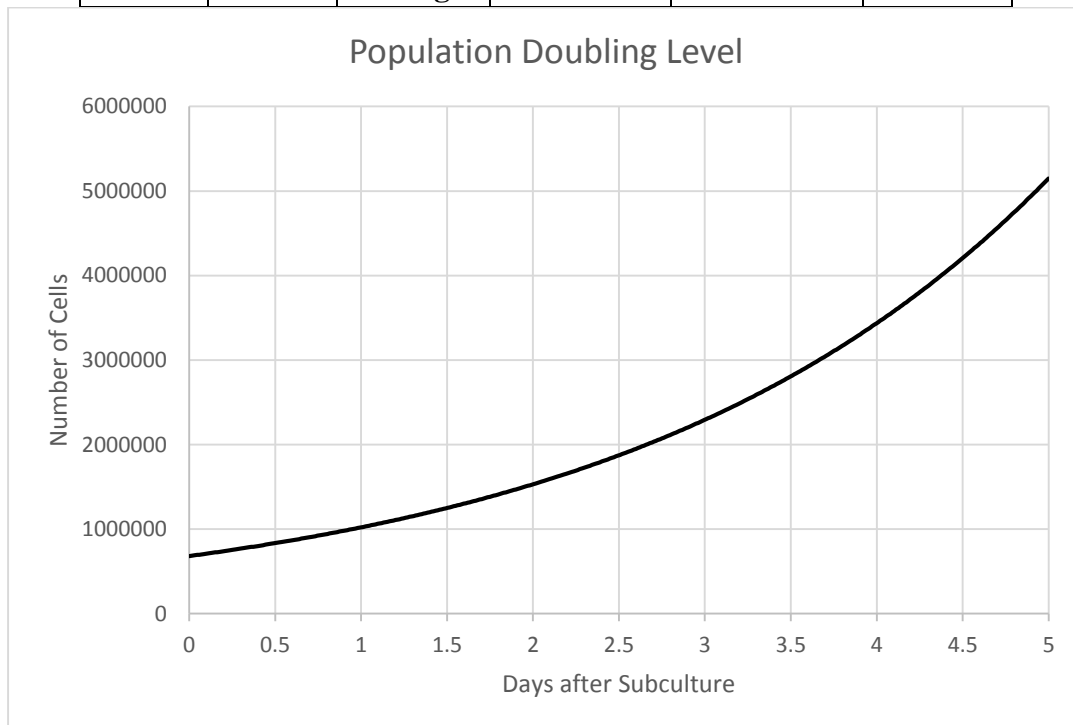


Figure 10: Graph of PDL Study of ATDC5 Cells

## 5.2 Cell Differentiation in 2D Culture

The images for Alizarin Red staining after four weeks can be seen in Figure 11. The most effective media for differentiation utilized the cell proliferation media described previously supplemented with ascorbic acid and insulin, achieving differentiation in fourteen days. The most effective concentration of FBS for 2D culture was 3%.

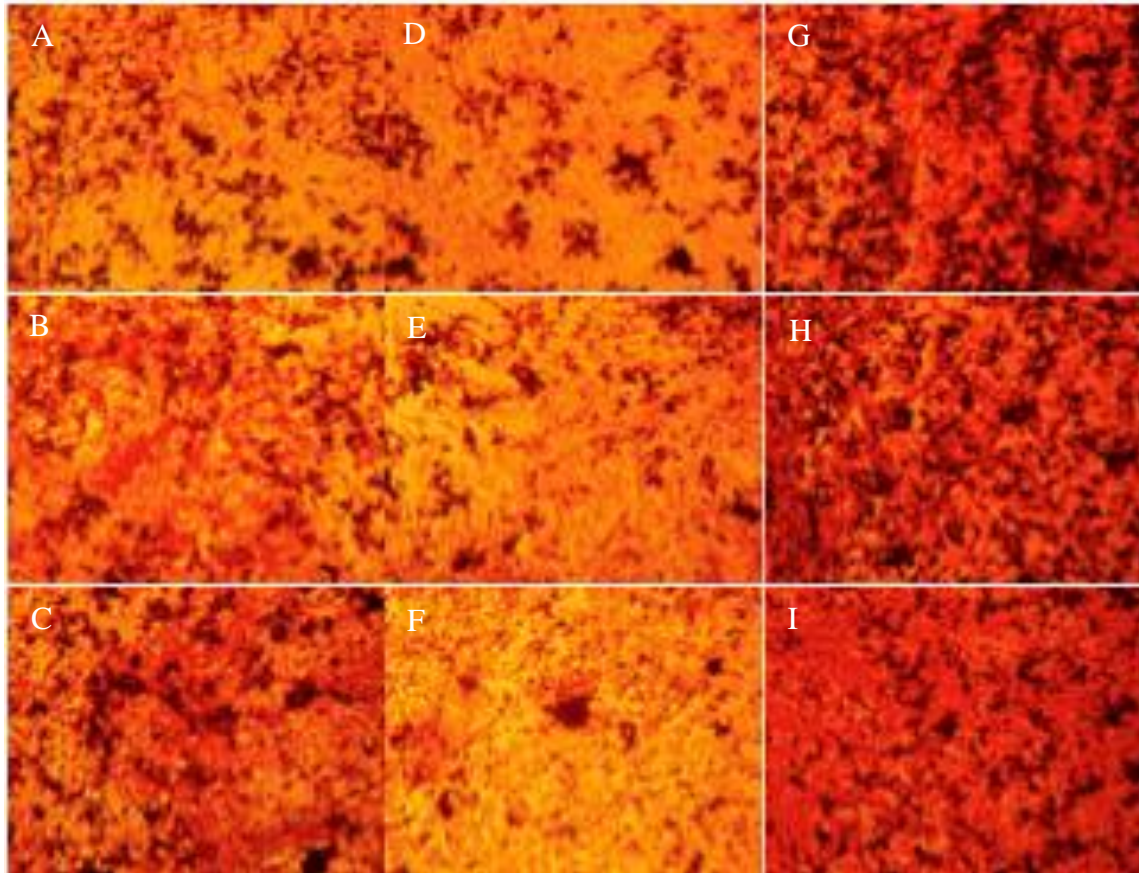
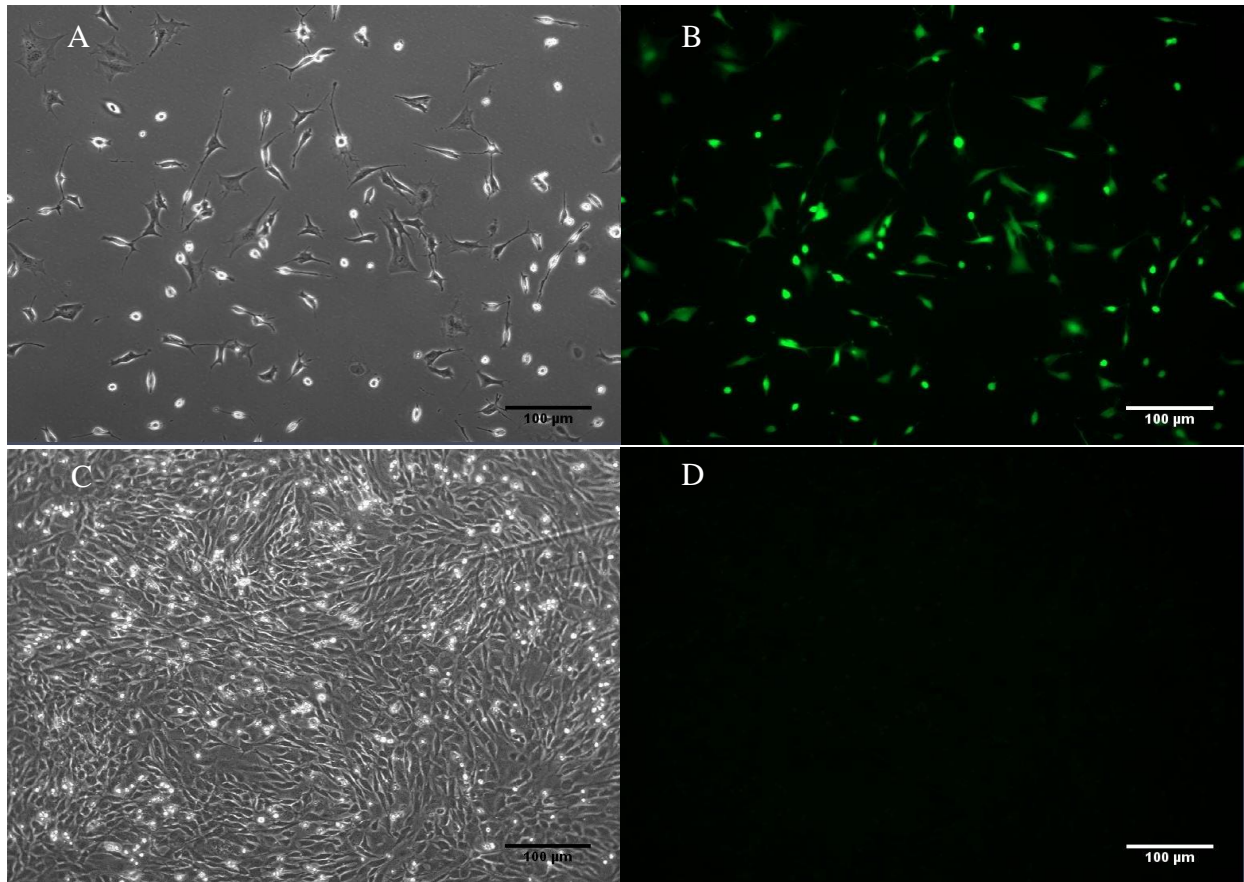


Figure 11: 2D Alizarin Red Staining at 4 Weeks

From top to bottom each column represents 2%, 3%, and 5% FBS concentrations. The dark blotches in each picture are calcium deposits. Column 1, A-C) Cells in proliferation media supplemented with insulin showed an increase in cell ECM. Column 2, D-F) Cells in proliferation media with ascorbic acid had a shrunken morphology and a small amount of calcium deposits. Column 3, G-I) Cells in proliferation media supplemented with both insulin and ascorbic acid showed a higher amount of calcium deposits than just insulin or ascorbic acid.

## 5.3 Calciin AM Live Cell Staining

A plate of live cells and a plate of fixed cells were stained with Calciin AM live stain. As shown in Figure 12, the live cells fluoresced while the fixed cells did not.



*Figure 12: Calcien AM Feasibility Study Results*

*All cells were stained with Calcien AM using the same protocol. The cells in the C and D were fixed with ice cold methanol for 10 minutes prior to staining. Image A is a phase contrast image of live cells. Image B shows the same cells, stained with Calcien AM, imaged with fluorescent microscopy. Image C is a phase contrast image of the fixed cells. Image D shows the same cells, stained with Calcien AM, imaged with fluorescent microscopy.*

### **5.3 Hydrogels**

Based on gelation time, the degree of cell dispersal, cell viability and the amount of shrinking, 4% alginate was chosen to culture and differentiate ATDC5 cells in the final scaffold design. To best avoid gel shrinking 77 mM CaCl<sub>2</sub> was used to crosslink. The experimental data was compiled in Table 6. The results from the mixtures of fibrin, PureCol EZ Gel and alginate are not included in Table 6 because the mixtures did not crosslink into a cohesive gel. The alginate shrinking was the most significant when it occurred therefore additional qualitative testing was done as seen in Figure 13.

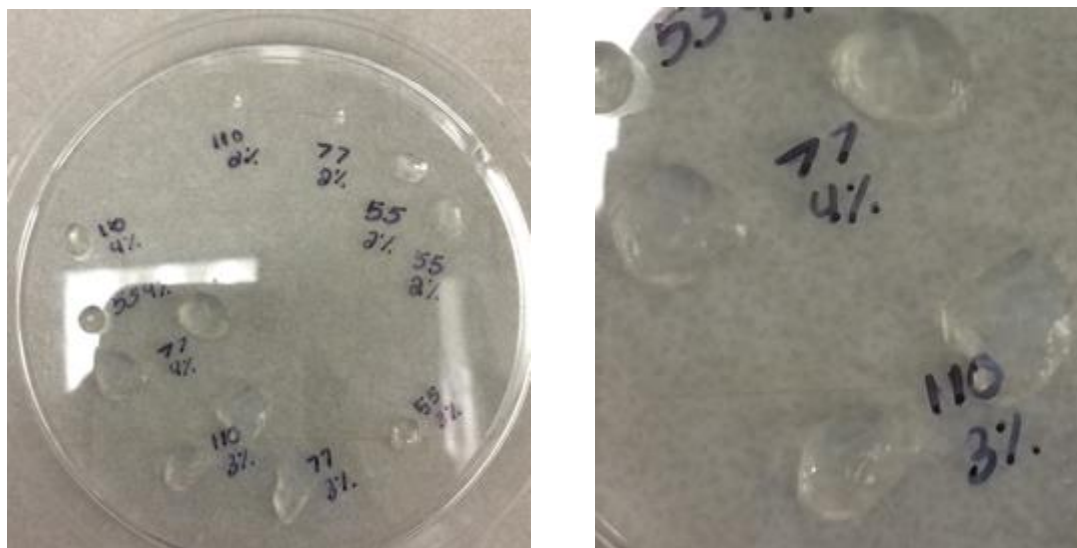


Figure 13: Alginate Shrinkage Testing

Alginate was determined to have the least amount of shrinkage with 4% alginate and 77mM CaCl<sub>2</sub>.

Table 6: Hydrogel Experimental Results

Cell dispersal and cell viability were assessed using confocal microscopy. All gels were seeded with 60,000 cells.

	Gel Time (min)	Cell Dispersal	Cell Viability	Gel shrinking			
<b>PureCol EZ Gel</b>	90+	Poor	Acceptable	Yes			
<b>Fibrin</b>	1.5	Acceptable	Acceptable	Yes			
<b>PureCol EZ Gel-Fibrin (60%-40%)</b>	50	Poor	Acceptable	Yes			
<b>PureCol EZ Gel - Fibrin (50%-50%)</b>	10	Poor	Acceptable	Yes			
<b>PureCol EZ Gel -Fibrin (40%-60%)</b>	4	<b>Excellent</b>	<b>Excellent</b>	Yes			
<b>Extracel</b>	7	<b>Excellent</b>	Poor	No			
<b>CaCl<sub>2</sub> Concentrations (mM)</b>				33	55	77	110
<b>2% Alginate</b>	<1	Acceptable	<b>Excellent</b>	No	Yes	Yes	Yes
<b>3% Alginate</b>	<1	Acceptable	<b>Excellent</b>	No	Yes	Yes	Yes
<b>4% Alginate</b>	<1	<b>Excellent</b>	<b>Excellent</b>	No	No	No	Yes

#### 5.4 Differentiation in 3D Hydrogel

Based on the hydrogel experimental results, 4% alginate crosslinked with 77 mM CaCl<sub>2</sub> was the hydrogel used for differentiation experimentation. Additionally, 40%-60% PureCol EZ Gel-Fibrin was tested for comparison. Each of these were tested with different cell densities of 10,000 cells/well, 30,000 cells/well, and 60,000 cells/well as seen in Figure 14. Based on these images, calcium deposits were observed regardless of cell density. In both gels calcium deposits were



observed at seven days. Alginate was shown to have a better retention of the calcium deposits when compared to the PureCol EZ Gel and fibrin gel.

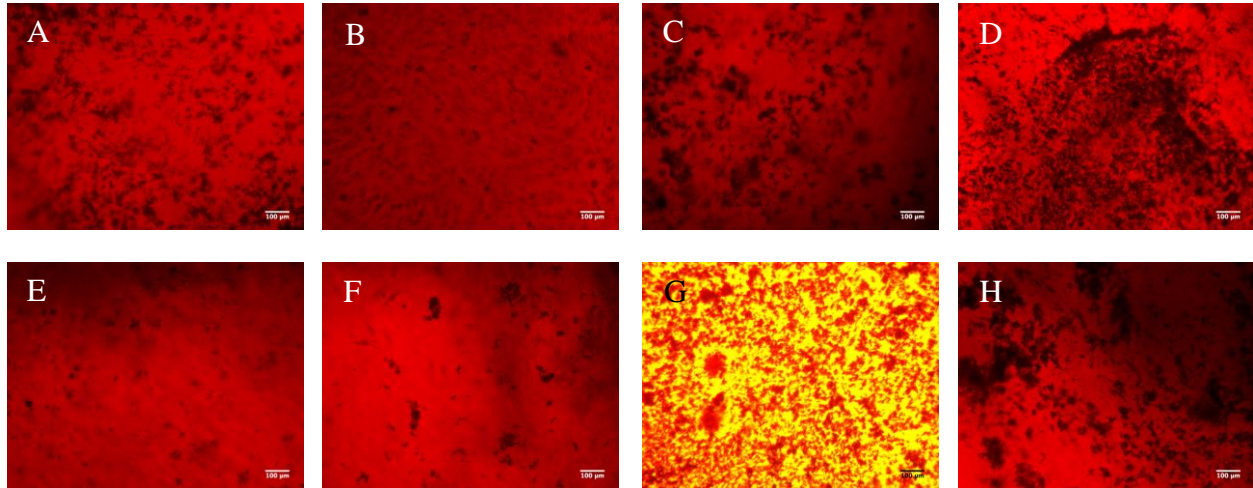


*Figure 14: Differentiation Comparison of Alginate and Fibrin- PureCol EZ Gel*

*Top row: 4% alginate gel crosslinked with 77 mM CaCl<sub>2</sub> for 2 minutes. Bottom row: 60% Fibrin and 40% PureCol EZ Gel mixture. Both rows from left to right are 10,000 cells, 30,000 cells, 60,000 cells, and 100,000 cells. Differentiation occurs regardless of cell density. The calcium deposits settled to the bottom of the fibrin and PureCol EZ Gel mixture and in G the gel was completely missing.*

## **5.5 PLA-PVA Dual Extruded Scaffold Results**

The scaffold that incorporated PLA with a PVA lattice work exhibited significant swelling during PVA degradation shown in Figure 15. Based on this result a swelling study was conducted with PVA as seen in Figure 16. ImageJ was used to measure the PVA at time points of 0, 15, and 30 minutes. The averaged observed swelling reached a maximum width of 0.83 mm and the average swelling rate was 0.03 mm/minute. During its degradation the PVA, absorbed the hydrogel and carried the material out of the scaffold during its swelling and dissolution. Minimum cell viability was observed using Hoechst 33342 and Propidium Iodide live/dead counter staining.





Figure 15: PVA Swelling out of a Scaffold  
PVA swelled during degradation to the point that it is extruding the hydrogel cell suspension.

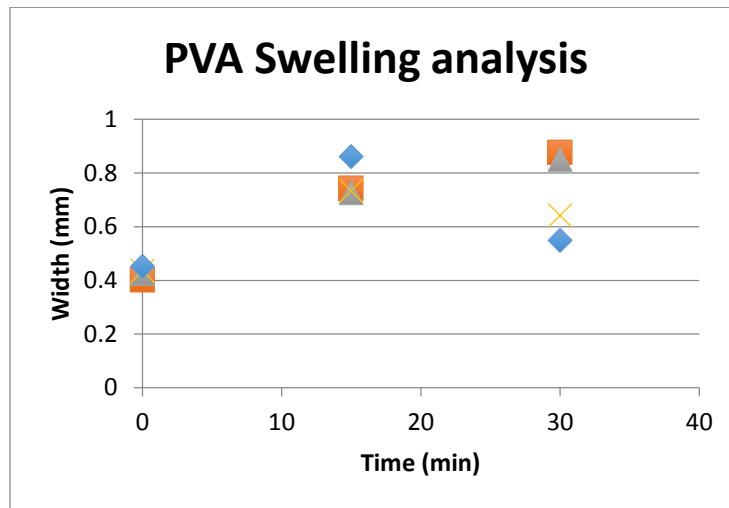


Figure 16: PVA Swelling Study

### 5.6 PLA-only Scaffold Results

Compared to the PVA lattice scaffold, better cell viability was observed in the PLA-only lattice, however, it did not aid in cell orientation as expected. A degradation study of the material showed that PLA would not degrade on a timeline conducive for the purposes of this project as shown in Table 7. The scaffolds were baked in an oven for one hour at 65° C to ensure the scaffolds were completely dry. Degradation was assessed by measuring the mass of the scaffolds before and after incubation.

Table 7: PLA Degradation Study

Week 1	
Initial weight (g)	After drying (g)
0.218	0.218
0.219	0.218
0.217	0.218
Week 2	
Initial weight (g)	After drying (g)
0.220	0.222
0.223	0.224
0.213	0.215
Week 3	
Initial weight (g)	After drying (g)
0.221	0.222
0.219	0.219
0.215	0.213

### 5.7 Threaded PLA Scaffold Results

Three iterations of the threaded scaffold can be seen in Figure 17. The different architectures were analyzed for ease of threading and seeding. The small scaffold with two holes and a PDMS cap was the easiest to thread and seed. During validation testing this design offered the best optical clarity for visualizing results. The silk and Vicryl sutures were both observed to have braided structures while the collagen suture was a single thread. Within the hydrogel, cells that were in direct contact with the silk and Vicryl sutures were not viable. Cells in direct contact with the collagen suture remained viable.



*Figure 17: Different Threaded PLA Scaffold Designs*

*From left to right, large diameter scaffold with small holes, large diameter scaffold with 6 holes, small diameter scaffold with two holes.*

## Chapter 6 Final Design Validation

Based on preliminary results the two hole threaded PLA scaffold incorporating collagen sutures through a PDMS cap was tested for further proof of concept that the scaffold would enhance nutrient perfusion and support cell viability, proliferation, and differentiation.

### 6.1 Cell Viability

Cell viability was analyzed using a Calcein AM live stain (C3100MP, Life Technologies). The staining was conducted on threaded scaffolds and control scaffolds without threads on day 7. The scaffolds were seeded with 4% alginate crosslinked with 77 mM CaCl<sub>2</sub> for 2 minutes at a cell density of 4.5\*10<sup>6</sup> cells each. Comparing the two images in Figure 18 showed that the threads were able to increase nutrient perfusion and maintain cell viability over the course of 7 days. Cell viability was not numerically analyzed due to lack of appropriate equipment.

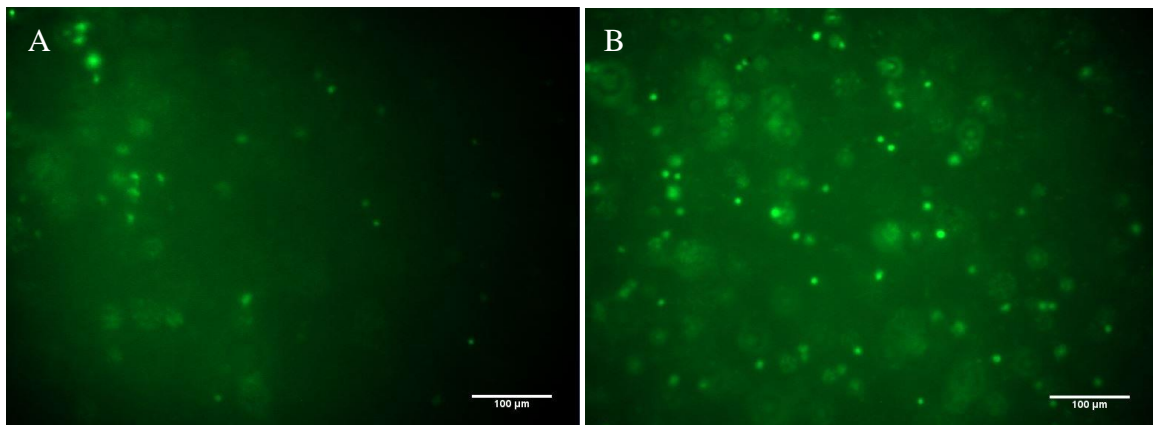


*Figure 18: Calcein AM Live Staining for Cell Viability*

*A) Cell viability in the center of a control scaffold without threads at day 7. B) Cell viability at the center of a threaded scaffold at day 7.*

## 6.2 Cell Proliferation

Calciem AM live stain was used to show living cells in a threaded scaffold at day 1 and a threaded scaffold at day 7. The resulting images in Figure 19 showed an increase in the number of cells at the center of the scaffold on day 7 versus day 1. These were not assessed qualitatively due to lack of appropriate equipment.

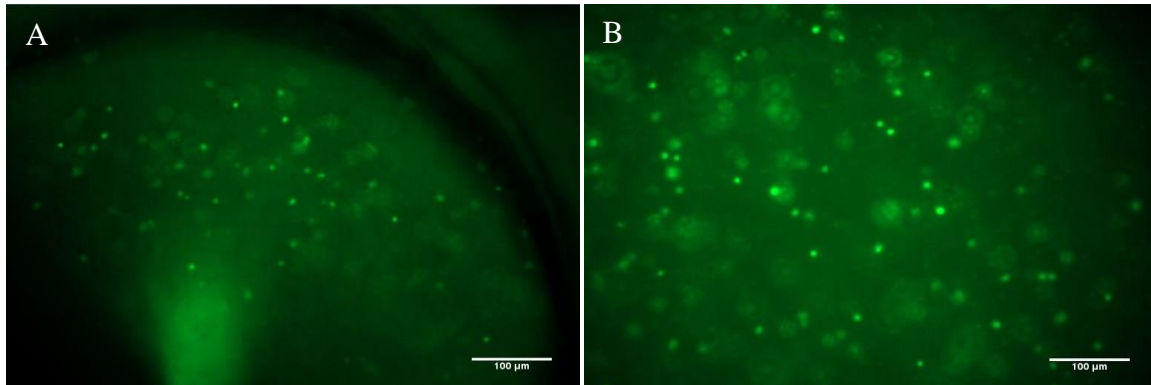


Figure 19: Calciem AM Live Staining for Cell Proliferation  
A) Cells in the center of a threaded scaffold at day 1. B) Cells at the center of threaded scaffold at day 7.

## 6.3 Cell Differentiation

Alizarin red staining was used to stain calcium deposits generated during differentiation. After being exposed to differentiation media for 7 days a threaded scaffold was stained along with a control threaded scaffold in proliferation media. Calcium deposits were visible in the scaffold that had been exposed to differentiation media but not in the control as shown in Figure 20.

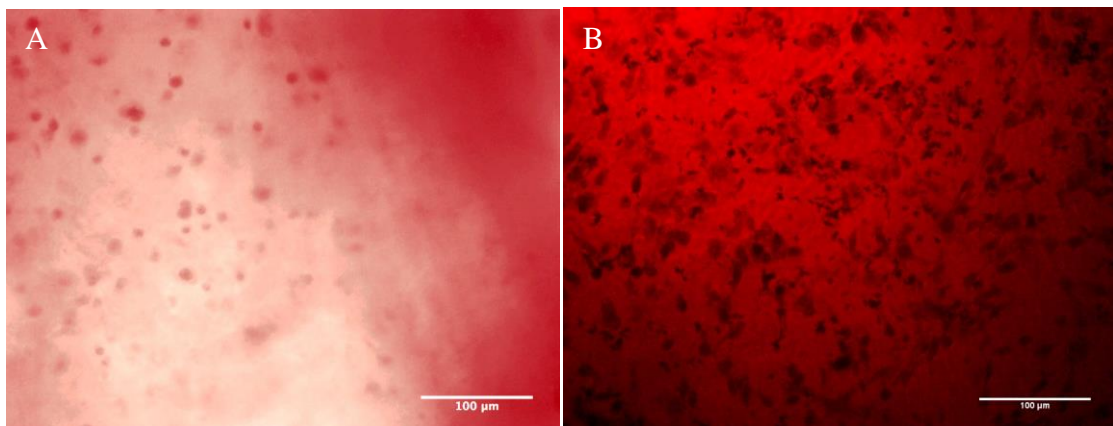


Figure 20: Alizarin Red Staining for Calcium Deposits  
A) Control scaffold cultured in proliferation media with no calcium deposits at day 7. B) Threaded scaffold at day 7 with calcium deposits present at different levels in the gel.

## Chapter 7 Discussion

Our experimental results show that cells are able to survive in a 3D environment at a depth deeper than the physiological limit to nutrient perfusion. This finding means that the scaffold is able to maintain cell viability, proliferation, and differentiation beyond the capabilities of the body.

### 7.1 Objectives Tree Assessment

The original objectives tree, depicted in Figure 6, has been marked to reflect accomplished objectives in Figure 21.

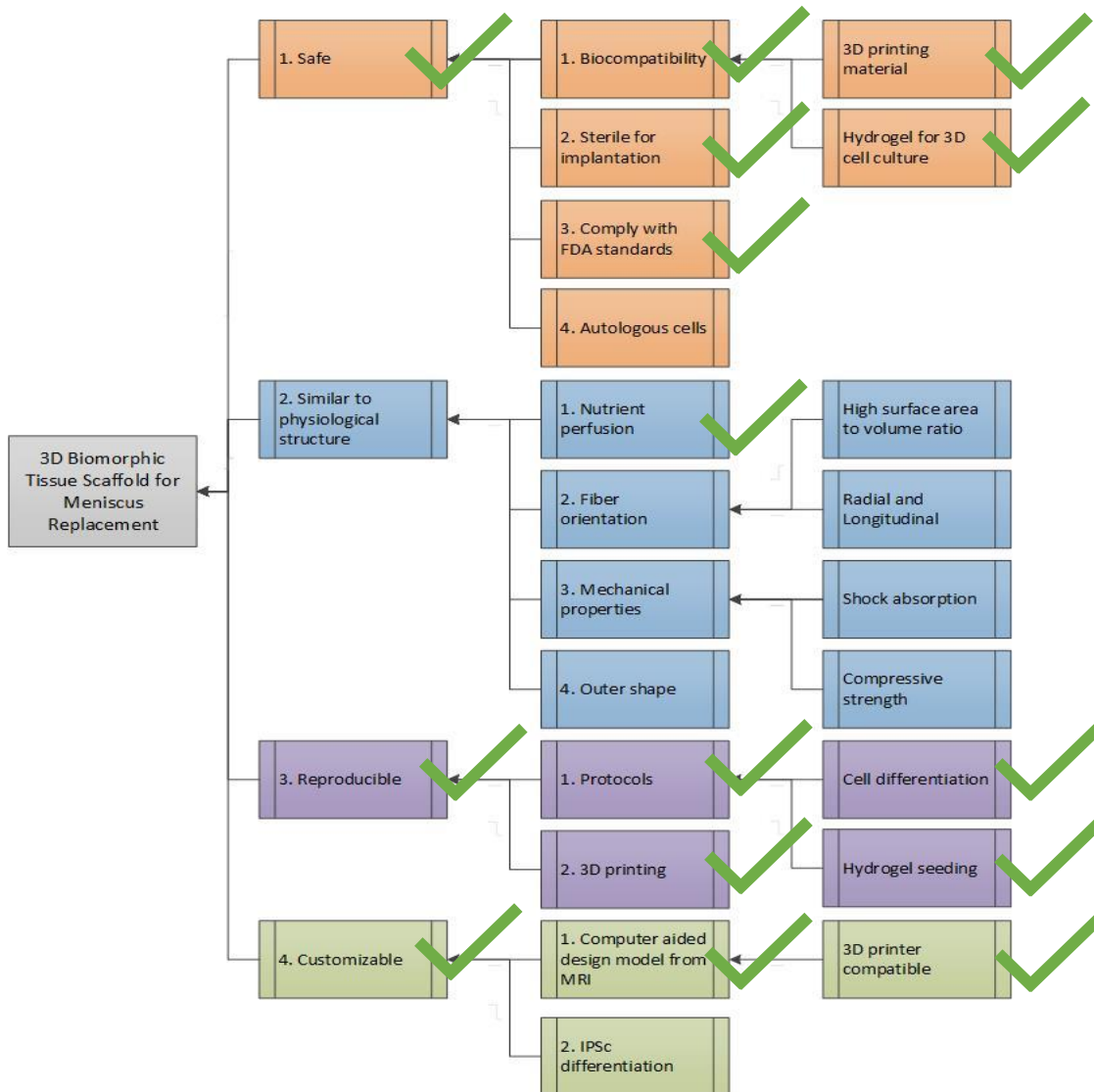


Figure 21: Objectives Tree Assessment

## **7.2 Safe**

A primary concern of this project was that the final product be safe for use in a clinical setting. To accomplish this only FDA approved materials were used. PLA is an FDA approved material, as is alginate, and the collagen threads used were surgical grade plain catgut sutures. However, in a clinical setting, none of these materials would come into contact with the patient as the replacement tissue would be grown *ex vivo* in the scaffold, but the implanted product would be made entirely of cells. In the case of a meniscus implant specifically, the cells used may be sourced from an existing human chondrogenic cell line. Additionally, a sterilization protocol was established to reduce the risk of scaffold contamination.

## **7.3 Similar to Physiological Structure**

During the course of this project the creation of a biomorphic scaffold could not be accomplished. The scope of the project changed so that the main challenge being addressed was the natural nutrient perfusion limit of 100  $\mu\text{m}$ . In order to devote more time to overcoming this challenge, the objectives associated with biomorphology were suspended. Based on the proof of concept provided by this project, the fabrication of a functional biomorphic scaffold is recommended for the future.

## **7.4 Reproducible**

The fabrication of the PLA scaffold is an extremely reproducible process. The 3D printer used can be purchased commercially and the G-code generated for the printer listed in 'Appendix E: G-code of Final Design' can be used to print the scaffold designed. Because there are only two holes in the bottom of the scaffold there is very little variability that can be introduced during the threading step of the fabrication. The step with the most potential for variation between users was the suspension of the cells in the hydrogel system. This step requires pipetting the cell suspension up

and down and depending on the person pipetting, this step can affect initial cell distribution throughout the scaffold.

## **7.5 Customizable**

The scaffold was designed to be printed with the Monoprice Dual Extrusion 3D printer, and should be printable on any printer with the same printing specifications. As the modeling of the scaffolds was completed in SolidWorks the scaffold may be changed and customized easily by a user with SolidWorks experience. In a clinical setting, MRI images may be used to create the scaffold morphology in order to create patient specific scaffolds to ensure that the implantable product fits each patient's affected area. In some settings the use of iPSCs may be necessary, depending on the immunogenicity of the area. However, when dealing with the meniscus specifically, the use of iPSCs are not necessary as the knee is an immune privileged area

## **7.6 Economic Impact**

Using a low-cost commercially available 3D printer and open source modeling program an effective tissue scaffold was successfully fabricated. By combining this scaffold with inexpensive materials such as alginate and plain collagen sutures the overall costs with this project were relatively low. The low budget necessary for this project may open up the opportunity for other research labs to utilize similar technologies.

## **7.7 Environmental Impact**

This project did not have any additional environmental impact beyond that of tissue engineering. The field of tissue engineering normally generates a significant amount of plastic waste in the form of the tissue culture petri dishes and pipette tips used during routine procedures. The materials used for the purposes of this specific project (PVA, PLA, collagen, alginate, etc.) are all naturally



biodegradable. Potential environmental improvements for this project would be to use recyclable materials for the routine laboratory procedures.

### **7.8 Societal Influence**

The most significant challenge overcome by this project was the natural nutrient perfusion limit within the body of 100  $\mu\text{m}$ . Using the research conducted during the course of this project, other labs may be able to successfully engineer full avascular tissues. The creation of these tissues have the potential to lead to improved quality of life for patients with cartilage injuries and/or degenerative bone disease.

### **7.9 Political Ramifications**

The political ramifications of this project at its current scope are minimal. However, if the project were to be advanced into a clinical setting the use of a human cell line or induced pluripotent stem cells could generate political friction due to the controversy associated with those aspects of biology.

### **7.10 Ethical Concerns**

Any ethical concerns with this project are concerns with the field of tissue engineering in general. There are ethical considerations that must be made when engineering tissues for the human body. However, at the project's current level with the use of mouse chondrogenic cells, these concerns were not a priority.

### **7.11 Health and Safety Issues**

Currently there are not health and safety issues with this project. However, if this project were to progress to the clinical level possible issues include the mechanical integrity of the tissue when

implanted, the interface between the engineered cartilage and the surrounding tissue, as well as any potential immune responses the body may have in an area that is not immune privileged.

### **7.12 Manufacturability**

The manufacturability of the scaffold was a primary consideration throughout the course of this project. The scaffold was designed such that the Monoprice Dual Extrusion 3D printer was capable of printing it. The printer utilizes a software called ReplicatorG which can import and convert files directly from SolidWorks, a modeling software that is commonly used in the industry setting. The threaded designs required more manual assembly as the thread had to be sewn through the PDMS cap and scaffold. However, this process can likely be automated, allowing the entire fabrication time to be scaled up significantly.

### **7.13 Sustainability**

As mentioned in 7.7 Environmental Impact, this project did not have a large environmental impact and did not require the use of limited resources. The largest sustainability issue would come from the basic laboratory supplies, but that may be overcome by streamlining the fabrication process.

## **Chapter 8 Conclusion and Recommendations**

We conclude that this system supports cell viability and differentiation in scaffolds that allow nutrient perfusion that are orders of magnitudes greater than the perfusion limits seen *in vivo*. Once further developed, this system holds promise for developing engineered meniscal tissue to replace damaged menisci.

### **8.1 Conclusions**

One of the greatest challenges in tissue engineering is generating tissue at sizes and depths which can be clinically applicable for implantation into the body (Costa-Almeida *et al*, 2014). The team's design of a 3D printed tissue scaffold was able to perfuse nutrients to depths significantly greater than the natural perfusion limit in the body. The team proved the hypothesis that the formation of channels through the hydrogel, in the scaffold, would improve cell viability in the center of the hydrogel, avoiding the formation of a necrotic.

Additionally, the team found after testing many iterations of different hydrogel concentrations and mixtures that a 4% alginate hydrogel cross-linked with 77 mM was the most effective hydrogel for the system. This hydrogel offered the best cell distribution and gel time to ensure cell layering throughout the entire depth and height of the scaffold. The hydrogel was also effective for cell viability both alone in a gel and in the scaffold system.

Differentiation in the 3D environment was found to occur more quickly than in the 2D cultures. Alizarin red staining for calcium deposits revealed that the ATDC5 cells in 3D differentiated after one week in media supplemented with insulin and ascorbic acid. In the 2D cultures, cells in the same media took two weeks to differentiate and generate comparable calcium deposits.

Finally, the experiments conducted with PVA as a scaffolding material revealed that PVA is not an applicable degradable material for use in this hydrogel system. The swelling induced as the PVA degrades expels the hydrogel and cells, making the material useless.

## **8.2 Recommendations**

Based on the results of the project, the team has several recommended areas for future research. The project was limited in time and other resources, which made certain goals unrealistic for the team to complete throughout the course of the project, however, these recommendations are still valuable for continued research. The recommended areas of research are to make the scaffold biomorphic, to mechanically condition the tissue during culture, and to use a proper human cell line for the scaffold.

### **8.2.1 Biomorphic**

For experimentation and proof of concept purposes, the scaffolds designed and tested in the project were cylindrical and 6.2 mm in diameter. These sizes were ideal for testing, however, they are not applicable for use in human transplantation. For future research, designing a scaffold model that mimics the geometric shape of the meniscus would be more appropriate. Additionally, situating the degradable collagen sutures in the same radial and longitudinal orientation naturally found in the meniscus could help with cell alignment and mechanical stability.

### **8.2.2 Mechanical Attributes**

The primary focus of the project was to overcome the natural perfusion limit in the body and generate living tissue at a clinically applicable depth without the development of a necrotic core. Another important consideration is the mechanical conditioning of the tissue to ensure the cells are appropriately prepared for the harsh environment of the knee. Culturing the system in a bioreactor equipped with an actuator and load cells would allow for proper cyclic loading during

the tissue growth. Cyclic loading of the cells and scaffold would influence the formation of proper fibers oriented through the meniscus and aid in the creation of a stable extracellular matrix able to support the weight and movement of each patient (Popp *et al*, 2012).

### **8.2.3 Cell Selection**

For the purposes of the project, mouse ATDC5 cells were tested as a model system. In order to apply the cartilage scaffold to human patients, a human cell line would need to be researched. An appropriate cell line for human application would be the H9 human chondrogenic cell line. These cells could be used for testing purposes and then, in a clinical setting, used as a source for human implantation.

### **8.2.4 Clinical Application**

In order to apply the nutrient enhancing cartilage tissue scaffold to a clinical setting, some scaling would have to occur. The following steps diagramed in Figure 22 outline how the team's proof of concept could be utilized for implantation into a human patient:

*Step 1:* The entire process would be conducted in a bioreactor to mechanically stimulate the cells to ensure they can develop the proper mechanical stability. The cells could be tuned to a patient specific mechanical strength.

*Step 2:* Human chondrocyte precursor cells would be cultured and maintained. This would allow cells to be available for use at any time.

*Step 3:* The cells would then be suspended in a 4% alginate gel.

*Step 4:* An MRI image of a patient's knee would be used to create a 3D model of the injured area of the patient's meniscus. This model would then be modified to include the holes necessary for threading. This scaffold would be 3D printed in PLA.

Step 5: The 3D printed scaffold would be covered with a cap and threaded in the same manner described in

#### 4.3.3 Threaded PLA Scaffold.

Step 6: The now threaded meniscus scaffold would be filled with the 4% alginate cell suspension and crosslinking would be induced using 77 mM CaCl<sub>2</sub> for two minutes.

Step 7: Cells would be allowed to proliferate in the meniscus scaffold until an appropriate cell density was reached.

Step 8: Once an appropriate cell density was reached, differentiation media would be added to the meniscus scaffold.

Step 9: After significant differentiation, the scaffold would be filled with living tissue and the alginate gel would be mostly, if not completely degraded.

Step 10: The tissue would be removed from the scaffold leaving a final product ready for implantation.

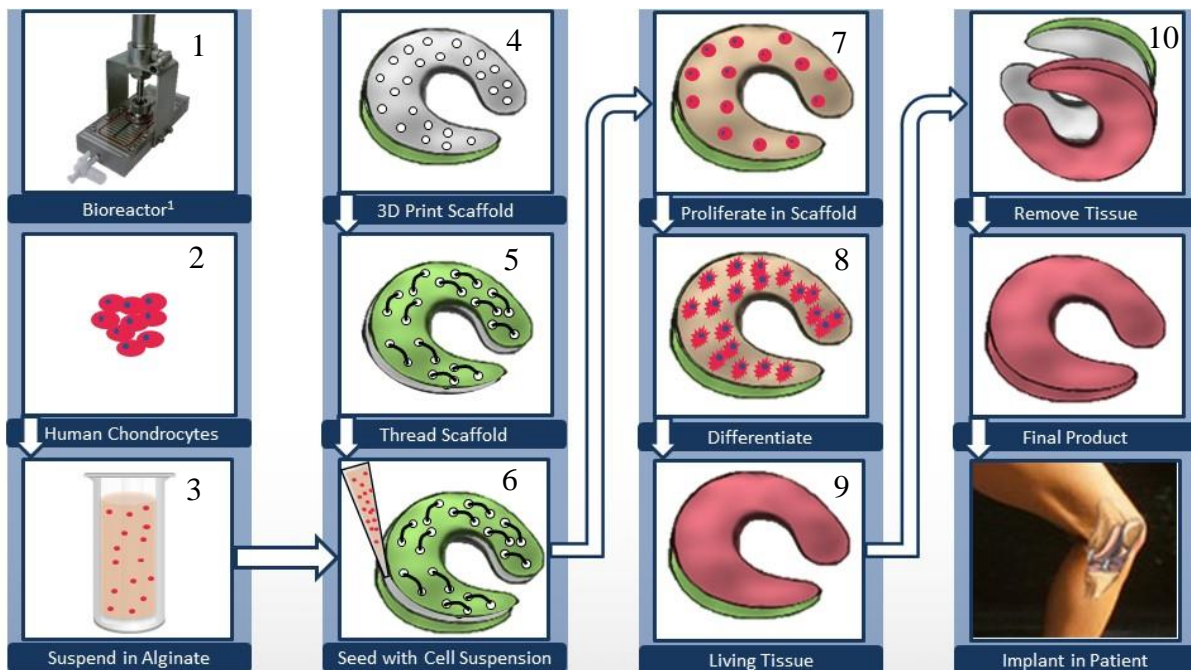


Figure 22: Concept Diagram of Clinical Application  
Clinically applicable use of a nutrient perfusion enhancing meniscus scaffold. Each step is labeled by number.

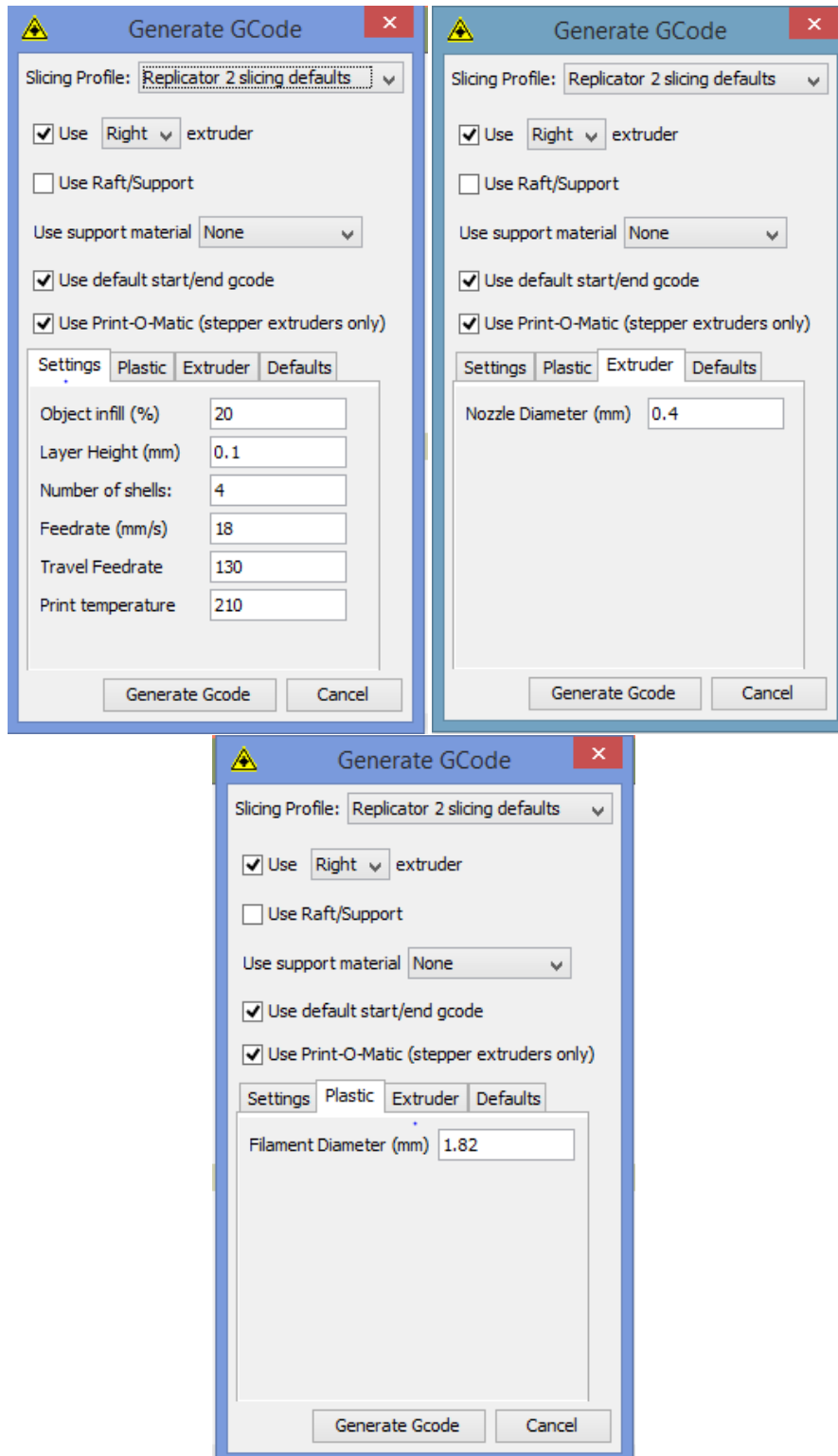
## Bibliography

- Baek, J., Jin, S., Sovani, S., Chen, X., D'Lima, D., & Grogan, S. (2014). Meniscal Tissue Engineering: Cell Encapsulation of Electrospun Collagen.
- Beaufils, P., & Verdonk, R. (2010). *The Meniscus*. Heidelberg: Springer-Verlag.
- Buckwalter, J. A., Einhorn, T. A., Simon, S. R., & Surgeons, A. A. o. O. (2000). Orthopaedic Basic Science: Biology and Biomechanics of the Musculoskeletal System: American Academy of Orthopaedic Surgeons.
- Buschmann, M. D., Gluzband, Y. A., Grodzinsky, A. J., Kimura, J. H., & Hunziker, E. B. (1992). Chondrocytes in agarose culture synthesize a mechanically functional extracellular matrix. *J Orthop Res*, 10(6), 745-758.
- Carmeliet, P., & Jain, R. K. (2000). Angiogenesis in cancer and other diseases. *Nature*, 407(6801), 249-257.
- Chadwick, Kellie, Manning, Kali, Skende, Johan, Walker, Sarah. (2013). Design and Fabrication of Biomorphic Scaffolds for Tissue Regrowth by 3D Printing, Worcester Polytechnic Institute.
- Chan, B. P., & Leong, K. W. (2008). Scaffolding in tissue engineering: general approaches and tissue-specific considerations *Eur Spine J* (Vol. 17, pp. 467-479).
- Costa-Almeida, R., Granja, P. L., Soares, R., & Guerreiro, S. G. (2014). Cellular strategies to promote vascularisation in tissue engineering applications *Eur Cell Mater* (Vol. 28, pp. 51-66; discussion 66-57). Scotland.
- DeCeuninck, F., Lesur, C., Pastoureau, P., Caliez, A., & Sabatini, M. (2004). Culture of chondrocytes in alginate beads. *Methods Mol Med*, 100, 15-22.
- Drosos, G.I. & Pozo, J.L. The causes and mechanisms of meniscal injuries in the sporting and non-sporting environment in an unselected population. *The Knee*. April 2004. Vol. 11 Iss. 2 p. 143-149
- Fox, A.J.S., Bedi, A., & Rodeo, S. A. (2009). The Basic Science of Articular Cartilage: Structure, Composition, and Function *Sports Health* (Vol. 1, pp. 461-468).
- Fox, A. J. S., Bedi, A., & Rodeo, S. A. (2012). The Basic Science of Human Knee Menisci: Structure, Composition, and Function *Sports Health* (Vol. 4, pp. 340-351).
- Frizziero, A., Ferrari, R., Giannotti, E., Ferroni, C., Poli, P., & Masiero, S. (2012). The meniscus tear: state of the art of rehabilitation protocols related to surgical procedures *Muscles Ligaments Tendons J* (Vol. 2, pp. 295-301).
- Garcia-Giralt, N., Cruz, D. M. G., Nogues, X., Ivirico, J. L. E., & Ribelles, J. L. G. (2013). Chitosan microparticles for “in vitro” 3D culture of human chondrocytes.

- Genes, N. G., Rowley, J. A., Mooney, D. J., & Bonassar, L. J. (2004). Effect of substrate mechanics on chondrocyte adhesion to modified alginate surfaces *Arch Biochem Biophys* (Vol. 422, pp. 161-167). United States.
- Miller, J. S. (2014). The Billion Cell Construct: Will Three-Dimensional Printing Get Us There? *PLoS Biol* (Vol. 12).
- Negishi, Y., Ui, N., Nakajima, M., Kawashima, K., Maruyama, K., Takizawa, T., *et al.* (2001). p21Cip-1/SDI-1/WAF-1 Gene Is Involved in Chondrogenic Differentiation of ATDC5 Cells in Vitro.
- Newton, P. T., Staines, K. A., Spevak, L., Boskey, A. L., Teixeira, C. C., Macrae, V. E., *et al.* (2012). Chondrogenic ATDC5 cells: an optimised model for rapid and physiological matrix mineralisation. *Int J Mol Med*, 30(5), 1187-1193.
- Popp, J. R., Roberts, J. J., Gallagher, D. V., Anseth, K. S., Bryant, S. J., & Quinn, T. P. (2012). An Instrumented Bioreactor for Mechanical Stimulation and Real-Time, Nondestructive Evaluation of Engineered Cartilage Tissue *J Med Device* (Vol. 6, p. 21006).
- Sanz-Ramos, P., Duarte, J., Rodríguez-Goñi, M. V., Vicente-Pascual, M., Dotor, J., Mora, G., *et al.* (2014). Improved Chondrogenic Capacity of Collagen Hydrogel Expanded Chondrocytes.
- Sanz-Ramos, P., Mora, G., Vicente-Pascual, M., Ochoa, I., Alcaine, C., Moreno, R., *et al.* (2013). Response of sheep chondrocytes to changes in substrate stiffness from 2 to 20 Pa: effect of cell passaging. *Connect Tissue Res*, 54(3), 159-166.
- Scarritt, M. E., Pashos, N. C., & Bunnell, B. A. (2015). A Review of Cellularization Strategies for Tissue Engineering of Whole Organs. *Front Bioeng Biotechnol*, 3.
- Tortelli, F., & Cancedda, R. (2009). Three-dimensional cultures of osteogenic and chondrogenic cells: a tissue engineering approach to mimic bone and cartilage in vitro. *Eur Cell Mater*, 17, 1-14.
- Wei, Y., Zeng, W., Wan, R., Wang, J., Zhou, Q., Qiu, S., *et al.* (2012). Chondrogenic differentiation of induced pluripotent stem cells from osteoarthritic chondrocytes in alginate matrix. *Eur Cell Mater*, 23, 1-12.
- Xu, T., Binder, K., Albanna, M., Dice, D., Zhao, W., Yoo, J., *et al.* (2012). Hybrid printing of mechanically and biologically improved constructs for cartilage tissue engineering applications. *Biofabrication*, 5.

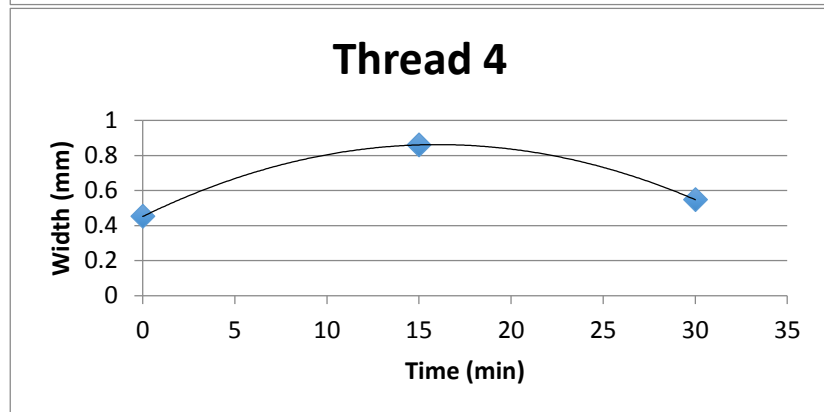
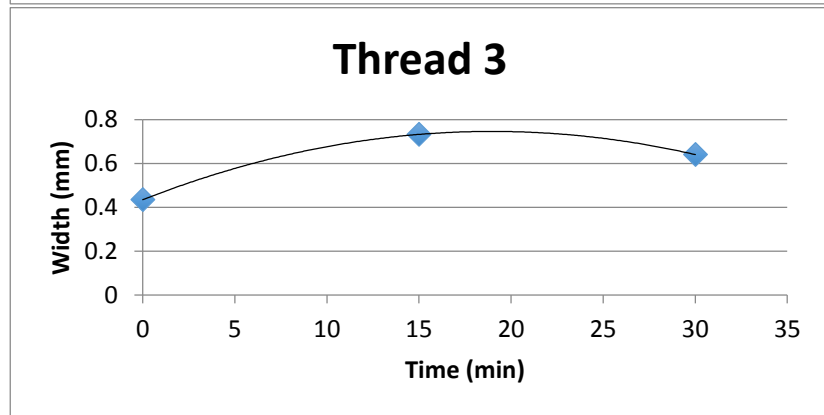
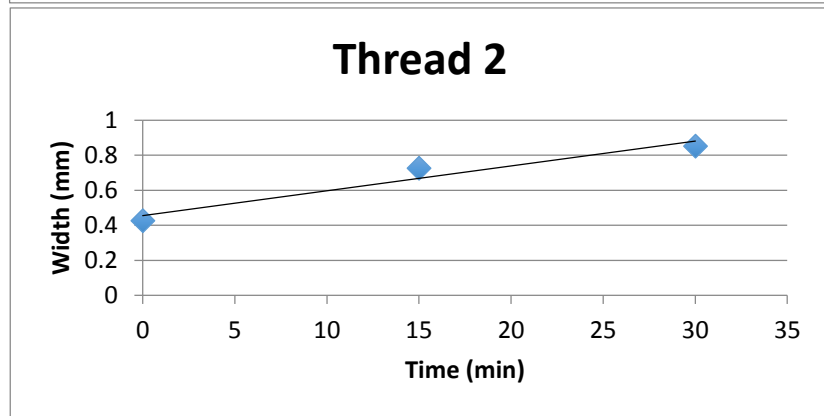
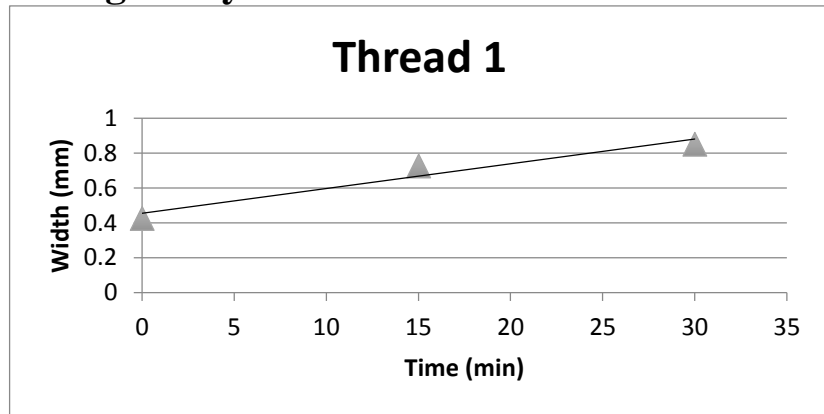


## Appendix A: ReplicatorG Print Settings for the Final Design



## Appendix B: PVA Swelling Study

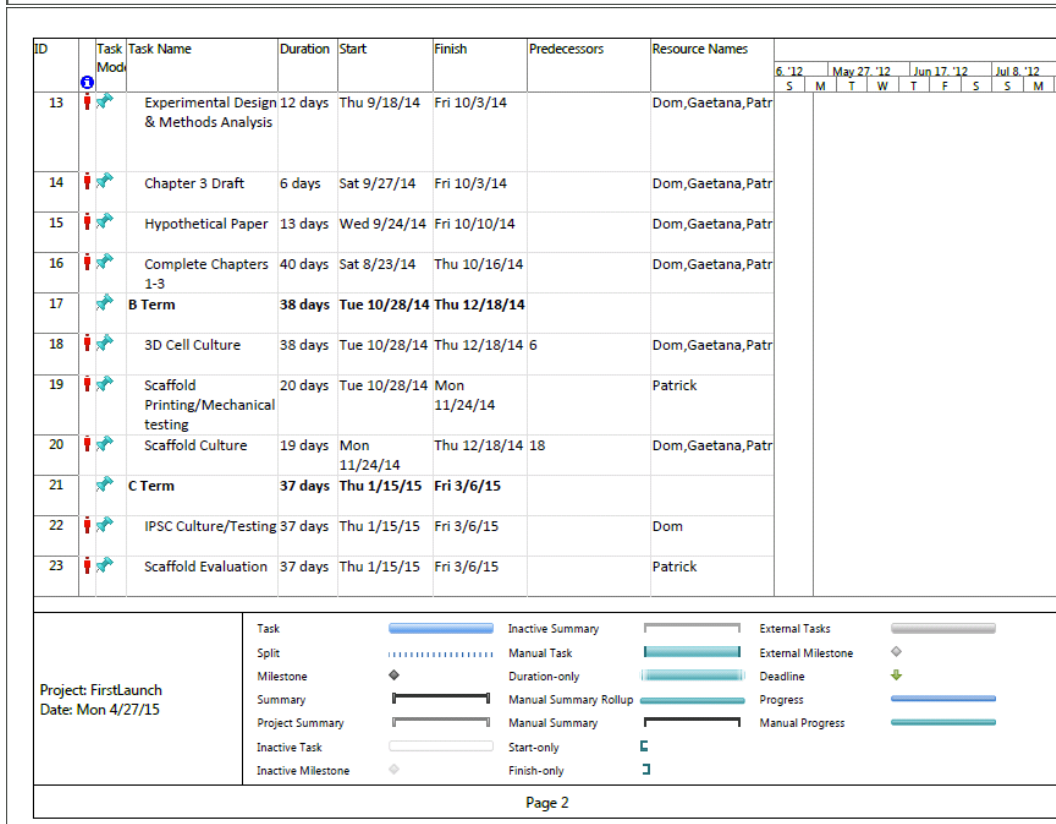
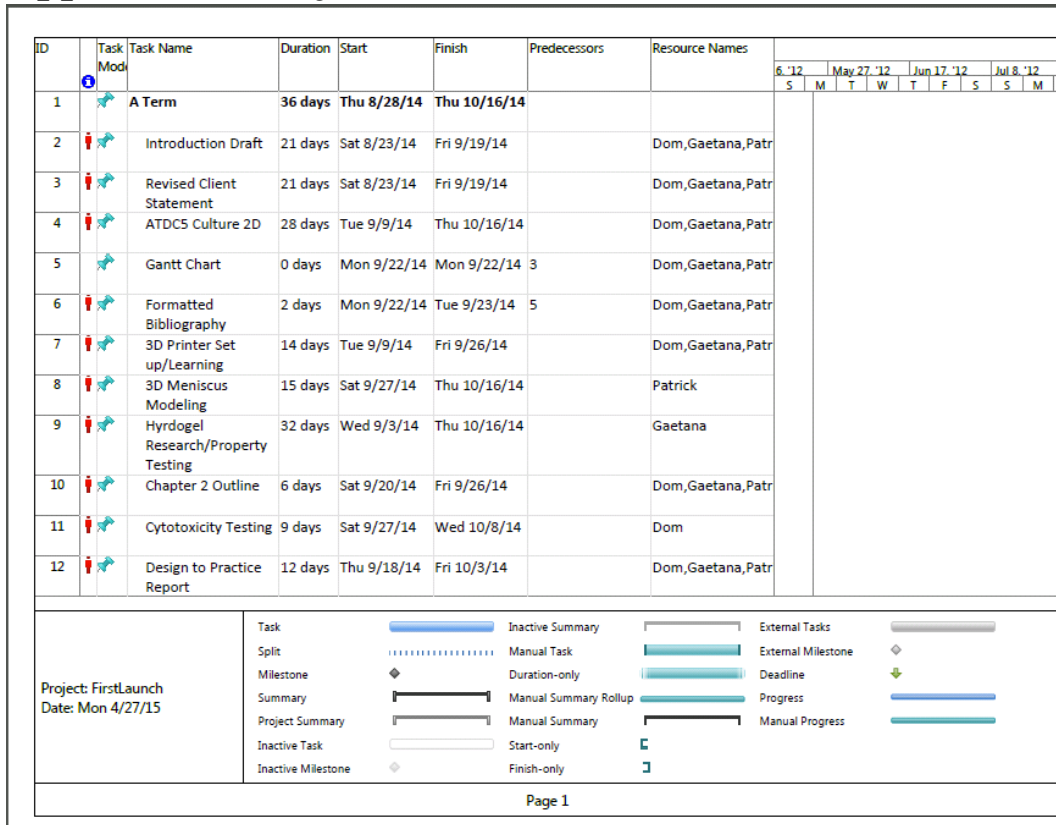
Time (min)	Width (mm)
Thread 1	
0	0.4
0	0.404
0	0.397
15	0.741
15	0.719
15	0.768
30	0.888
30	0.882
30	0.858
Thread 2	
0	0.441
0	0.414
0	0.423
15	0.721
15	0.726
15	0.73
30	0.827
30	0.873
30	0.852
Thread 3	
0	0.43
0	0.424
0	0.452
15	0.717
15	0.74
15	0.743
30	0.661
30	0.64
30	0.623
Thread 4	
0	0.446
0	0.451
0	0.459
15	0.871
15	0.855
15	0.856
30	0.537
30	0.513
30	0.595



## Appendix C: Project Budget

Product	Cost/Unit	Quantity	Total Cost	Cost for Group
Monoprice 3D Printer	\$1200/Printer	1 Printer	\$1,200	\$0
Polyvinyl Alcohol	\$58-\$167/kg	2 kg	\$116-\$334	\$0
Polylactic Acid	\$20/kg	2 kg	\$40	\$0
Plain catgut collagen sutures	\$16.42/packet	12 packets	\$197	\$0
Vicryl Violet sutures	\$37.50/packet	12 packets	\$450	\$0
Silk suture	\$8/packet	12 packets	\$96	\$0
Calcien AM live stain	\$241/mL	1 mL	\$241	\$241
<b>Lab Fee</b>			\$100	\$100
Alginate				
DMEM				
DPBS(-)				
DPBS(+)				
Ham's F12				
Penicillin/Streptomycin				
Pipette tips				
Tissue culture plates				
		<b>Final Costs:</b>	\$2,324	\$341
			<b>Total Project Budget:</b>	\$468
			<b>Remaining Budget:</b>	\$127

# Appendix D: Project Gantt Chart



ID	Task Mod	Task Name	Duration	Start	Finish	Predecessors	Resource Names									
								6 '12	May 27 '12	Jun 17 '12	Jul 8 '12					
								S	M	T	W	T	F	S	S	M
24		D Term	34 days	Mon 3/16/15	Thu 4/30/15											
25		Project Complete			Sun 3/29/15		Dom,Gaetana,Patr									
26		Report First Draft	146 days	Thu 9/18/14	Thu 4/9/15		Dom,Gaetana,Patr									
27		Project Presentation Day	20 days	Sun 3/29/15	Thu 4/23/15		Dom,Gaetana,Patr									
28		eCDR Due	25 days	Sun 3/29/15	Thu 4/30/15		Dom,Gaetana,Patr									

Project: FirstLaunch  
Date: Mon 4/27/15

Task		Inactive Summary		External Tasks	
Split		Manual Task		External Milestone	
Milestone		Duration-only		Deadline	
Summary		Manual Summary Rollup		Progress	
Project Summary		Manual Summary		Manual Progress	
Inactive Task		Start-only			
Inactive Milestone		Finish-only			

Jul 29 '12	Aug 19 '12	Sep 9 '12	Sep 30 '12	Oct 21 '12	Nov 11 '12	Dec 2 '12	Dec 23 '12	Jan 13 '13	Feb 3 '13	Feb 24 '13	Mar 17 '13	Apr 7 '13
T	W	T	F	S	S	M	T	W	T	F	S	S

Project: FirstLaunch  
Date: Mon 4/27/15

Task		Inactive Summary		External Tasks	
Split		Manual Task		External Milestone	
Milestone		Duration-only		Deadline	
Summary		Manual Summary Rollup		Progress	
Project Summary		Manual Summary		Manual Progress	
Inactive Task		Start-only			
Inactive Milestone		Finish-only			

Jul 29 '12	Aug 19 '12	Sep 9 '12	Sep 30 '12	Oct 21 '12	Nov 11 '12	Dec 2 '12	Dec 23 '12	Jan 13 '13	Feb 3 '13	Feb 24 '13	Mar 17 '13	Apr						
T	W	T	F	S	S	M	T	W	T	F	S	S	M	T	W	T	F	S

<b>Project: FirstLaunch</b> Date: Mon 4/27/15	Task		Inactive Summary		External Tasks	
	Split		Manual Task		External Milestone	
	Milestone		Duration-only		Deadline	
	Summary		Manual Summary Rollup		Progress	
	Project Summary		Manual Summary		Manual Progress	
	Inactive Task		Start-only			
	Inactive Milestone		Finish-only			
Page 5						

Jul 29 '12	Aug 19 '12	Sep 9 '12	Sep 30 '12	Oct 21 '12	Nov 11 '12	Dec 2 '12	Dec 23 '12	Jan 13 '13	Feb 3 '13	Feb 24 '13	Mar 17 '13	Apr						
T	W	T	F	S	S	M	T	W	T	F	S	S	M	T	W	T	F	S

<b>Project: FirstLaunch</b> Date: Mon 4/27/15	Task		Inactive Summary		External Tasks	
	Split		Manual Task		External Milestone	
	Milestone		Duration-only		Deadline	
	Summary		Manual Summary Rollup		Progress	
	Project Summary		Manual Summary		Manual Progress	
	Inactive Task		Start-only			
	Inactive Milestone		Finish-only			
Page 6						

7 '13	Apr 28 '13	May 19 '13	Jun 9 '13	Jun 30 '13	Jul 21 '13	Aug 11 '13	Sep 1 '13	Sep 22 '13	Oct 13 '13	Nov 3 '13	Nov 24 '13	Dec 15 '13	
S	M	T	W	T	F	S	S	M	T	W	T	F	S

Project: FirstLaunch  
Date: Mon 4/27/15

Task		Inactive Summary		External Tasks	
Split		Manual Task		External Milestone	
Milestone		Duration-only		Deadline	
Summary		Manual Summary Rollup		Progress	
Project Summary		Manual Summary		Manual Progress	
Inactive Task		Start-only			
Inactive Milestone		Finish-only			

Page 7

7 '13	Apr 28 '13	May 19 '13	Jun 9 '13	Jun 30 '13	Jul 21 '13	Aug 11 '13	Sep 1 '13	Sep 22 '13	Oct 13 '13	Nov 3 '13	Nov 24 '13	Dec 15 '13	
S	M	T	W	T	F	S	S	M	T	W	T	F	S

Project: FirstLaunch  
Date: Mon 4/27/15

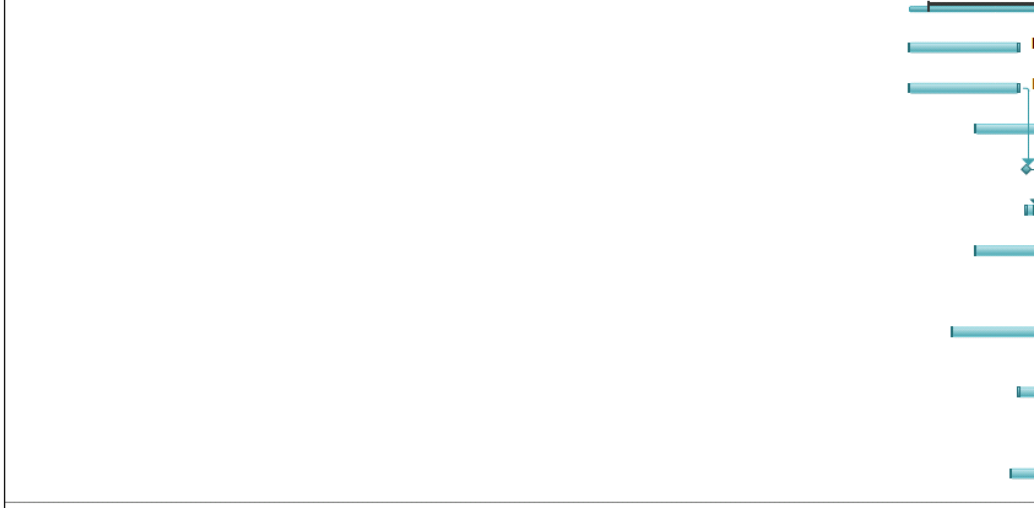
Task		Inactive Summary		External Tasks	
Split		Manual Task		External Milestone	
Milestone		Duration-only		Deadline	
Summary		Manual Summary Rollup		Progress	
Project Summary		Manual Summary		Manual Progress	
Inactive Task		Start-only			
Inactive Milestone		Finish-only			

Page 8

Feb '13	Apr 28 '13	May 19 '13	Jun 9 '13	Jun 30 '13	Jul 21 '13	Aug 11 '13	Sep 1 '13	Sep 22 '13	Oct 13 '13	Nov 3 '13	Nov 24 '13	Dec 15 '13						
S	M	T	W	T	F	S	S	M	T	W	T	F	S	S	M	T	W	T

Project: FirstLaunch Date: Mon 4/27/15	Task		Inactive Summary		External Tasks	
	Split		Manual Task		External Milestone	
	Milestone		Duration-only		Deadline	
	Summary		Manual Summary Rollup		Progress	
	Project Summary		Manual Summary		Manual Progress	
	Inactive Task		Start-only			
	Inactive Milestone		Finish-only			

Jan 5 '14	Jan 26 '14	Feb 16 '14	Mar 9 '14	Mar 30 '14	Apr 20 '14	May 11 '14	Jun 1 '14	Jun 22 '14	Jul 13 '14	Aug 3 '14	Aug 24 '14	Sep 14	
F	S	S	M	T	W	T	F	S	S	M	T	W	T



Project: FirstLaunch Date: Mon 4/27/15	Task		Inactive Summary		External Tasks	
	Split		Manual Task		External Milestone	
	Milestone		Duration-only		Deadline	
	Summary		Manual Summary Rollup		Progress	
	Project Summary		Manual Summary		Manual Progress	
	Inactive Task		Start-only			
	Inactive Milestone		Finish-only			



Jan 5 '14 Jan 26 '14 Feb 16 '14 Mar 9 '14 Mar 30 '14 Apr 20 '14 May 11 '14 Jun 1 '14 Jun 22 '14 Jul 13 '14 Aug 3 '14 Aug 24 '14 Sep 14

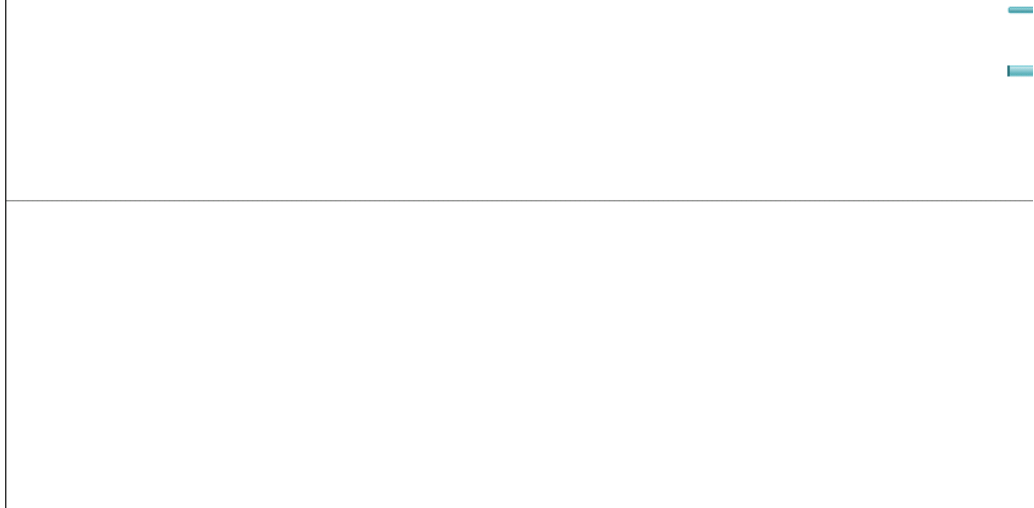


Project: FirstLaunch  
Date: Mon 4/27/15

Task		Inactive Summary		External Tasks	
Split		Manual Task		External Milestone	
Milestone		Duration-only		Deadline	
Summary		Manual Summary Rollup		Progress	
Project Summary		Manual Summary		Manual Progress	
Inactive Task		Start-only			
Inactive Milestone		Finish-only			

Page 11

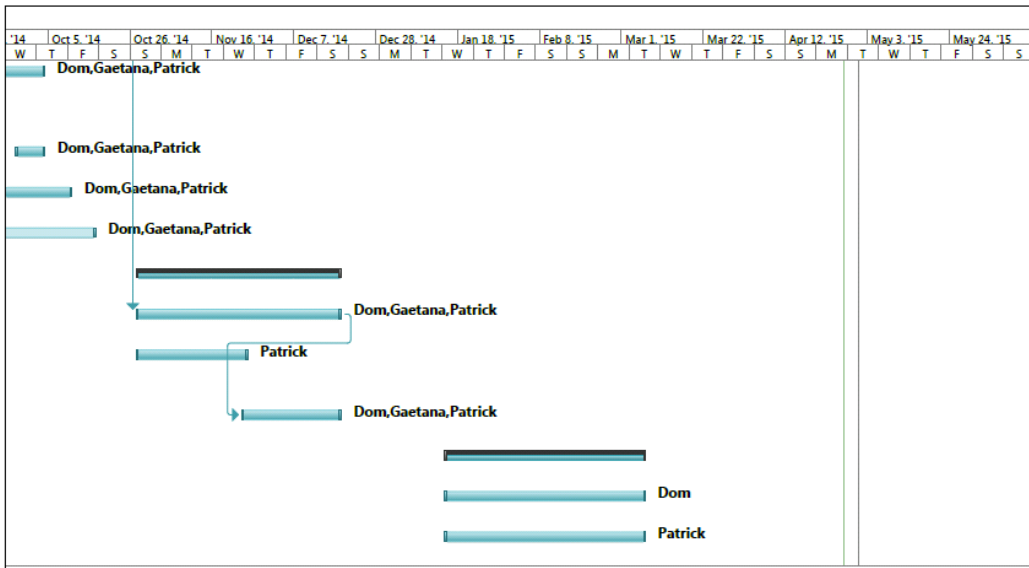
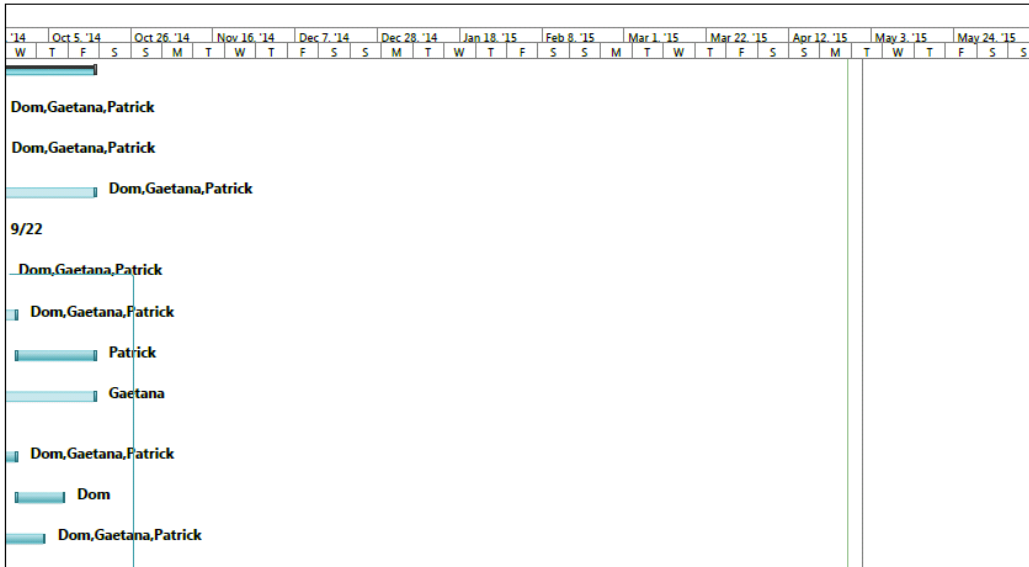
Jan 5 '14 Jan 26 '14 Feb 16 '14 Mar 9 '14 Mar 30 '14 Apr 20 '14 May 11 '14 Jun 1 '14 Jun 22 '14 Jul 13 '14 Aug 3 '14 Aug 24 '14 Sep 14



Project: FirstLaunch  
Date: Mon 4/27/15

Task		Inactive Summary		External Tasks	
Split		Manual Task		External Milestone	
Milestone		Duration-only		Deadline	
Summary		Manual Summary Rollup		Progress	
Project Summary		Manual Summary		Manual Progress	
Inactive Task		Start-only			
Inactive Milestone		Finish-only			

Page 12

























































































GI X10.1 Y7 99.23.85 F840.0 E80.161 GI X9.98 Y8.45 23.85 F840.0 E80.171 GI X9.59 Y8.87 23.85 F840.0 E80.182 GI X9.26 Y9.26 23.85 F840.0 E80.191 GI X8.87 Y9.99 23.85 F840.0 E80.2 GI X8.45 Y9.88 23.85 F840.0 E80.21 GI X7.99 Y10.1 23.85 F840.0 E80.219 GI X7.51 Y10.27 23.85 F840.0 E80.228 GI X7.01 Y10.37 23.85 F840.0 E80.237 GI X6.5 Y10.4 23.85 F840.0 E80.246 GI X6.09 Y10.71 23.85 F840.0 E80.256 GI X5.59 Y10.27 23.85 F840.0 E80.265 GI X5.11 Y10.1 23.85 F840.0 E80.274 GI X4.55 Y9.88 23.85 F840.0 E80.283 GI X4.13 Y9.59 23.85 F840.0 E80.292 GI X3.74 Y9.26 23.85 F840.0 E80.302 GI X3.34 Y9.87 23.85 F840.0 E80.311 GI X2.92 Y9.45 23.85 F840.0 E80.32 GI X2.5 Y9.99 23.85 F840.0 E80.33 GI X2.09 Y9.23 23.85 F840.0 E80.339 GI X1.67 Y7.01 23.85 F840.0 E80.348 GI X1.26 Y6.23 85 F840.0 E80.357 GI X0.83 Y9.23 85 F840.0 E80.366 GI X0.41 Y8.49 23.85 F840.0 E80.376 GI X0.36 Y8.01 23.85 F840.0 E80.384 GI X0.31 Y8.45 23.85 F840.0 E80.393 GI X0.27 Y9.23 85 F840.0 E80.402 GI X0.23 Y7.01 23.85 F840.0 E80.411 GI X0.19 Y8.45 23.85 F840.0 E80.42 GI X0.15 Y9.23 85 F840.0 E80.429 GI X0.11 Y7.01 23.85 F840.0 E80.438 GI X0.07 Y8.45 23.85 F840.0 E80.447 GI X0.03 Y9.23 85 F840.0 E80.456 GI X0.39 Y9.23 85 F840.0 E80.465 GI X0.34 Y8.45 23.85 F840.0 E80.474 GI X0.3 Y9.23 85 F840.0 E80.483 GI X0.26 Y9.23 85 F840.0 E80.492 GI X0.22 Y8.45 23.85 F840.0 E80.501 GI X0.18 Y9.23 85 F840.0 E80.51 GI X0.14 Y8.45 23.85 F840.0 E80.519 GI X0.1 Y9.23 85 F840.0 E80.528 GI X0.06 Y8.45 23.85 F840.0 E80.537 GI X0.02 Y9.23 85 F840.0 E80.546 GI X0.59 Y8.23 85 F840.0 E80.555 GI X0.54 Y7.01 23.85 F840.0 E80.564 GI X0.5 Y9.23 85 F840.0 E80.573 GI X0.46 Y8.45 23.85 F840.0 E80.582 GI X0.42 Y9.23 85 F840.0 E80.591 GI X0.38 Y8.45 23.85 F840.0 E80.6 GI X0.34 Y9.23 85 F840.0 E80.609 GI X0.3 Y9.23 85 F840.0 E80.618 GI X0.26 Y8.45 23.85 F840.0 E80.627 GI X0.22 Y9.23 85 F840.0 E80.636 GI X0.18 Y8.45 23.85 F840.0 E80.645 GI X0.14 Y9.23 85 F840.0 E80.654 GI X0.1 Y9.23 85 F840.0 E80.663 GI X0.06 Y8.45 23.85 F840.0 E80.672 GI X0.02 Y9.23 85 F840.0 E80.681 GI X0.59 Y8.23 85 F840.0 E80.69 GI X0.54 Y7.01 23.85 F840.0 E80.699 GI X0.5 Y9.23 85 F840.0 E80.708 GI X0.46 Y8.45 23.85 F840.0 E80.717 GI X0.42 Y9.23 85 F840.0 E80.726 GI X0.38 Y8.45 23.85 F840.0 E80.735 GI X0.34 Y9.23 85 F840.0 E80.744 GI X0.3 Y9.23 85 F840.0 E80.753 GI X0.26 Y8.45 23.85 F840.0 E80.762 GI X0.22 Y9.23 85 F840.0 E80.771 GI X0.18 Y8.45 23.85 F840.0 E80.78 GI X0.14 Y9.23 85 F840.0 E80.789 GI X0.1 Y9.23 85 F840.0 E80.798 GI X0.06 Y8.45 23.85 F840.0 E80.807 GI X0.02 Y9.23 85 F840.0 E80.816 GI X0.59 Y8.23 85 F840.0 E80.825 GI X0.54 Y7.01 23.85 F840.0 E80.834 GI X0.5 Y9.23 85 F840.0 E80.843 GI X0.46 Y8.45 23.85 F840.0 E80.852 GI X0.42 Y9.23 85 F840.0 E80.861 GI X0.38 Y8.45 23.85 F840.0 E80.87 GI X0.34 Y9.23 85 F840.0 E80.88 GI X0.3 Y9.23 85 F840.0 E80.889 GI X0.26 Y8.45 23.85 F840.0 E80.898 GI X0.22 Y9.23 85 F840.0 E80.907 GI X0.18 Y8.45 23.85 F840.0 E80.916 GI X0.14 Y9.23 85 F840.0 E80.925 GI X0.1 Y9.23 85 F840.0 E80.934 GI X0.06 Y8.45 23.85 F840.0 E80.943 GI X0.02 Y9.23 85 F840.0 E80.952 GI X0.59 Y8.23 85 F840.0 E80.961 GI X0.54 Y7.01 23.85 F840.0 E80.97 GI X0.5 Y9.23 85 F840.0 E80.98 GI X0.46 Y8.45 23.85 F840.0 E80.989 GI X0.42 Y9.23 85 F840.0 E81 GI X0.38 Y8.45 23.85 F840.0 E81.009 GI X0.34 Y9.23 85 F840.0 E81.018 GI X0.3 Y9.23 85 F840.0 E81.027 GI X0.26 Y8.45 23.85 F840.0 E81.036 GI X0.22 Y9.23 85 F840.0 E81.045 GI X0.18 Y8.45 23.85 F840.0 E81.054 GI X0.14 Y9.23 85 F840.0 E81.063 GI X0.1 Y9.23 85 F840.0 E81.072 GI X0.06 Y8.45 23.85 F840.0 E81.081 GI X0.02 Y9.23 85 F840.0 E81.09 GI X0.59 Y8.23 85 F840.0 E81.099 GI X0.54 Y7.01 23.85 F840.0 E81.108 GI X0.5 Y9.23 85 F840.0 E81.117 GI X0.46 Y8.45 23.85 F840.0 E81.126 GI X0.42 Y9.23 85 F840.0 E81.135 GI X0.38 Y8.45 23.85 F840.0 E81.144 GI X0.34 Y9.23 85 F840.0 E81.153 GI X0.3 Y9.23 85 F840.0 E81.162 GI X0.26 Y8.45 23.85 F840.0 E81.171 GI X0.22 Y9.23 85 F840.0 E81.18 GI X0.18 Y8.45 23.85 F840.0 E81.189 GI X0.14 Y9.23 85 F840.0 E81.198 GI X0.1 Y9.23 85 F840.0 E81.207 GI X0.06 Y8.45 23.85 F840.0 E81.216 GI X0.02 Y9.23 85 F840.0 E81.225 GI X0.59 Y8.23 85 F840.0 E81.234 GI X0.54 Y7.01 23.85 F840.0 E81.243 GI X0.5 Y9.23 85 F840.0 E81.252 GI X0.46 Y8.45 23.85 F840.0 E81.261 GI X0.42 Y9.23 85 F840.0 E81.27 GI X0.38 Y8.45 23.85 F840.0 E81.28 GI X0.34 Y9.23 85 F840.0 E81.289 GI X0.3 Y9.23 85 F840.0 E81.298 GI X0.26 Y8.45 23.85 F840.0 E81.307 GI X0.22 Y9.23 85 F840.0 E81.316 GI X0.18 Y8.45 23.85 F840.0 E81.325 GI X0.14 Y9.23 85 F840.0 E81.334 GI X0.1 Y9.23 85 F840.0 E81.343 GI X0.06 Y8.45 23.85 F840.0 E81.352 GI X0.02 Y9.23 85 F840.0 E81.361 GI X0.59 Y8.23 85 F840.0 E81.37 GI X0.54 Y7.01 23.85 F840.0 E81.38 GI X0.5 Y9.23 85 F840.0 E81.389 GI X0.46 Y8.45 23.85 F840.0 E81.398 GI X0.42 Y9.23 85 F840.0 E81.407 GI X0.38 Y8.45 23.85 F840.0 E81.416 GI X0.34 Y9.23 85 F840.0 E81.425 GI X0.3 S Y9.23 85 F840.0 E81.434 GI X0.3 Y9.23 85 F840.0 E81.443 GI X0.26 Y8.45 23.85 F840.0 E81.452 GI X0.22 Y9.23 85 F840.0 E81.461 GI X0.18 Y8.45 23.85 F840.0 E81.47 GI X0.14 Y9.23 85 F840.0 E81.48 GI X0.1 Y9.23 85 F840.0 E81.489 GI X0.06 Y8.45 23.85 F840.0 E81.498 GI X0.02 Y9.23 85 F840.0 E81.507 GI X0.59 Y8.23 85 F840.0 E81.516 GI X0.54 Y7.01 23.85 F840.0 E81.525 GI X0.5 Y9.23 85 F840.0 E81.534 GI X0.46 Y8.45 23.85 F840.0 E81.543 GI X0.42 Y9.23 85 F840.0 E81.552 GI X0.38 Y8.45 23.85 F840.0 E81.561 GI X0.34 Y9.23 85 F840.0 E81.57 GI X0.3 S Y9.23 85 F840.0 E81.58 GI X0.3 Y9.23 85 F840.0 E81.589 GI X0.26 Y8.45 23.85 F840.0 E81.598 GI X0.22 Y9.23 85 F840.0 E81.607 GI X0.18 Y8.45 23.85 F840.0 E81.616 GI X0.14 Y9.23 85 F840.0 E81.625 GI X0.1 Y9.23 85 F840.0 E81.634 GI X0.06 Y8.45 23.85 F840.0 E81.643 GI X0.02 Y9.23 85 F840.0 E81.652 GI X0.59 Y8.23 85 F840.0 E81.661 GI X0.54 Y7.01 23.85 F840.0 E81.67 GI X0.5 Y9.23 85 F840.0 E81.68 GI X0.46 Y8.45 23.85 F840.0 E81.689 GI X0.42 Y9.23 85 F840.0 E81.698 GI X0.38 Y8.45 23.85 F840.0 E81.707 GI X0.34 Y9.23 85 F840.0 E81.716 GI X0.3 Y9.23 85 F840.0 E81.725 GI X0.26 Y8.45 23.85 F840.0 E81.734 GI X0.22 Y9.23 85 F840.0 E81.743 GI X0.18 Y8.45 23.85 F840.0 E81.752 GI X0.14 Y9.23 85 F840.0 E81.761 GI X0.1 Y9.23 85 F840.0 E81.77 GI X0.06 Y8.45 23.85 F840.0 E81.78 GI X0.02 Y9.23 85 F840.0 E81.789 GI X0.59 Y8.23 85 F840.0 E81.798 GI X0.54 Y7.01 23.85 F840.0 E81.807 GI X0.5 Y9.23 85 F840.0 E81.816 GI X0.46 Y8.45 23.85 F840.0 E81.825 GI X0.42 Y9.23 85 F840.0 E81.834 GI X0.38 Y8.45 23.85 F840.0 E81.843 GI X0.34 Y9.23 85 F840.0 E81.852 GI X0.3 S Y9.23 85 F840.0 E81.861 GI X0.3 Y9.23 85 F840.0 E81.87 GI X0.26 Y8.45 23.85 F840.0 E81.88 GI X0.22 Y9.23 85 F840.0 E81.889 GI X0.18 Y8.45 23.85 F840.0 E81.898 GI X0.14 Y9.23 85 F840.0 E81.907 GI X0.1 Y9.23 85 F840.0 E81.916 GI X0.06 Y8.45 23.85 F840.0 E81.925 GI X0.02 Y9.23 85 F840.0 E81.934 GI X0.59 Y8.23 85 F840.0 E81.943 GI X0.54 Y7.01 23.85 F840.0 E81.952 GI X0.5 Y9.23 85 F840.0 E81.961 GI X0.46 Y8.45 23.85 F840.0 E81.97 GI X0.42 Y9.23 85 F840.0 E81.98 GI X0.38 Y8.45 23.85 F840.0 E81.989 GI X0.34 Y9.23 85 F840.0 E82	(cedge) inner F780.0 GI X12.00 GI Y9.94 23.85 MI0 GI X1.2 Y4.21 23.85 F840.0 E80.411 GI X3.8 Y4.6 23.85 F840.0 E80.422 GI X3.54 Y5.04 23.85 F840.0 E80.431 GI X3.25 Y5.4 23.85 F840.0 E80.44 GI X3.24 Y6.0 23.85 F840.0 E80.449 GI X3.2 Y6.23 85 F840.0 E80.458 F840.0 E80.467 GI X3.25 Y7.5 23.85 F840.0 E80.476 GI X3.24 Y7.96 23.85 F840.0 E80.486 GI X3.25 Y8.4 23.85 F840.0 E80.495 GI X4.12 Y8.19 23.85 F840.0 E80.504 GI X4.5 Y9.11 23.85 F840.0 E80.513 GI X4.2 Y9.41 23.85 F840.0 E80.522 GI X3.87 Y9.74 23.85 F840.0 E80.531 GI X3.67 Y9.8 23.85 F840.0 E80.54 GI X3.88 Y9.78 23.85 F840.0 E80.559 GI X3.7 Y9.68 23.85 F840.0 E80.568 GI X3.55 Y9.51 23.85 F840.0 E80.577 GI X3.29 Y9.27 23.85 F840.0 E80.586 GI X3.78 Y9.6 23.85 F840.0 E80.595 GI X3.29 Y9.23 85 F840.0 E80.604 GI X3.24 Y8.13 23.85 F840.0 E80.613 GI X3.19 Y8.45 23.85 F840.0 E80.622 GI X3.19 Y9.75 23.85 F840.0 E80.631 GI X3.18 Y9.25 23.85 F840.0 E80.64 GI X3.17 Y8.25 23.85 F840.0 E80.649 GI X3.16 Y8.25 23.85 F840.0 E80.658 GI X3.15 Y7.75 23.85 F840.0 E80.667 GI X3.14 Y8.23 85 F840.0 E80.676 GI X3.13 Y8.23 85 F840.0 E80.685 GI X3.12 Y8.23 85 F840.0 E80.694 GI X3.11 Y8.23 85 F840.0 E80.703 GI X3.1 Y8.23 85 F840.0 E80.712 GI X3.09 Y8.23 85 F840.0 E80.721 GI X3.08 Y8.23 85 F840.0 E80.73 GI X3.07 Y8.23 85 F840.0 E80.739 GI X3.06 Y8.23 85 F840.0 E80.748 GI X3.05 Y8.23 85 F840.0 E80.757 GI X3.04 Y8.23 85 F840.0 E80.766 GI X3.03 Y8.23 85 F840.0 E80.775 GI X3.02 Y8.23 85 F840.0 E80.784 GI X3.01 Y8.23 85 F840.0 E80.793 GI X3.0 Y8.23 85 F840.0 E80.802 GI X2.99 Y8.23 85 F840.0 E80.811 GI X2.98 Y8.23 85 F840.0 E80.82 GI X2.97 Y8.23 85 F840.0 E80.829 GI X2.96 Y8.23 85 F840.0 E80.838 GI X2.95 Y8.23 85 F840.0 E80.847 GI X2.94 Y8.23 85 F840.0 E80.856 GI X2.93 Y8.23 85 F840.0 E80.865 GI X2.92 Y8.23 85 F840.0 E80.874 GI X2.91 Y8.23 85 F840.0 E80.883 GI X2.9 Y8.23 85 F840.0 E80.892 GI X2.89 Y8.23 85 F840.0 E80.901 GI X2.88 Y8.23 85 F840.0 E80.91 GI X2.87 Y8.23 85 F840.0 E80.919 GI X2.86 Y8.23 85 F840.0 E80.928 GI X2.85 Y8.23 85 F840.0 E80.937 GI X2.84 Y8.23 85 F840.0 E80.946 GI X2.83 Y8.23 85 F840.0 E80.955 GI X2.82 Y8.23 85 F840.0 E80.964 GI X2.81 Y8.23 85 F840.0 E80.973 GI X2.8 Y8.23 85 F840.0 E80.982 GI X2.79 Y8.23 85 F840.0 E80.991 GI X2.78 Y8.23 85 F840.0 E80.999 GI X2.77 Y8.23 85 F840.0 E81.008 GI X2.76 Y8.23 85 F840.0 E81.017 GI X2.75 Y8.23 85 F840.0 E81.026 GI X2.74 Y8.23 85 F840.0 E81.035 GI X2.73 Y8.23 85 F840.0 E81.044 GI X2.72 Y8.23 85 F840.0 E81.053 GI X2.71 Y8.23 85 F840.0 E81.062 GI X2.7 Y8.23 85 F840.0 E81.071 GI X2.69 Y8.23 85 F840.0 E81.08 GI X2.68 Y8.23 85 F840.0 E81.089 GI X2.67 Y8.23 85 F840.0 E81.098 GI X2.66 Y8.23 85 F840.0 E81.107 GI X2.65 Y8.23 85 F840.0 E81.116 GI X2.64 Y8.23 85 F840.0 E81.125 GI X2.63 Y8.23 85 F840.0 E81.134 GI X2.62 Y8.23 85 F840.0 E81.143 GI X2.61 Y8.23 85 F840.0 E81.152 GI X2.6 Y8.23 85 F840.0 E81.161 GI X2.59 Y8.23 85 F840.0 E81.17 GI X2.58 Y8.23 85 F840.0 E81.18 GI X2.57 Y8.23 85 F840.0 E81.189 GI X2.56 Y8.23 85 F840.0 E81.198 GI X2.55 Y8.23 85 F840.0 E81.207 GI X2.54 Y8.23 85 F840.0 E81.216 GI X2.53 Y8.23 85 F840.0 E81.225 GI X2.52 Y8.23 85 F840.0 E81.234 GI X2.51 Y8.23 85 F840.0 E81.243 GI X2.5 Y8.23 85 F840.0 E81.252 GI X2.49 Y8.23 85 F840.0 E81.261 GI X2.48 Y8.23 85 F840.0 E81.27 GI X2.47 Y8.23 85 F840.0 E81.28 GI X2.46 Y8.23 85 F840.0 E81.289 GI X2.45 Y8.23 85 F840.0 E81.298 GI X2.44 Y8.23 85 F840.0 E81.307 GI X2.43 Y8.23 85 F840.0 E81.316 GI X2.42 Y8.23 85 F840.0 E81.325 GI X2.41 Y8.23 85 F840.0 E81.334 GI X2.4 Y8.23 85 F840.0 E81.343 GI X2.39 Y8.23 85 F840.0 E81.352 GI X2.38 Y8.23 85 F840.0 E81.361 GI X2.37 Y8.23 85 F840.0 E81.37 GI X2.36 Y8.23 85 F840.0 E81.38 GI X2.35 Y8.23 85 F840.0 E81.389 GI X2.34 Y8.23 85 F840.0 E81.398 GI X2.33 Y8.23 85 F840.0 E81.407 GI X2.32 Y8.23 85 F840.0 E81.416 GI X2.31 Y8.23 85 F840.0 E81.425 GI X2.3 Y8.23 85 F840.0 E81.434 GI X2.29 Y8.23 85 F840.0 E81.443 GI X2.28 Y8.23 85 F840.0 E81.452 GI X2.27 Y8.23 85 F840.0 E81.461 GI X2.26 Y8.23 85 F840.0 E81.47 GI X2.25 Y8.23 85 F840.0 E81.48 GI X2.24 Y8.23 85 F840.0 E81.489 GI X2.23 Y8.23 85 F840.0 E81.498 GI X2.22 Y8.23 85 F840.0 E81.507 GI X2.21 Y8.23 85 F840.0 E81.516 GI X2.2 Y8.23 85 F840.0 E81.525 GI X2.19 Y8.23 85 F840.0 E81.534 GI X2.18 Y8.23 85 F840.0 E81.543 GI X2.17 Y8.23 85 F840.0 E81.552 GI X2.16 Y8.23 85 F840.0 E81.561 GI X2.15 Y8.23 85 F840.0 E81.57 GI X2.14 Y8.23 85 F840.0 E81.58 GI X2.13 Y8.23 85 F840.0 E81.589 GI X2.12 Y8.23 85 F840.0 E81.598 GI X2.11 Y8.23 85 F840.0 E81.607 GI X2.1 Y8.23 85 F840.0 E81.616 GI X1.99 Y8.23 85 F840.0 E81.625 GI X1.98 Y8.23 85 F840.0 E81.634 GI X1.97 Y8.23 85 F840.0 E81.643 GI X1.96 Y8.23 85 F840.0 E81.652 GI X1.95 Y8.23 85 F840.0 E81.661 GI X1.94 Y8.23 85 F840.0 E81.67 GI X1.93 Y8.23 85 F840.0 E81.68 GI X1.92 Y8.23 85 F840.0 E81.689 GI X1.91 Y8.23 85 F840.0 E81.698 GI X1.9 Y8.23 85 F840.0 E81.707 GI X1.89 Y8.23 85 F840.0 E81.716 GI X1.88 Y8.23 85 F840.0 E81.725 GI X1.87 Y8.23 85 F840.0 E81.734 GI X1.86 Y8.23 85 F840.0 E81.743 GI X1.85 Y8.23 85 F840.0 E81.752 GI X1.84 Y8.23 85 F840.0 E81.761 GI X1.83 Y8.23 85 F840.0 E81.77 GI X1.82 Y8.23 85 F840.0 E81.78 GI X1.81 Y8.23 85 F840.0 E81.789 GI X1.8 Y8.23 85 F840.0 E81.798 GI X1.79 Y8.23 85 F840.0 E81.807 GI X1.78 Y8.23 85 F840.0 E81.816 GI X1.77 Y8.23 85 F840.0 E81.825 GI X1.76 Y8.23 85 F840.0 E81.834 GI X1.75 Y8.23 85 F840.0 E81.843 GI X1.74 Y8.23 85 F840.0 E81.852 GI X1.73 Y8.23 85 F840.0 E81.861 GI X1.72 Y8.23 85 F840.0 E81.87 GI X1.71 Y8.23 85 F840.0 E81.88 GI X1.7 Y8.23 85 F840.0 E81.889 GI X1.69 Y8.23 85 F840.0 E81.898 GI X1.68 Y8.23 85 F840.0 E81.907 GI X1.67 Y8.23 85 F840.0 E81.916 GI X1.66 Y8.23 85 F840.0 E81.925 GI X1.65 Y8.23 85 F840.0 E81.934 GI X1.64 Y8.23 85 F840.0 E81.943 GI X1.63 Y8.23 85 F840.0 E81.952 GI X1.62 Y8.23 85 F840.0 E81.961 GI X1.61 Y8.23 85 F840.0 E81.97 GI X1.6 Y8.23 85 F840.0 E81.98 GI X1.59 Y8.23 85 F840.0 E81.989 GI X1.58 Y8.23 85 F840.0 E82	GI X2.7 Y87.23.85 F780.0 GI X12.00 GI X10.8 Y8.874 GI Y7.800 MI0 GI X12.2 Y97.23.85 F800.0 E80.782 GI X3.6 Y100.23.85 F800.0 E80.796 GI X4.0 Y106.23.85 F800.0 E80.806 GI X4.0 Y91.23.85 F800.0 E80.807 GI X4.4 Y99.23.85 F800.0 E80.817 GI X4.4 Y94.23.85 F800.0 E80.825 GI X4.8 Y99.23.85 F800.0 E80.826 GI X5.2 Y98.23.85 F800.0 E80.834 GI X5.2 Y98.23.85 F800.0 E80.843 GI X5.6 Y96.23.85 
---	---	--

(cncIRPoint) XT.009	GI X3.58 Y4.2 23.95	(cncBoundaryPoint)	GI X3.42 Y8.87 24.05	(cncIRPoint) X4.55	GI X4.92 Y9.4 24.05	(cncIRPoint) X4.55	GI X6.6 Y9.96 24.05
(cncIRPoint) Y10.166 Z3.95	F10M0.0 E82.007	(cncBoundaryPoint)	X8.009 Y17.112 24.05	(cncIRPoint)	F9.877 Z4.008	(cncIRPoint)	F10M0.0 E82.279
(cncIRPoint) X6.5	GI X3.38 Y4.8 23.95	(cncBoundaryPoint)	GI X3.12 Y8.45 24.05	(cncIRPoint) X4.126	GI X3.58 Y9.61 24.05	(cncIRPoint)	GI X5.6 Y10.24 24.05
(cncIRPoint) Y10.4 Z3.95	(cncBoundaryPoint)	(cncBoundaryPoint)	F540.0 E82.1097	(cncIRPoint) Y9.594 24.05	F540.0 E82.1097	(cncIRPoint) Y9.594 24.05	GI X6.0 Y10.04 24.05
(cncIRPoint) X5.991	GI X3.13 Y4.8 23.95	(cncBoundaryPoint)	Y2.949 24.05	(cncIRPoint)	GI X3.71 Y9.24 24.05	(cncIRPoint)	F10M0.0 E83.23
(cncIRPoint) Y10.166 Z3.95	F10M0.0 E82.016	(cncBoundaryPoint)	(cncBoundaryPoint)	(cncIRPoint)	GI X3.27 Y8.4 24.05	(cncIRPoint)	GI X6.0 Y10.08 24.05
(cncIRPoint) X5.491	GI X3.13 Y4.2 23.95	(cncBoundaryPoint)	X8.996 Y3.247 24.05	(cncIRPoint)	F540.0 E82.126	(cncIRPoint)	GI X6.0 Y10.04 24.05
(cncIRPoint) Y10.166 Z3.95	F10M0.0 E82.023	(cncBoundaryPoint)	(cncBoundaryPoint)	(cncIRPoint)	GI X3.68 Y9.78 24.05	(cncIRPoint)	GI X6.0 Y10.04 24.05
(cncIRPoint) X5.008	GI X3.13 Y4.6 23.95	(cncBoundaryPoint)	F540.0 E82.171	(cncIRPoint) X3.406	F540.0 E82.315	(cncIRPoint)	GI X6.4 Y10.11 24.05
(cncIRPoint) Y10.163 Z3.95	F10M0.0 E82.032	(cncBoundaryPoint)	X3.242 Y4.6 24.05	(cncIRPoint)	F540.0 E82.374	(cncIRPoint)	F10M0.0 E83.238
(cncIRPoint) X4.55	F10M0.0 E82.032	(cncBoundaryPoint)	F540.0 E82.73	(cncIRPoint) X3.123	GI X7.89 Y9.51 24.05	(cncIRPoint)	GI X6.8 Y10.1 24.05
(cncIRPoint) Y9.877 Z3.95	GI X2.96 Y4.0 23.95	(cncBoundaryPoint)	F540.0 E82.161	(cncIRPoint) X2.897	F540.0 E82.95	(cncIRPoint)	GI X6.8 Y10.06 24.05
(cncIRPoint) X4.126	GI X2.92 Y4.0 23.95	(cncBoundaryPoint)	X10.051 Y4.45 24.05	(cncIRPoint) Y7.992 24.05	(cncIRPoint) X2.897	(cncIRPoint)	GI X7.0 Y10.04 24.05
(cncIRPoint) Y9.594 Z3.95	F10M0.0 E82.04	(cncBoundaryPoint)	X10.288 Y4.931 24.05	(cncIRPoint) X2.734	F540.0 E82.981	(cncIRPoint)	F10M0.0 E83.254
(cncIRPoint) X3.743	GI X2.94 Y4.2 23.95	(cncBoundaryPoint)	(cncBoundaryPoint)	(cncIRPoint) X2.634	GI X3.89 Y8.24 24.05	(cncIRPoint)	GI X7.6 Y9.92 24.05
(cncIRPoint) Y9.257 Z3.95	F10M0.0 E82.048	(cncBoundaryPoint)	X10.46 Y4.49 24.05	(cncIRPoint) X2.897	F540.0 E82.999	(cncIRPoint)	F10M0.0 E83.262
(cncIRPoint) X3.406	GI X2.9 Y6.8 23.95	(cncBoundaryPoint)	(cncBoundaryPoint)	(cncIRPoint) X2.897	F540.0 E83.007	(cncIRPoint)	F10M0.0 E83.268
(cncIRPoint) Y8.874 Z3.95	F10M0.0 E82.056	(cncBoundaryPoint)	X10.565 Y5.965 24.05	(cncIRPoint) X2.897	F540.0 E83.016	(cncIRPoint)	F10M0.0 E83.275
(cncIRPoint) X3.123	GI X2.9 Y7.2 23.95	(cncBoundaryPoint)	(cncBoundaryPoint)	(cncIRPoint) X2.897	F540.0 E83.025	(cncIRPoint)	F10M0.0 E83.282
(cncIRPoint) Y8.45 Z3.95	F10M0.0 E82.064	(cncBoundaryPoint)	X10.716 Y7.23 24.05	(cncIRPoint) X2.897	F540.0 E83.034	(cncIRPoint)	F10M0.0 E83.289
(cncIRPoint) X3.289	GI X3.0 Y7.6 23.95	(cncBoundaryPoint)	X10.869 Y8.71 24.05	(cncIRPoint) X2.897	F540.0 E83.043	(cncIRPoint)	F10M0.0 E83.296
(cncIRPoint) Y7.992 Z3.95	F10M0.0 E82.072	(cncBoundaryPoint)	X10.965 Y10.209 24.05	(cncIRPoint) X2.897	F540.0 E83.052	(cncIRPoint)	F10M0.0 E83.303
(cncIRPoint) X2.734	GI X3.09 Y7.6 23.95	(cncBoundaryPoint)	X10.965 Y12.45 24.05	(cncIRPoint) X2.897	F540.0 E83.061	(cncIRPoint)	F10M0.0 E83.31
(cncIRPoint) Y7.409 Z3.95	F10M0.0 E82.079	(cncBoundaryPoint)	X10.965 Y14.69 24.05	(cncIRPoint) X2.897	F540.0 E83.07	(cncIRPoint)	F10M0.0 E83.317
(cncIRPoint) X2.634	GI X3.23 Y8.0 23.95	(cncBoundaryPoint)	X10.965 Y16.93 24.05	(cncIRPoint) X2.897	F540.0 E83.079	(cncIRPoint)	F10M0.0 E83.324
(cncIRPoint) Y7.009 Z3.95	F10M0.0 E82.08	(cncBoundaryPoint)	X10.965 Y19.17 24.05	(cncIRPoint) X2.897	F540.0 E83.088	(cncIRPoint)	F10M0.0 E83.331
(cncIRPoint) X2.634	GI X3.23 Y8.4 23.95	(cncBoundaryPoint)	X10.965 Y21.41 24.05	(cncIRPoint) X2.897	F540.0 E83.097	(cncIRPoint)	F10M0.0 E83.338
(cncIRPoint) Y7.009 Z3.95	F10M0.0 E82.081	(cncBoundaryPoint)	X10.965 Y23.65 24.05	(cncIRPoint) X2.897	F540.0 E83.106	(cncIRPoint)	F10M0.0 E83.345
(cncIRPoint) X2.634	GI X3.43 Y8.4 23.95	(cncBoundaryPoint)	X10.965 Y25.89 24.05	(cncIRPoint) X2.897	F540.0 E83.115	(cncIRPoint)	F10M0.0 E83.352
(cncIRPoint) Y7.009 Z3.95	F10M0.0 E82.082	(cncBoundaryPoint)	X10.965 Y28.13 24.05	(cncIRPoint) X2.897	F540.0 E83.124	(cncIRPoint)	F10M0.0 E83.359
(cncIRPoint) X2.634	GI X3.43 Y8.8 23.95	(cncBoundaryPoint)	X10.965 Y30.37 24.05	(cncIRPoint) X2.897	F540.0 E83.133	(cncIRPoint)	F10M0.0 E83.366
(cncIRPoint) Y7.009 Z3.95	F10M0.0 E82.083	(cncBoundaryPoint)	X10.965 Y32.61 24.05	(cncIRPoint) X2.897	F540.0 E83.142	(cncIRPoint)	F10M0.0 E83.373
(cncIRPoint) X2.634	GI X3.43 Y9.2 23.95	(cncBoundaryPoint)	X10.965 Y34.85 24.05	(cncIRPoint) X2.897	F540.0 E83.151	(cncIRPoint)	F10M0.0 E83.38
(cncIRPoint) Y7.009 Z3.95	F10M0.0 E82.084	(cncBoundaryPoint)	X10.965 Y37.09 24.05	(cncIRPoint) X2.897	F540.0 E83.16	(cncIRPoint)	F10M0.0 E83.387
(cncIRPoint) X2.634	GI X3.43 Y9.6 23.95	(cncBoundaryPoint)	X10.965 Y39.33 24.05	(cncIRPoint) X2.897	F540.0 E83.169	(cncIRPoint)	F10M0.0 E83.394
(cncIRPoint) Y7.009 Z3.95	F10M0.0 E82.085	(cncBoundaryPoint)	X10.965 Y41.57 24.05	(cncIRPoint) X2.897	F540.0 E83.178	(cncIRPoint)	F10M0.0 E83.401
(cncIRPoint) X2.634	GI X3.43 Y10.0 23.95	(cncBoundaryPoint)	X10.965 Y43.81 24.05	(cncIRPoint) X2.897	F540.0 E83.187	(cncIRPoint)	F10M0.0 E83.408
(cncIRPoint) Y7.009 Z3.95	F10M0.0 E82.086	(cncBoundaryPoint)	X10.965 Y46.05 24.05	(cncIRPoint) X2.897	F540.0 E83.196	(cncIRPoint)	F10M0.0 E83.415
(cncIRPoint) X2.634	GI X3.43 Y10.4 23.95	(cncBoundaryPoint)	X10.965 Y48.29 24.05	(cncIRPoint) X2.897	F540.0 E83.205	(cncIRPoint)	F10M0.0 E83.422
(cncIRPoint) Y7.009 Z3.95	F10M0.0 E82.087	(cncBoundaryPoint)	X10.965 Y50.53 24.05	(cncIRPoint) X2.897	F540.0 E83.214	(cncIRPoint)	F10M0.0 E83.429
(cncIRPoint) X2.634	GI X3.43 Y10.8 23.95	(cncBoundaryPoint)	X10.965 Y52.77 24.05	(cncIRPoint) X2.897	F540.0 E83.223	(cncIRPoint)	F10M0.0 E83.436
(cncIRPoint) Y7.009 Z3.95	F10M0.0 E82.088	(cncBoundaryPoint)	X10.965 Y55.01 24.05	(cncIRPoint) X2.897	F540.0 E83.232	(cncIRPoint)	F10M0.0 E83.443
(cncIRPoint) X2.634	GI X3.43 Y11.2 23.95	(cncBoundaryPoint)	X10.965 Y57.25 24.05	(cncIRPoint) X2.897	F540.0 E83.241	(cncIRPoint)	F10M0.0 E83.45
(cncIRPoint) Y7.009 Z3.95	F10M0.0 E82.089	(cncBoundaryPoint)	X10.965 Y59.49 24.05	(cncIRPoint) X2.897	F540.0 E83.25	(cncIRPoint)	F10M0.0 E83.457
(cncIRPoint) X2.634	GI X3.43 Y11.6 23.95	(cncBoundaryPoint)	X10.965 Y61.73 24.05	(cncIRPoint) X2.897	F540.0 E83.259	(cncIRPoint)	F10M0.0 E83.464
(cncIRPoint) Y7.009 Z3.95	F10M0.0 E82.09	(cncBoundaryPoint)	X10.965 Y63.97 24.05	(cncIRPoint) X2.897	F540.0 E83.268	(cncIRPoint)	F10M0.0 E83.471
(cncIRPoint) X2.634	GI X3.43 Y12.0 23.95	(cncBoundaryPoint)	X10.965 Y66.21 24.05	(cncIRPoint) X2.897	F540.0 E83.277	(cncIRPoint)	F10M0.0 E83.478
(cncIRPoint) Y7.009 Z3.95	F10M0.0 E82.091	(cncBoundaryPoint)	X10.965 Y68.45 24.05	(cncIRPoint) X2.897	F540.0 E83.286	(cncIRPoint)	F10M0.0 E83.485
(cncIRPoint) X2.634	GI X3.43 Y12.4 23.95	(cncBoundaryPoint)	X10.965 Y70.69 24.05	(cncIRPoint) X2.897	F540.0 E83.295	(cncIRPoint)	F10M0.0 E83.492
(cncIRPoint) Y7.009 Z3.95	F10M0.0 E82.092	(cncBoundaryPoint)	X10.965 Y72.93 24.05	(cncIRPoint) X2.897	F540.0 E83.304	(cncIRPoint)	F10M0.0 E83.499
(cncIRPoint) X2.634	GI X3.43 Y12.8 23.95	(cncBoundaryPoint)	X10.965 Y75.17 24.05	(cncIRPoint) X2.897	F540.0 E83.313	(cncIRPoint)	F10M0.0 E83.506
(cncIRPoint) Y7.009 Z3.95	F10M0.0 E82.093	(cncBoundaryPoint)	X10.965 Y77.41 24.05	(cncIRPoint) X2.897	F540.0 E83.322	(cncIRPoint)	F10M0.0 E83.513
(cncIRPoint) X2.634	GI X3.43 Y13.2 23.95	(cncBoundaryPoint)	X10.965 Y79.65 24.05	(cncIRPoint) X2.897	F540.0 E83.331	(cncIRPoint)	F10M0.0 E83.52
(cncIRPoint) Y7.009 Z3.95	F10M0.0 E82.094	(cncBoundaryPoint)	X10.965 Y81.89 24.05	(cncIRPoint) X2.897	F540.0 E83.34	(cncIRPoint)	F10M0.0 E83.527
(cncIRPoint) X2.634	GI X3.43 Y13.6 23.95	(cncBoundaryPoint)	X10.965 Y84.13 24.05	(cncIRPoint) X2.897	F540.0 E83.349	(cncIRPoint)	F10M0.0 E83.534
(cncIRPoint) Y7.009 Z3.95	F10M0.0 E82.095	(cncBoundaryPoint)	X10.965 Y86.37 24.05	(cncIRPoint) X2.897	F540.0 E83.358	(cncIRPoint)	F10M0.0 E83.541
(cncIRPoint) X2.634	GI X3.43 Y14.0 23.95	(cncBoundaryPoint)	X10.965 Y88.61 24.05	(cncIRPoint) X2.897	F540.0 E83.367	(cncIRPoint)	F10M0.0 E83.548
(cncIRPoint) Y7.009 Z3.95	F10M0.0 E82.096	(cncBoundaryPoint)	X10.965 Y90.85 24.05	(cncIRPoint) X2.897	F540.0 E83.376	(cncIRPoint)	F10M0.0 E83.555
(cncIRPoint) X2.634	GI X3.43 Y14.4 23.95	(cncBoundaryPoint)	X10.965 Y93.09 24.05	(cncIRPoint) X2.897	F540.0 E83.385	(cncIRPoint)	F10M0.0 E83.562
(cncIRPoint) Y7.009 Z3.95	F10M0.0 E82.097	(cncBoundaryPoint)	X10.965 Y95.33 24.05	(cncIRPoint) X2.897	F540.0 E83.394	(cncIRPoint)	F10M0.0 E83.569
(cncIRPoint) X2.634	GI X3.43 Y14.8 23.95	(cncBoundaryPoint)	X10.965 Y97.57 24.05	(cncIRPoint) X2.897	F540.0 E83.403	(cncIRPoint)	F10M0.0 E83.576
(cncIRPoint) Y7.009 Z3.95	F10M0.0 E82.098	(cncBoundaryPoint)	X10.965 Y99.81 24.05	(cncIRPoint) X2.897	F540.0 E83.412	(cncIRPoint)	F10M0.0 E83.583
(cncIRPoint) X2.634	GI X3.43 Y15.2 23.95	(cncBoundaryPoint)	X10.965 Y102.05 24.05	(cncIRPoint) X2.897	F540.0 E83.421	(cncIRPoint)	F10M0.0 E83.59
(cncIRPoint) Y7.009 Z3.95	F10M0.0 E82.099	(cncBoundaryPoint)	X10.965 Y104.29 24.05	(cncIRPoint) X2.897	F540.0 E83.43	(cncIRPoint)	F10M0.0 E83.597
(cncIRPoint) X2.634	GI X3.43 Y15.6 23.95	(cncBoundaryPoint)	X10.965 Y106.53 24.05	(cncIRPoint) X2.897	F540.0 E83.44	(cncIRPoint)	F10M0.0 E83.604
(cncIRPoint) Y7.009 Z3.95	F10M0.0 E82.1	(cncBoundaryPoint)	X10.965 Y108.77 24.05	(cncIRPoint) X2.897	F540.0 E83.45	(cncIRPoint)	F10M0.0 E83.611
(cncIRPoint) X2.634	GI X3.43 Y16.0 23.95	(cncBoundaryPoint)	X10.965 Y111.01 24.05	(cncIRPoint) X2.897	F540.0 E83.46	(cncIRPoint)	F10M0.0 E83.618
(cncIRPoint) Y7.009 Z3.95	F10M0.0 E82.101	(cncBoundaryPoint)	X10.965 Y113.25 24.05	(cncIRPoint) X2.897	F540.0 E83.47	(cncIRPoint)	F10M0.0 E83.625
(cncIRPoint) X2.634	GI X3.43 Y16.4 23.95	(cncBoundaryPoint)	X10.965 Y115.49 24.05	(cncIRPoint) X2.897	F540.0 E83.48	(cncIRPoint)	F10M0.0 E83.632
(cncIRPoint) Y7.009 Z3.95	F10M0.0 E82.102	(cncBoundaryPoint)	X10.965 Y117.73 24.05	(cncIRPoint) X2.897	F540.0 E83.49	(cncIRPoint)	F10M0.0 E83.639
(cncIRPoint) X2.634	GI X3.43 Y16.8 23.95	(cncBoundaryPoint)	X10.965 Y119.97 24.05	(cncIRPoint) X2.897	F540.0 E83.5	(cncIRPoint)	F10M0.0 E83.646
(cncIRPoint) Y7.009 Z3.95	F10M0.0 E82.103	(cncBoundaryPoint)	X10.965 Y122.21 24.05	(cncIRPoint) X2.897	F540.0 E83.51	(cncIRPoint)	F10M0.0 E83.653
(cncIRPoint) X2.634	GI X3.43 Y17.2 23.95	(cncBoundaryPoint)	X10.965 Y124.45 24.05	(cncIRPoint) X2.897	F540.0 E83.52	(cncIRPoint)	F10M0.0 E83.66
(cncIRPoint) Y7.009 Z3.95	F10M0.0 E82.104	(cncBoundaryPoint)	X10.965 Y126.69 24.05	(cncIRPoint) X2.897	F540.0 E83.53	(cncIRPoint)	F10M0.0 E83.667
(cncIRPoint) X2.634	GI X3.43 Y17.6 23.95	(cncBoundaryPoint)	X10.965 Y128.93 24.05	(cncIRPoint) X2.897	F540.0 E83.54	(cncIRPoint)	F10M0.0 E83.674
(cncIRPoint) Y7.009 Z3.95	F10M0.0 E82.105	(cncBoundaryPoint)	X10.965 Y131.17 24.05	(cncIRPoint) X2.897	F540.0 E83.55	(cncIRPoint)	F10M0.0 E83.681
(cncIRPoint) X2.634	GI X3.43 Y18.0 23.95	(cncBoundaryPoint)	X10.965 Y133.41 24.05	(cncIRPoint) X2.897	F540.0 E83.56	(cncIRPoint)	F10M0.0 E83.688
(cncIRPoint) Y7.009 Z3.95	F10M0.0 E82.106	(cncBoundaryPoint)	X10.965 Y135.65 24.05	(cncIRPoint) X2.897	F540.0 E83.57	(cncIRPoint)	F10M0.0 E83.695
(cncIRPoint) X2.634	GI X3.43 Y18.4 23.95	(cncBoundaryPoint)	X10.965 Y137.89 24.05	(cncIRPoint) X2.897	F540.0 E83.58	(cncIRPoint)	F10M0.0 E83.702
(cncIRPoint) Y7.009 Z3.95	F10M0.0 E82.107	(cncBoundaryPoint)	X10.965 Y140.13 24.05	(cncIRPoint) X2.897	F540.0 E83.59	(cncIRPoint)	F10M0.0 E83.709
(cncIRPoint) X2.634	GI X3.43 Y18.8 23.95	(cncBoundaryPoint)	X10.965 Y142.37 24.05	(cncIRPoint) X2.897	F540.0 E83.6	(cncIRPoint)	F10M0.0 E83.716
(cncIRPoint) Y7.009 Z3.95	F10M0.0 E82.108	(cncBoundaryPoint)	X10.965 Y144.61 24.05	(cncIRPoint) X2.897	F540.0 E83.61	(cncIRPoint)	F10M0.0 E83.723
(cncIRPoint) X2.634	GI X3.43 Y19.2 23.95	(cncBoundaryPoint)	X10.965 Y146.85 24.05	(cncIRPoint) X2.897	F540.0 E83.62	(cncIRPoint)	F10M0.0 E83.73
(cncIRPoint) Y7.009 Z3.95	F10M0.0 E82.109	(cncBoundaryPoint)	X10.965 Y149.09 24.05	(cncIRPoint) X2.897	F540.0 E83.63	(cncIRPoint)	F10M0.0 E83.737
(cncIRPoint) X2.634	GI X3.43 Y19.6 23.95	(cncBoundaryPoint)	X10.965 Y151.33 24.05	(cncIRPoint) X2.897	F540.0 E83.64	(cncIRPoint)	F10M0.0 E83.744
(cncIRPoint) Y7.009 Z3.95	F10M0.0 E82.11	(cncBoundaryPoint)	X10.965 Y153.57 24.05				













GI X7.51 Y2.73 Z4.85  
 F540.0 E91.939  
 GI X7.99 Y2.59 Z4.85  
 F540.0 E91.944  
 GI X8.45 Y3.12 Z4.85  
 F540.0 E91.958  
 GI X8.45 Y3.41 Z4.85  
 F540.0 E91.967  
 GI X8.59 Y3.74 Z4.85  
 F540.0 E91.976  
 GI X8.59 Y3.13 Z4.85  
 F540.0 E91.985  
 GI X8.98 Y4.55 Z4.85  
 F540.0 E91.994  
 GI X10.1 Y5.01 Z4.85  
 F540.0 E92.004  
 GI X10.27 Y5.49 Z4.85  
 F540.0 E92.013  
 GI X10.37 Y5.99 Z4.85  
 F540.0 E92.022  
 GI X10.4 Y6.5 Z4.85  
 F540.0 E92.031  
 GI X10.37 Y7.13 Z4.85  
 F540.0 E92.041  
 GI X10.27 Y7.51 Z4.85  
 F540.0 E92.05  
 GI X10.1 Y7.99 Z4.85  
 F540.0 E92.059  
 GI X9.88 Y8.45 Z4.85  
 F540.0 E92.068  
 GI X9.59 Y8.7 Z4.85  
 F540.0 E92.077  
 GI X9.26 Y9.26 Z4.85  
 F540.0 E92.086  
 GI X8.97 Y9.45 Z4.85  
 F540.0 E92.096  
 GI X8.59 Y9.88 Z4.85  
 F540.0 E92.105  
 GI X8.28 Y10.4 Z4.85  
 F540.0 E92.114  
 GI X7.99 Y10.1 Z4.85  
 F540.0 E92.123  
 GI X7.72 Y10.4 Z4.85  
 F540.0 E92.132  
 GI X7.51 Y10.7 Z4.85  
 F540.0 E92.141  
 GI X7.26 Y11.01 Z4.85  
 F540.0 E92.150  
 GI X7.01 Y11.27 Z4.85  
 F540.0 E92.159  
 GI X6.76 Y11.54 Z4.85  
 F540.0 E92.168  
 GI X6.51 Y11.81 Z4.85  
 F540.0 E92.177  
 GI X6.26 Y12.08 Z4.85  
 F540.0 E92.186  
 GI X6.01 Y12.35 Z4.85  
 F540.0 E92.195  
 GI X5.76 Y12.62 Z4.85  
 F540.0 E92.204  
 GI X5.51 Y12.89 Z4.85  
 F540.0 E92.213  
 GI X5.26 Y13.16 Z4.85  
 F540.0 E92.222  
 GI X5.01 Y13.43 Z4.85  
 F540.0 E92.231  
 GI X4.76 Y13.7 Z4.85  
 F540.0 E92.240  
 GI X4.51 Y13.97 Z4.85  
 F540.0 E92.249  
 GI X4.26 Y14.24 Z4.85  
 F540.0 E92.258  
 GI X4.01 Y14.51 Z4.85  
 F540.0 E92.267  
 GI X3.76 Y14.78 Z4.85  
 F540.0 E92.276  
 GI X3.51 Y15.05 Z4.85  
 F540.0 E92.285  
 GI X3.26 Y15.32 Z4.85  
 F540.0 E92.294  
 GI X3.01 Y15.59 Z4.85  
 F540.0 E92.303  
 GI X2.76 Y15.86 Z4.85  
 F540.0 E92.312  
 GI X2.51 Y16.13 Z4.85  
 F540.0 E92.321  
 GI X2.26 Y16.4 Z4.85  
 F540.0 E92.330  
 GI X2.01 Y16.67 Z4.85  
 F540.0 E92.339  
 GI X1.76 Y16.94 Z4.85  
 F540.0 E92.348  
 GI X1.51 Y17.21 Z4.85  
 F540.0 E92.357  
 GI X1.26 Y17.48 Z4.85  
 F540.0 E92.366  
 GI X1.01 Y17.75 Z4.85  
 F540.0 E92.375  
 GI X0.76 Y18.02 Z4.85  
 F540.0 E92.384  
 GI X0.51 Y18.29 Z4.85  
 F540.0 E92.393  
 GI X0.26 Y18.56 Z4.85  
 F540.0 E92.402  
 GI X0.01 Y18.83 Z4.85  
 F540.0 E92.411  
 GI X0.01 Y19.1  
 F540.0 E92.420  
 GI X0.01 Y19.37  
 F540.0 E92.429  
 GI X0.01 Y19.64  
 F540.0 E92.438  
 GI X0.01 Y19.91  
 F540.0 E92.447  
 GI X0.01 Y20.18  
 F540.0 E92.456  
 GI X0.01 Y20.45  
 F540.0 E92.465  
 GI X0.01 Y20.72  
 F540.0 E92.474  
 GI X0.01 Y20.99  
 F540.0 E92.483  
 GI X0.01 Y21.26  
 F540.0 E92.492  
 GI X0.01 Y21.53  
 F540.0 E92.501  
 GI X0.01 Y21.8  
 F540.0 E92.510  
 GI X0.01 Y22.07  
 F540.0 E92.519  
 GI X0.01 Y22.34  
 F540.0 E92.528  
 GI X0.01 Y22.61  
 F540.0 E92.537  
 GI X0.01 Y22.88  
 F540.0 E92.546  
 GI X0.01 Y23.15  
 F540.0 E92.555  
 GI X0.01 Y23.42  
 F540.0 E92.564  
 GI X0.01 Y23.69  
 F540.0 E92.573  
 GI X0.01 Y23.96  
 F540.0 E92.582  
 GI X0.01 Y24.23  
 F540.0 E92.591  
 GI X0.01 Y24.5  
 F540.0 E92.600  
 GI X0.01 Y24.77  
 F540.0 E92.609  
 GI X0.01 Y25.04  
 F540.0 E92.618  
 GI X0.01 Y25.31  
 F540.0 E92.627  
 GI X0.01 Y25.58  
 F540.0 E92.636  
 GI X0.01 Y25.85  
 F540.0 E92.645  
 GI X0.01 Y26.12  
 F540.0 E92.654  
 GI X0.01 Y26.39  
 F540.0 E92.663  
 GI X0.01 Y26.66  
 F540.0 E92.672  
 GI X0.01 Y26.93  
 F540.0 E92.681  
 GI X0.01 Y27.2  
 F540.0 E92.690  
 GI X0.01 Y27.47  
 F540.0 E92.699  
 GI X0.01 Y27.74  
 F540.0 E92.708  
 GI X0.01 Y28.01  
 F540.0 E92.717  
 GI X0.01 Y28.28  
 F540.0 E92.726  
 GI X0.01 Y28.55  
 F540.0 E92.735  
 GI X0.01 Y28.82  
 F540.0 E92.744  
 GI X0.01 Y29.09  
 F540.0 E92.753  
 GI X0.01 Y29.36  
 F540.0 E92.762  
 GI X0.01 Y29.63  
 F540.0 E92.771  
 GI X0.01 Y29.9  
 F540.0 E92.780  
 GI X0.01 Y30.17  
 F540.0 E92.789  
 GI X0.01 Y30.44  
 F540.0 E92.798  
 GI X0.01 Y30.71  
 F540.0 E92.807  
 GI X0.01 Y30.98  
 F540.0 E92.816  
 GI X0.01 Y31.25  
 F540.0 E92.825  
 GI X0.01 Y31.52  
 F540.0 E92.834  
 GI X0.01 Y31.79  
 F540.0 E92.843  
 GI X0.01 Y32.06  
 F540.0 E92.852  
 GI X0.01 Y32.33  
 F540.0 E92.861  
 GI X0.01 Y32.6  
 F540.0 E92.870  
 GI X0.01 Y32.87  
 F540.0 E92.879  
 GI X0.01 Y33.14  
 F540.0 E92.888  
 GI X0.01 Y33.41  
 F540.0 E92.897  
 GI X0.01 Y33.68  
 F540.0 E92.906  
 GI X0.01 Y33.95  
 F540.0 E92.915  
 GI X0.01 Y34.22  
 F540.0 E92.924  
 GI X0.01 Y34.49  
 F540.0 E92.933  
 GI X0.01 Y34.76  
 F540.0 E92.942  
 GI X0.01 Y35.03  
 F540.0 E92.951  
 GI X0.01 Y35.3  
 F540.0 E92.960  
 GI X0.01 Y35.57  
 F540.0 E92.969  
 GI X0.01 Y35.84  
 F540.0 E92.978  
 GI X0.01 Y36.11  
 F540.0 E92.987  
 GI X0.01 Y36.38  
 F540.0 E92.996  
 GI X0.01 Y36.65  
 F540.0 E93.005  
 GI X0.01 Y36.92  
 F540.0 E93.014  
 GI X0.01 Y37.19  
 F540.0 E93.023  
 GI X0.01 Y37.46  
 F540.0 E93.032  
 GI X0.01 Y37.73  
 F540.0 E93.041  
 GI X0.01 Y38.0  
 F540.0 E93.050  
 GI X0.01 Y38.27  
 F540.0 E93.059  
 GI X0.01 Y38.54  
 F540.0 E93.068  
 GI X0.01 Y38.81  
 F540.0 E93.077  
 GI X0.01 Y39.08  
 F540.0 E93.086  
 GI X0.01 Y39.35  
 F540.0 E93.095  
 GI X0.01 Y39.62  
 F540.0 E93.104  
 GI X0.01 Y39.89  
 F540.0 E93.113  
 GI X0.01 Y40.16  
 F540.0 E93.122  
 GI X0.01 Y40.43  
 F540.0 E93.131  
 GI X0.01 Y40.7  
 F540.0 E93.140  
 GI X0.01 Y40.97  
 F540.0 E93.149  
 GI X0.01 Y41.24  
 F540.0 E93.158  
 GI X0.01 Y41.51  
 F540.0 E93.167  
 GI X0.01 Y41.78  
 F540.0 E93.176  
 GI X0.01 Y42.05  
 F540.0 E93.185  
 GI X0.01 Y42.32  
 F540.0 E93.194  
 GI X0.01 Y42.59  
 F540.0 E93.203  
 GI X0.01 Y42.86  
 F540.0 E93.212  
 GI X0.01 Y43.13  
 F540.0 E93.221  
 GI X0.01 Y43.4  
 F540.0 E93.230  
 GI X0.01 Y43.67  
 F540.0 E93.239  
 GI X0.01 Y43.94  
 F540.0 E93.248  
 GI X0.01 Y44.21  
 F540.0 E93.257  
 GI X0.01 Y44.48  
 F540.0 E93.266  
 GI X0.01 Y44.75  
 F540.0 E93.275  
 GI X0.01 Y45.02  
 F540.0 E93.284  
 GI X0.01 Y45.29  
 F540.0 E93.293  
 GI X0.01 Y45.56  
 F540.0 E93.302  
 GI X0.01 Y45.83  
 F540.0 E93.311  
 GI X0.01 Y46.1  
 F540.0 E93.320  
 GI X0.01 Y46.37  
 F540.0 E93.329  
 GI X0.01 Y46.64  
 F540.0 E93.338  
 GI X0.01 Y46.91  
 F540.0 E93.347  
 GI X0.01 Y47.18  
 F540.0 E93.356  
 GI X0.01 Y47.45  
 F540.0 E93.365  
 GI X0.01 Y47.72  
 F540.0 E93.374  
 GI X0.01 Y47.99  
 F540.0 E93.383  
 GI X0.01 Y48.26  
 F540.0 E93.392  
 GI X0.01 Y48.53  
 F540.0 E93.401  
 GI X0.01 Y48.8  
 F540.0 E93.410  
 GI X0.01 Y49.07  
 F540.0 E93.419  
 GI X0.01 Y49.34  
 F540.0 E93.428  
 GI X0.01 Y49.61  
 F540.0 E93.437  
 GI X0.01 Y49.88  
 F540.0 E93.446  
 GI X0.01 Y50.15  
 F540.0 E93.455  
 GI X0.01 Y50.42  
 F540.0 E93.464  
 GI X0.01 Y50.69  
 F540.0 E93.473  
 GI X0.01 Y50.96  
 F540.0 E93.482  
 GI X0.01 Y51.23  
 F540.0 E93.491  
 GI X0.01 Y51.5  
 F540.0 E93.500  
 GI X0.01 Y51.77  
 F540.0 E93.509  
 GI X0.01 Y52.04  
 F540.0 E93.518  
 GI X0.01 Y52.31  
 F540.0 E93.527  
 GI X0.01 Y52.58  
 F540.0 E93.536  
 GI X0.01 Y52.85  
 F540.0 E93.545  
 GI X0.01 Y53.12  
 F540.0 E93.554  
 GI X0.01 Y53.39  
 F540.0 E93.563  
 GI X0.01 Y53.66  
 F540.0 E93.572  
 GI X0.01 Y53.93  
 F540.0 E93.581  
 GI X0.01 Y54.2  
 F540.0 E93.590  
 GI X0.01 Y54.47  
 F540.0 E93.599  
 GI X0.01 Y54.74  
 F540.0 E93.608  
 GI X0.01 Y55.01  
 F540.0 E93.617  
 GI X0.01 Y55.28  
 F540.0 E93.626  
 GI X0.01 Y55.55  
 F540.0 E93.635  
 GI X0.01 Y55.82  
 F540.0 E93.644  
 GI X0.01 Y56.09  
 F540.0 E93.653  
 GI X0.01 Y56.36  
 F540.0 E93.662  
 GI X0.01 Y56.63  
 F540.0 E93.671  
 GI X0.01 Y56.9  
 F540.0 E93.680  
 GI X0.01 Y57.17  
 F540.0 E93.689  
 GI X0.01 Y57.44  
 F540.0 E93.698  
 GI X0.01 Y57.71  
 F540.0 E93.707  
 GI X0.01 Y57.98  
 F540.0 E93.716  
 GI X0.01 Y58.25  
 F540.0 E93.725  
 GI X0.01 Y58.52  
 F540.0 E93.734  
 GI X0.01 Y58.79  
 F540.0 E93.743  
 GI X0.01 Y59.06  
 F540.0 E93.752  
 GI X0.01 Y59.33  
 F540.0 E93.761  
 GI X0.01 Y59.6  
 F540.0 E93.770  
 GI X0.01 Y59.87  
 F540.0 E93.779  
 GI X0.01 Y60.14  
 F540.0 E93.788  
 GI X0.01 Y60.41  
 F540.0 E93.797  
 GI X0.01 Y60.68  
 F540.0 E93.806  
 GI X0.01 Y60.95  
 F540.0 E93.815  
 GI X0.01 Y61.22  
 F540.0 E93.824  
 GI X0.01 Y61.49  
 F540.0 E93.833  
 GI X0.01 Y61.76  
 F540.0 E93.842  
 GI X0.01 Y62.03  
 F540.0 E93.851  
 GI X0.01 Y62.3  
 F540.0 E93.860  
 GI X0.01 Y62.57  
 F540.0 E93.869  
 GI X0.01 Y62.84  
 F540.0 E93.878  
 GI X0.01 Y63.11  
 F540.0 E93.887  
 GI X0.01 Y63.38  
 F540.0 E93.896  
 GI X0.01 Y63.65  
 F540.0 E93.905  
 GI X0.01 Y63.92  
 F540.0 E93.914  
 GI X0.01 Y64.19  
 F540.0 E93.923  
 GI X0.01 Y64.46  
 F540.0 E93.932  
 GI X0.01 Y64.73  
 F540.0 E93.941  
 GI X0.01 Y65.0  
 F540.0 E93.950  
 GI X0.01 Y65.27  
 F540.0 E93.959  
 GI X0.01 Y65.54  
 F540.0 E93.968  
 GI X0.01 Y65.81  
 F540.0 E93.977  
 GI X0.01 Y66.08  
 F540.0 E93.986  
 GI X0.01 Y66.35  
 F540.0 E93.995  
 GI X0.01 Y66.62  
 F540.0 E94.004  
 GI X0.01 Y66.89  
 F540.0 E94.013  
 GI X0.01 Y67.16  
 F540.0 E94.022  
 GI X0.01 Y67.43  
 F540.0 E94.031  
 GI X0.01 Y67.7  
 F540.0 E94.040  
 GI X0.01 Y67.97  
 F540.0 E94.049  
 GI X0.01 Y68.24  
 F540.0 E94.058  
 GI X0.01 Y68.51  
 F540.0 E94.067  
 GI X0.01 Y68.78  
 F540.0 E94.076  
 GI X0.01 Y69.05  
 F540.0 E94.085  
 GI X0.01 Y69.32  
 F540.0 E94.094  
 GI X0.01 Y69.59  
 F540.0 E94.103  
 GI X0.01 Y69.86  
 F540.0 E94.112  
 GI X0.01 Y70.13  
 F540.0 E94.121  
 GI X0.01 Y70.4  
 F540.0 E94.130  
 GI X0.01 Y70.67  
 F540.0 E94.139  
 GI X0.01 Y70.94  
 F540.0 E94.148  
 GI X0.01 Y71.21  
 F540.0 E94.157  
 GI X0.01 Y71.48  
 F540.0 E94.166  
 GI X0.01 Y71.75  
 F540.0 E94.175  
 GI X0.01 Y72.02  
 F540.0 E94.184  
 GI X0.01 Y72.29  
 F540.0 E94.193  
 GI X0.01 Y72.56  
 F540.0 E94.202  
 GI X0.01 Y72.83  
 F540.0 E94.211  
 GI X0.01 Y73.1  
 F540.0 E94.220  
 GI X0.01 Y73.37  
 F540.0 E94.229  
 GI X0.01 Y73.64  
 F540.0 E94.238  
 GI X0.01 Y73.91  
 F540.0 E94.247  
 GI X0.01 Y74.18  
 F540.0 E94.256  
 GI X0.01 Y74.45  
 F540.0 E94.265  
 GI X0.01 Y74.72  
 F540.0 E94.274  
 GI X0.01 Y74.99  
 F540.0 E94.283  
 GI X0.01 Y75.26  
 F540.0 E94.292  
 GI X0.01 Y75.53  
 F540.0 E94.301  
 GI X0.01 Y75.8  
 F540.0 E94.310  
 GI X0.01 Y76.07  
 F540.0 E94.319  
 GI X0.01 Y76.34  
 F540.0 E94.328  
 GI X0.01 Y76.61  
 F540.0 E94.337  
 GI X0.01 Y76.88  
 F540.0 E94.346  
 GI X0.01 Y77.15  
 F540.0 E94.355  
 GI X0.01 Y77.42  
 F540.0 E94.364  
 GI X0.01 Y77.69  
 F540.0 E94.373  
 GI X0.01 Y77.96  
 F540.0 E94.382  
 GI X0.01 Y78.23  
 F540.0 E94.391  
 GI X0.01 Y78.5  
 F540.0 E94.400  
 GI X0.01 Y78.77  
 F540.0 E94.409  
 GI X0.01 Y79.04  
 F540.0 E94.418  
 GI X0.01 Y79.31  
 F540.0 E94.427  
 GI X0.01 Y79.58  
 F540.0 E94.436  
 GI X0.01 Y79.85  
 F540.0 E94.445  
 GI X0.01 Y80.12  
 F540.0 E94.454  
 GI X0.01 Y80.39  
 F540.0 E94.463  
 GI X0.01 Y80.66  
 F540.0 E94.472  
 GI X0.01 Y80.93  
 F540.0 E94.481  
 GI X0.01 Y81.2  
 F540.0 E94.490  
 GI X0.01 Y81.47  
 F540.0 E94.499  
 GI X0.01 Y81.74  
 F540.0 E94.508  
 GI X0.01 Y82.01  
 F540.0 E94.517  
 GI X0.01 Y82.28  
 F540.0 E94.526  
 GI X0.01 Y82.55  
 F540.0 E94.535  
 GI X0.01 Y82.82  
 F540.0 E94.544  
 GI X0.01 Y83.09  
 F540.0 E94.553  
 GI X0.01 Y83.36  
 F540.0 E94.562  
 GI X0.01 Y83.63  
 F540.0 E94.571  
 GI X0.01 Y83.9  
 F540.0 E94.580  
 GI X0.01 Y84.17  
 F540.0 E94.589  
 GI X0.01 Y84.44  
 F540.0 E94.598  
 GI X0.01 Y84.71  
 F540.0 E94.607  
 GI X0.01 Y84.98  
 F540.0 E94.616  
 GI X0.01 Y85.25  
 F540.0 E94.625  
 GI X0.01 Y85.52  
 F540.0 E94.634  
 GI X0.01 Y85.79  
 F540.0 E94.643  
 GI X0.01 Y86.06  
 F540.0 E94.652  
 GI X0.01 Y86.33  
 F540.0 E94.661  
 GI X0.01 Y86.6  
 F540.0 E94.670  
 GI X0.01 Y86.87  
 F540.0 E94.679  
 GI X0.01 Y87.14  
 F540.0 E94.688  
 GI X0.01 Y87.41  
 F540.0 E94.697  
 GI X0.01 Y87.68  
 F540.0 E94.706  
 GI X0.01 Y87.95  
 F540.0 E94.715  
 GI X0.01 Y88.22  
 F540.0 E94.724  
 GI X0.01 Y88.49  
 F540.0 E94.733  
 GI X0.01 Y88.76  
 F540.0 E94.742  
 GI X0.01 Y89.03  
 F540.0 E94.751  
 GI X0.01 Y89.3  
 F540.0 E94.760  
 GI X0.01 Y89.57  
 F540.0 E94.769  
 GI X0.01 Y89.84  
 F540.0 E94.778  
 GI X0.01 Y90.11  
 F540.0 E94.787  
 GI X0.01 Y90.38  
 F540.0 E94.796  
 GI X0.01 Y90.65  
 F540.0 E94.805  
 GI X0.01 Y90.92  
 F540.0 E94.814  
 GI X0.01 Y91.19  
 F540.0 E94.823  
 GI X0.01 Y91.46  
 F540.0 E94.832  
 GI X0.01 Y91.73  
 F540.0 E94.841  
 GI X0.01 Y92.0  
 F540.0 E94.850  
 GI X0.01 Y92.27  
 F540.0 E94.859  
 GI X0.01 Y92.54  
 F540.0 E94.868  
 GI X0.01 Y92.81  
 F540.0 E94.877  
 GI X0.01 Y93.08  
 F540.0 E94.886  
 GI X0.01 Y93.35  
 F540.0 E94.895  
 GI X0.01 Y93.62  
 F540.0 E94.904  
 GI X0.01 Y93.89  
 F540.0 E94.913  
 GI X0.01 Y94.16  
 F540.0 E94.922  
 GI X0.01 Y94.43  
 F540.0 E94.931  
 GI X0.01 Y94.7  
 F540.0 E94.940  
 GI X0.01 Y94.97  
 F540.0 E94.949  
 GI X0.01 Y95.24  
 F540.0 E94.958  
 GI X0.01 Y95.51  
 F540.0 E94.967  
 GI X0.01 Y95.78  
 F540.0 E94.976  
 GI X0.01 Y96.05  
 F540.0 E94.985  
 GI X0.01 Y96.32  
 F540.0 E94.994  
 GI X0.01 Y96.59  
 F540.0 E95.003  
 GI X0.01 Y96.86  
 F540.0 E95.012  
 GI X0.01 Y97.13  
 F540.0 E95.021  
 GI X0.01 Y97.4  
 F540.0 E95.030  
 GI X0.01 Y97.67  
 F540.0 E95.039  
 GI X0.01 Y97.94  
 F540.0 E95.048  
 GI X0.01 Y98.21  
 F540.0 E95.057  
 GI X0.01 Y98.48  
 F540.0 E95.066  
 GI X0.01 Y98.75  
 F540.0 E95.075  
 GI X0.01 Y99.02  
 F540.0 E95.084  
 GI X0.01 Y99.29  
 F540.0 E95.093  
 GI X0.01 Y99.56  
 F540.0 E95.102  
 GI X0.01 Y99.83  
 F540.0 E95.111  
 GI X0.01 Y100.1  
 F540.0 E95.120  
 GI X0.01 Y100.37  
 F540.0 E95.129  
 GI X0.01 Y100.64  
 F540.0 E95.138  
 GI X0.01 Y100.91  
 F540.0 E95.147  
 GI X0.01 Y101.18  
 F540.0 E95.156  
 GI X0.01 Y101.45  
 F540.0 E95.165  
 GI X0.01 Y101.72  
 F540.0 E95.174  
 GI X0.01 Y101.99  
 F540.0 E95.183  
 GI X0.01 Y102.26  
 F540.0 E95.192  
 GI X0.01 Y102.53  
 F540.0 E95.201  
 GI X0.01 Y102.8  
 F540.0 E95.210  
 GI X0.01 Y103.07  
 F540.0 E95.219  
 GI X0.01 Y103.34  
 F540.0 E95.228  
 GI X0.01 Y103.61  
 F540.0 E95.237  
 GI X0.01 Y103.88







GI X8.87 Y9.74 25.25	<(null)Point> X4.126	GI X8.6 Y10.04 25.25	<(boundaryPoint)>	GI X3.41 Y4.13 25.35	<(null)Point> X2.734
P840.8.189.189	<(null)Point>	F1000.0.897.507	<(boundaryPoint)>	F1000.0.898.447	P7.509.25.35
GI X6.37 Y9.8 25.25	<(null)Point>	GI X6.0 Y10.08 25.25	<(boundaryPoint)>	GI X6.56 Y1.73 25.35	<(null)Point>
P840.8.197.198	<(null)Point> X3.743	F1000.0.897.508	<(boundaryPoint)>	F840.0.896.466	P840.0.896.466
GI X6.88 Y9.78 25.25	<(null)Point> X7.25	GI X6.4 Y10.11 25.25	<(boundaryPoint)>	GI F1200.0	GI X0.71 Y7.25 25.35
P840.8.197.207	<(null)Point> X4.406	F1000.0.897.515	<(boundaryPoint)>	GI E98.252	P840.0.898.475
GI X7.17 Y9.68 25.25	<(null)Point> Y8.474 25.25	F1000.0.897.516	<(boundaryPoint)>	F1000.0.897.400	P840.0.898.484
P840.8.197.216	<(null)Point>	GI X6.8 Y10.16 25.25	<(boundaryPoint)>	M101	<(edge)>
GI X7.85 Y9.51 25.25	<(null)Point>	F1000.0.897.523	<(boundaryPerimeter)>	GI X8.79 Y9.25 25.35	P840.0.898.494
P840.8.197.225	<(null)Point> X3.123	GI X6.8 Y10.26 25.25	<(boundaryPerimeter)>	GI X5.25 Y5.75 25.35	<(null)Point>
GI X8.29 Y9.27 25.25	<(null)Point>	F1000.0.897.524	<(boundaryPerimeter)>	P840.0.898.503	<(null)Point> X6.713
P840.8.197.234	<(null)Point> X2.897	GI X7.2 Y10.04 25.25	<(boundaryPoint)>	GI X6.56 Y7.27 25.35	<(null)Point>
GI X8.7 Y8.96 25.25	<(null)Point> Y7.992 25.25	F1000.0.897.531	<(boundaryPoint)>	P840.0.898.512	<(null)Point> X9.561
P840.8.197.243	<(null)Point>	GI X7.2 Y10.0 25.25	<(boundaryPoint)>	GI X9.34 Y4.81 25.35	Y5.266 25.35
GI X9.05 Y8.25 25.25	<(null)Point> X2.734	F1000.0.897.532	<(boundaryPoint)>	P840.0.898.521	<(null)Point>
P840.8.197.255	<(null)Point> Y7.509 25.25	GI X7.6 Y9.94 25.25	<(boundaryPoint)>	GI X0.98 Y4.4 25.35	<(null)Point> X9.337
GI X9.34 Y8.19 25.25	<(null)Point> X2.634	F1000.0.897.539	<(boundaryPoint)>	GI X3.7 Y3.32 25.35	P840.0.898.531
P840.8.197.266	<(null)Point> Y7.009 25.25	GI X7.6 Y9.29 25.25	<(boundaryPoint)>	GI X8.7 Y4.4 25.35	<(null)Point> X8.904
GI X8.7 Y7.25 25.25	<(null)Point> Y7.009 25.25	F1000.0.897.544	<(boundaryPoint)>	GI X0.98 Y4.4 25.35	P840.0.898.542
P840.8.197.275	<(null)Point> X5.713	GI X8.8 Y9.37 25.25	<(boundaryPoint)>	GI X7.3 Y3.32 25.35	<(null)Point> X9.047
P840.8.197.284	<(null)Point> X2.6.16.5	GI X8.0 Y10.11 25.25	<(boundaryPoint)>	GI X8.29 Y3.73 25.35	<(null)Point> X9.474
GI X8.79 Y6.75 25.25	<(null)Point> Y5.748 25.25	F1000.0.897.548	<(boundaryPoint)>	P840.0.898.548	<(null)Point> X8.696
P840.8.197.289	<(null)Point>	GI X8.0 Y9.78 25.25	<(boundaryPoint)>	GI X7.85 Y1.49 25.35	Y4.036 25.35
GI X8.79 Y6.75 25.25	<(null)Point> X9.713	F1000.0.897.549	<(boundaryPoint)>	P840.0.898.558	<(null)Point> X8.294
P840.8.197.298	<(null)Point> Y5.748 25.25	GI X8.8 Y9.53 25.25	<(boundaryPoint)>	GI X0.98 Y4.4 25.35	<(null)Point> X8.785
GI X0.71 Y7.25 25.25	<(null)Point>	F1000.0.897.557	<(boundaryPoint)>	GI X6.88 Y3.22 25.35	Y3.121 25.35
P840.8.197.307	<(null)Point>	GI X8.8 Y9.29 25.25	<(boundaryPoint)>	GI X7.85 Y1.49 25.35	<(null)Point> X8.696
GI X9.56 Y7.27 25.25	<(null)Point> X9.561	F1000.0.897.565	<(boundaryPoint)>	GI X8.7 Y3.26 25.35	<(null)Point> X7.374
P840.8.197.317	<(null)Point> Y4.036 25.25	GI X8.8 Y9.34 25.25	<(boundaryPoint)>	GI X5.25 Y5.75 25.35	<(null)Point> X8.696
GI X9.34 Y4.81 25.25	<(null)Point> X9.047	F1000.0.897.576	<(boundaryPoint)>	GI X8.7 Y3.26 25.35	<(null)Point> X7.879
P840.8.197.325	<(null)Point> X3.337	GI X9.2 Y8.9 25.25	<(boundaryPoint)>	GI X8.5 Y3.19 25.35	Y3.118 25.35
GI X9.05 Y4.25 25.25	<(null)Point> X9.561	F1000.0.897.576	<(boundaryPoint)>	P840.0.898.603	<(null)Point> X9.379
P840.8.197.335	<(null)Point> X9.047	GI X9.2 Y8.9 25.25	<(boundaryPoint)>	GI X4.82 Y3.6 25.35	<(null)Point> X9.870
GI X8.79 Y4.04 25.25	<(null)Point> X9.047	F1000.0.897.588	<(boundaryPoint)>	P840.0.898.627	Y3.221 25.35
P840.8.197.344	<(null)Point> Y4.25 25.25	GI X0.71 Y7.27 25.25	<(boundaryPoint)>	GI X8.5 Y3.18 25.35	<(null)Point> X9.379
GI X8.29 Y9.27 25.25	<(null)Point> X9.294	F1000.0.897.597	<(boundaryPoint)>	GI X4.5 Y2.08 25.35	<(null)Point> X8.696
P840.8.197.353	<(null)Point> X8.696	GI X0.71 Y7.27 25.25	<(boundaryPoint)>	GI X8.5 Y3.19 25.35	<(null)Point> X8.696
GI X8.79 Y4.25 25.25	<(null)Point> X8.696	GI X8.6 Y10.28 25.25	<(boundaryPoint)>	GI X8.7 Y3.26 25.35	<(null)Point> X8.696
P840.8.197.362	<(null)Point> X9.337	GI X9.8 Y9.29 25.25	<(boundaryPoint)>	GI X8.7 Y3.26 25.35	<(null)Point> X8.696
P840.8.197.371	<(null)Point> X9.294	F1000.0.897.597	<(boundaryPoint)>	GI X8.7 Y3.26 25.35	<(null)Point> X8.696
GI X6.88 Y3.22 25.25	<(null)Point> X7.85	GI X8.6 Y10.28 25.25	<(boundaryPoint)>	GI X8.7 Y3.26 25.35	<(null)Point> X8.696
P840.8.197.381	<(null)Point> Y3.848 25.25	GI X8.6 Y10.28 25.25	<(boundaryPoint)>	GI X8.7 Y3.26 25.35	<(null)Point> X8.696
GI X6.37 Y3.2 25.25	<(null)Point> X9.374	F1000.0.897.603	<(boundaryPoint)>	GI X8.7 Y3.26 25.35	<(null)Point> X8.696
P840.8.197.390	<(null)Point> Y3.118 25.25	GI X9.8 Y9.16 25.25	<(boundaryPoint)>	GI X8.7 Y3.26 25.35	<(null)Point> X8.696
GI X5.18 Y3.19 25.25	<(null)Point> X6.879	F1000.0.897.617	<(boundaryPoint)>	GI X8.7 Y3.26 25.35	<(null)Point> X8.696
P840.8.197.400	<(null)Point> X6.879	GI X8.6 Y10.28 25.25	<(boundaryPoint)>	GI X8.7 Y3.26 25.35	<(null)Point> X8.696
GI X4.5 Y3.6 25.25	<(null)Point> X5.25	F1000.0.897.627	<(boundaryPoint)>	GI X8.7 Y3.26 25.35	<(null)Point> X8.696
P840.8.197.417	<(null)Point> X6.374	GI X8.6 Y10.28 25.25	<(boundaryPoint)>	GI X8.7 Y3.26 25.35	<(null)Point> X8.696
GI X4.5 Y3.88 25.25	<(null)Point> X6.374	GI X8.8 Y9.29 25.25	<(boundaryPoint)>	GI X8.7 Y3.26 25.35	<(null)Point> X8.696
P840.8.197.426	<(null)Point> X6.374	F1000.0.897.648	<(boundaryPoint)>	GI X8.7 Y3.26 25.35	<(null)Point> X8.696
GI X4.12 Y4.21 25.25	<(null)Point> X8.872	GI X8.8 Y9.17 25.25	<(boundaryPoint)>	GI X8.7 Y3.26 25.35	<(null)Point> X8.696
P840.8.197.435	<(null)Point> X8.872	F1000.0.897.681	<(boundaryPoint)>	GI X8.7 Y3.26 25.35	<(null)Point> X8.696
GI X4.08 Y4.29 25.25	<(null)Point> X8.872	GI X8.8 Y9.47 25.25	<(boundaryPoint)>	GI X8.7 Y3.26 25.35	<(null)Point> X8.696
P840.8.197.447	<(null)Point> X8.872	F1000.0.897.69	<(boundaryPoint)>	GI X8.7 Y3.26 25.35	<(null)Point> X8.696
GI F1200.0	<(null)Point> X3.384	GI X8.8 Y9.48 25.25	<(boundaryPoint)>	GI X8.7 Y3.26 25.35	<(null)Point> X8.696
GI E96.437	<(null)Point> Y3.393 25.25	F1000.0.897.691	<(boundaryPoint)>	GI X8.7 Y3.26 25.35	<(null)Point> X8.696
GI F1540.0	<(null)Point> X4.923	GI X8.8 Y9.28 25.25	<(boundaryPoint)>	GI X8.7 Y3.26 25.35	<(null)Point> X8.696
<(boundaryPerimeter)>	<(null)Point> X4.923	F1000.0.897.703	<(boundaryPoint)>	GI X8.7 Y3.26 25.35	<(null)Point> X8.696
<(nestedRing)>	<(null)Point> X4.5	GI X8.8 Y9.28 25.25	<(boundaryPoint)>	GI X8.7 Y3.26 25.35	<(null)Point> X8.696
<(null)>	<(null)Point> X6.879	F1000.0.897.707	<(boundaryPoint)>	GI X8.7 Y3.26 25.35	<(null)Point> X8.696
<(null)Point> X2.634	<(null)Point> X6.879	GI X8.7 Y3.26 25.25	<(boundaryPoint)>	GI X8.7 Y3.26 25.35	<(null)Point> X8.696
Y5.991 25.25	<(null)Point> X4.122	F1000.0.897.707	<(boundaryPoint)>	GI X8.7 Y3.26 25.35	<(null)Point> X8.696
<(null)Point>	Y4.211 25.25	GI X7.2 Y3.25 25.25	<(boundaryPoint)>	GI X8.7 Y3.26 25.35	<(null)Point> X8.696
<(null)Point> X2.734	Y5.491 25.25	F1000.0.897.735	<(boundaryPoint)>	GI X8.7 Y3.26 25.35	<(null)Point> X8.696
Y5.491 25.25	<(null)Point> X3.8	GI X7.2 Y9.26 25.25	<(boundaryPoint)>	GI X8.7 Y3.26 25.35	<(null)Point> X8.696
<(null)Point> X2.897	<(null)Point>	GI X6.8 Y9.24 25.25	<(boundaryPoint)>	GI X8.7 Y3.26 25.35	<(null)Point> X8.696
Y5.008 25.25	<(null)Point> X3.542	F1000.0.897.723	<(boundaryPoint)>	GI X8.7 Y3.26 25.35	<(null)Point> X8.696
<(null)Point> X3.123	Y4.55 25.25	GI X6.8 Y9.25 25.25	<(boundaryPoint)>	GI X8.7 Y3.26 25.35	<(null)Point> X8.696
Y4.55 25.25	<(null)Point> X3.353	F1000.0.897.731	<(boundaryPoint)>	GI X8.7 Y3.26 25.35	<(null)Point> X8.696
<(null)Point> X4.106	Y5.404 25.25	GI X6.4 Y9.28 25.25	<(boundaryPoint)>	GI X8.7 Y3.26 25.35	<(null)Point> X8.696
P840.8.197.454	<(null)Point> X4.126	GI X6.4 Y9.28 25.25	<(boundaryPoint)>	GI X8.7 Y3.26 25.35	<(null)Point> X8.696
P840.8.197.463	<(null)Point> X3.743	F1000.0.897.731	<(boundaryPoint)>	GI X8.7 Y3.26 25.35	<(null)Point> X8.696
Y5.142 25.25	<(null)Point> X3.238	GI X6.8 Y9.28 25.25	<(boundaryPoint)>	GI X8.7 Y3.26 25.35	<(null)Point> X8.696
<(null)Point> X4.126	Y6.5 25.25	GI X6.8 Y9.28 25.25	<(boundaryPoint)>	GI X8.7 Y3.26 25.35	<(null)Point> X8.696
Y5.406 25.25	<(null)Point> X3.238	F1000.0.897.739	<(boundaryPoint)>	GI X8.7 Y3.26 25.35	<(null)Point> X8.696
<(null)Point> X4.55	Y7.004 25.25	GI X6.8 Y9.28 25.25	<(boundaryPoint)>	GI X8.7 Y3.26 25.35	<(null)Point> X8.696
Y3.123 25.25	<(null)Point> X3.353	F1000.0.897.747	<(boundaryPoint)>	GI X8.7 Y3.26 25.35	<(null)Point> X8.696
<(null)Point> X5.008	Y7.496 25.25	GI X6.8 Y9.28 25.25	<(boundaryPoint)>	GI X8.7 Y3.26 25.35	<(null)Point> X8.696
Y2.907 25.25	<(null)Point> X3.542	F1000.0.897.756	<(boundaryPoint)>	GI X8.7 Y3.26 25.35	<(null)Point> X8.696
P840.8.197.474	<(null)Point> X3.542	GI X6.8 Y9.28 25.25	<(boundaryPoint)>	GI X8.7 Y3.26 25.35	<(null)Point> X8.696
Y2.74 25.25	<(null)Point> X3.8	F1000.0.897.763	<(boundaryPoint)>	GI X8.7 Y3.26 25.35	<(null)Point> X8.696
<(null)Point> X3.991	X8.198 25.25	GI X8.8 Y9.35 25.25	<(boundaryPoint)>	GI X8.7 Y3.26 25.35	<(null)Point> X8.696
Y2.634 25.25	<(null)Point> X4.122	F1000.0.897.764	<(boundaryPoint)>	GI X8.7 Y3.26 25.35	<(null)Point> X8.696
GI X4.12 Y4.25 25.25	<(null)Point> X8.198 25.25	GI X4.4 Y3.56 25.25	<(boundaryPoint)>	GI X8.7 Y3.26 25.35	<(null)Point> X8.696
Y5.25.25<(null)Point> X3.606	Y7.859 25.25	F1000.0.897.773	<(boundaryPoint)>	GI X8.7 Y3.26 25.35	<(null)Point> X8.696
Y2.634 25.25	<(null)Point> X4.5	GI X4.0 Y3.89 25.25	<(boundaryPoint)>	GI X8.7 Y3.26 25.35	<(null)Point> X8.696
<(null)Point> X3.509	Y9.125 25.25	F1000.0.897.782	<(boundaryPoint)>	GI X8.7 Y3.26 25.35	<(null)Point> X8.696
Y2.714 25.25	<(null)Point> X4.923	GI X4.0 Y3.89 25.25	<(boundaryPoint)>	GI X8.7 Y3.26 25.35	<(null)Point> X8.696
Y2.907 25.25	<(null)Point> X3.384	F1000.0.897.791	<(boundaryPoint)>	GI X8.7 Y3.26 25.35	<(null)Point> X8.696
<(null)Point> X4.5	Y9.607 25.25	GI X4.4 Y3.56 25.25	<(boundaryPoint)>	GI X8.7 Y3.26 25.35	<(null)Point> X8.696
Y3.123 25.25	<(null)Point> X3.872	F1000.0.897.796	<(boundaryPoint)>	GI X8.7 Y3.26 25.35	<(null)Point> X8.696
<(null)Point> X8.874	Y9.74 25.25	GI X6.8 Y9.28 25.25	<(boundaryPoint)>	GI X8.7 Y3.26 25.35	<(null)Point> X8.696
Y3.406 25.25	<(null)Point> X6.373	GI X6.8 Y9.28 25.25	<(boundaryPoint)>	GI X8.7 Y3.26 25.35	<(null)Point> X8.696
<(null)Point> X9.561	Y9.798 25.25	F1000.0.897.807	<(boundaryPoint)>	GI X8.7 Y3.26 25.35	<(null)Point> X8.696
Y3.743 25.25	<(null)Point> X6.879	GI X6.8 Y9.28 25.25	<(boundaryPoint)>	GI X8.7 Y3.26 25.35	<(null)Point> X8.696
Y4.126 25.25	<(null)Point> X7.374	F1000.0.897.809	<(boundaryPoint)>	GI X8.7 Y3.26 25.35	<(null)Point> X8.696
Y4.5 25.25	<(null)Point> X3.384	GI X3.2 Y5.13 25.25	<(boundaryPoint)>	GI X8.7 Y3.26 25.35	<(null)Point> X8.696
<(null)Point> X9.594	Y9.79 25.25	GI X3.2 Y5.13 25.25	<(boundaryPoint)>	GI X8.7 Y3.26 25.35	<(null)Point> X8.696
Y4.5 25.25	<(null)Point> X8.874	GI X8.7 Y3.26 25.25	<(boundaryPoint)>	GI X8.7 Y3.26 25.35	<(null)Point> X8.696
Y5.08 25.25	<(null)Point> X10.103	GI X8.7 Y3.26 25.25	<(boundaryPoint)>	GI X8.7 Y3.26 25.35	<(null)Point> X8.696
Y5.491 25.25	<(null)Point> X10.266	GI X8.7 Y3.26 25.25	<(boundaryPoint)>	GI X8.7 Y3.26 25.35	<(null)Point> X8.696
<(null)Point> X10.366	X8.894 25.25	GI X8.7 Y3.26 25.25	<(boundaryPoint)>	GI X8.7 Y3.26 25.35	<(null)Point> X8.696
Y5.991 25.25	<(null)Point> X9.047	GI X8.7 Y3.26 25.25	<(boundaryPoint)>	GI X8.7 Y3.26 25.35	<(null)Point> X8.696
<(null)Point> X10.4	Y8. 25.25	X2.712 4.931 25.35	<(boundaryPoint)>	GI X8.7 Y3.26 25.35	<(null)Point> X8.696
Y6.5 25.25	<(null)Point> X9.337	<(boundaryPoint)>	<(boundaryPoint)>	GI X8.7 Y3.26 25.35	<(null)Point> X8.696
<(null)Point> X10.366	Y8.186 25.25	GI X2.49 Y4.25 25.35	<(boundaryPoint)>	GI X8.7 Y3.26 25.35	<(null)Point> X8.696
Y7.009 25.25	<(null)Point> X9.561	F1000.0.898.016	<(boundaryPoint)>	GI X8.7 Y3.26 25.35	<(null)Point> X8.696
<(null)Point> X10.266	Y7.509 25.25	GI X8.7 Y3.26 25.35	<(boundaryPoint)>	GI X8.7 Y3.26 25.35	<(null)Point> X8.696
Y7.509 25.25	<(null)Point> X9.713	F1000.0.898.017	<(boundaryPoint)>	GI X8.7 Y3.26 25.35	<(null)Point> X8.696
<(null)Point> X10.103	Y7.992 25.25	GI X8.7 Y3.26 25.35	<(boundaryPoint)>	GI X8.7 Y3.26 25.35	<(null)Point> X8.696
<(null)Point>	Y8.475 25.25	GI X8.7 Y3.26 25.35	<(boundaryPoint)>	GI X8.7 Y3.26 25.35	<(null)Point> X8.696
<(null)Point> X8.874	Y9.594 25.25	GI X8.7 Y3.26 25.35	<(boundaryPoint)>	GI X8.7 Y3.26 25.35	















(creation> 42)
14.224444(9915e-16)
(creationRing)
(creationPerimeter)
(creationPoint)
X2.435 Y5.965 Z6.15
(creationPoint) X2.54 Y5.439 Z6.15
(creationPoint) X2.81 Z7.71 Z6.15
(creationPoint) X2.112 Y4.91 Z6.15
(creationPoint) X2.849 Y4.45 Z6.15
(creationPoint) X2.547 Y4.04 Z6.15
(creationPoint) X3.601 Y3.601 Z6.15
(creationPoint) X4.084 Y3.247 Z6.15
(creationPoint) X2.949 Z6.15
(creationPoint) X4.91 Y2.712 Z6.15
(creationPoint) X5.439 Y2.54 Z6.15
(creationPoint) X5.965 Y2.435 Z6.15
(creationPoint) X6.5 Y2. Z6.15
(creationPoint) X7.035 Y2.435 Z6.15
(creationPoint) X7.561 Y2.126 Z6.15
(creationPoint) X8.087 Y2.126 Z6.15
(creationPoint) X8.613 Y2.51 Z6.15
(creationPoint) X9.139 Y2.62 Z6.15
(creationPoint) X9.665 Y2.98 Z6.15
(creationPoint) X10.191 Y3.42 Z6.15
(creationPoint) X10.717 Y4.26 Z6.15
(creationPoint) X11.243 Y5.18 Z6.15
(creationPoint) X11.769 Y6.26 Z6.15
(creationPoint) X12.295 Y7.51 Z6.15
(creationPoint) X12.821 Y8.98 Z6.15
(creationPoint) X13.347 Y10.59 Z6.15
(creationPoint) X13.873 Y12.36 Z6.15
(creationPoint) X14.4 Y14.26 Z6.15
(creationPoint) X14.926 Y16.15 Z6.15
(creationPoint) X15.452 Y18.15 Z6.15
(creationPoint) X15.978 Y19.26 Z6.15
(creationPoint) X16.504 Y20.45 Z6.15
(creationPoint) X17.03 Y21.71 Z6.15
(creationPoint) X17.556 Y23.06 Z6.15
(creationPoint) X18.082 Y24.45 Z6.15
(creationPoint) X18.608 Y25.87 Z6.15
(creationPoint) X19.134 Y27.31 Z6.15
(creationPoint) X19.66 Y28.76 Z6.15
(creationPoint) X20.186 Y30.26 Z6.15
(creationPoint) X20.712 Y31.76 Z6.15
(creationPoint) X21.238 Y33.26 Z6.15
(creationPoint) X21.764 Y34.76 Z6.15
(creationPoint) X22.29 Y36.26 Z6.15
(creationPoint) X22.816 Y37.76 Z6.15
(creationPoint) X23.342 Y39.26 Z6.15
(creationPoint) X23.868 Y40.76 Z6.15
(creationPoint) X24.394 Y42.26 Z6.15
(creationPoint) X24.92 Y43.76 Z6.15
(creationPoint) X25.446 Y45.26 Z6.15
(creationPoint) X25.972 Y46.76 Z6.15
(creationPoint) X26.5 Y48.26 Z6.15
(creationPoint) X27.026 Y49.76 Z6.15
(creationPoint) X27.552 Y51.26 Z6.15
(creationPoint) X28.078 Y52.76 Z6.15
(creationPoint) X28.604 Y54.26 Z6.15
(creationPoint) X29.13 Y55.76 Z6.15
(creationPoint) X29.656 Y57.26 Z6.15
(creationPoint) X30.182 Y58.76 Z6.15
(creationPoint) X30.708 Y60.26 Z6.15
(creationPoint) X31.234 Y61.76 Z6.15
(creationPoint) X31.76 Y63.26 Z6.15
(creationPoint) X32.286 Y64.76 Z6.15
(creationPoint) X32.812 Y66.26 Z6.15
(creationPoint) X33.338 Y67.76 Z6.15
(creationPoint) X33.864 Y69.26 Z6.15
(creationPoint) X34.39 Y70.76 Z6.15
(creationPoint) X34.916 Y72.26 Z6.15
(creationPoint) X35.442 Y73.76 Z6.15
(creationPoint) X35.968 Y75.26 Z6.15
(creationPoint) X36.494 Y76.76 Z6.15
(creationPoint) X37.02 Y78.26 Z6.15
(creationPoint) X37.546 Y79.76 Z6.15
(creationPoint) X38.072 Y81.26 Z6.15
(creationPoint) X38.598 Y82.76 Z6.15
(creationPoint) X39.124 Y84.26 Z6.15
(creationPoint) X39.65 Y85.76 Z6.15
(creationPoint) X40.176 Y87.26 Z6.15
(creationPoint) X40.702 Y88.76 Z6.15
(creationPoint) X41.228 Y90.26 Z6.15
(creationPoint) X41.754 Y91.76 Z6.15
(creationPoint) X42.28 Y93.26 Z6.15
(creationPoint) X42.806 Y94.76 Z6.15
(creationPoint) X43.332 Y96.26 Z6.15
(creationPoint) X43.858 Y97.76 Z6.15
(creationPoint) X44.384 Y99.26 Z6.15
(creationPoint) X44.91 Y100.76 Z6.15
(creationPoint) X45.436 Y102.26 Z6.15
(creationPoint) X45.962 Y103.76 Z6.15
(creationPoint) X46.5 Y105.26 Z6.15
(creationPoint) X47.026 Y106.76 Z6.15
(creationPoint) X47.552 Y108.26 Z6.15
(creationPoint) X48.078 Y109.76 Z6.15
(creationPoint) X48.604 Y111.26 Z6.15
(creationPoint) X49.13 Y112.76 Z6.15
(creationPoint) X49.656 Y114.26 Z6.15
(creationPoint) X50.182 Y115.76 Z6.15
(creationPoint) X50.708 Y117.26 Z6.15
(creationPoint) X51.234 Y118.76 Z6.15
(creationPoint) X51.76 Y120.26 Z6.15
(creationPoint) X52.286 Y121.76 Z6.15
(creationPoint) X52.812 Y123.26 Z6.15
(creationPoint) X53.338 Y124.76 Z6.15
(creationPoint) X53.864 Y126.26 Z6.15
(creationPoint) X54.39 Y127.76 Z6.15
(creationPoint) X54.916 Y129.26 Z6.15
(creationPoint) X55.442 Y130.76 Z6.15
(creationPoint) X55.968 Y132.26 Z6.15
(creationPoint) X56.494 Y133.76 Z6.15
(creationPoint) X57.02 Y135.26 Z6.15
(creationPoint) X57.546 Y136.76 Z6.15
(creationPoint) X58.072 Y138.26 Z6.15
(creationPoint) X58.598 Y139.76 Z6.15
(creationPoint) X59.124 Y141.26 Z6.15
(creationPoint) X59.65 Y142.76 Z6.15
(creationPoint) X60.176 Y144.26 Z6.15
(creationPoint) X60.702 Y145.76 Z6.15
(creationPoint) X61.228 Y147.26 Z6.15
(creationPoint) X61.754 Y148.76 Z6.15
(creationPoint) X62.28 Y150.26 Z6.15
(creationPoint) X62.806 Y151.76 Z6.15
(creationPoint) X63.332 Y153.26 Z6.15
(creationPoint) X63.858 Y154.76 Z6.15
(creationPoint) X64.384 Y156.26 Z6.15
(creationPoint) X64.91 Y157.76 Z6.15
(creationPoint) X65.436 Y159.26 Z6.15
(creationPoint) X65.962 Y160.76 Z6.15
(creationPoint) X66.5 Y162.26 Z6.15
(creationPoint) X67.026 Y163.76 Z6.15
(creationPoint) X67.552 Y165.26 Z6.15
(creationPoint) X68.078 Y166.76 Z6.15
(creationPoint) X68.604 Y168.26 Z6.15
(creationPoint) X69.13 Y169.76 Z6.15
(creationPoint) X69.656 Y171.26 Z6.15
(creationPoint) X70.182 Y172.76 Z6.15
(creationPoint) X70.708 Y174.26 Z6.15
(creationPoint) X71.234 Y175.76 Z6.15
(creationPoint) X71.76 Y177.26 Z6.15
(creationPoint) X72.286 Y178.76 Z6.15
(creationPoint) X72.812 Y180.26 Z6.15
(creationPoint) X73.338 Y181.76 Z6.15
(creationPoint) X73.864 Y183.26 Z6.15
(creationPoint) X74.39 Y184.76 Z6.15
(creationPoint) X74.916 Y186.26 Z6.15
(creationPoint) X75.442 Y187.76 Z6.15
(creationPoint) X75.968 Y189.26 Z6.15
(creationPoint) X76.494 Y190.76 Z6.15
(creationPoint) X77.02 Y192.26 Z6.15
(creationPoint) X77.546 Y193.76 Z6.15
(creationPoint) X78.072 Y195.26 Z6.15
(creationPoint) X78.598 Y196.76 Z6.15
(creationPoint) X79.124 Y198.26 Z6.15
(creationPoint) X79.65 Y199.76 Z6.15
(creationPoint) X80.176 Y201.26 Z6.15
(creationPoint) X80.702 Y202.76 Z6.15
(creationPoint) X81.228 Y204.26 Z6.15
(creationPoint) X81.754 Y205.76 Z6.15
(creationPoint) X82.28 Y207.26 Z6.15
(creationPoint) X82.806 Y208.76 Z6.15
(creationPoint) X83.332 Y210.26 Z6.15
(creationPoint) X83.858 Y211.76 Z6.15
(creationPoint) X84.384 Y213.26 Z6.15
(creationPoint) X84.91 Y214.76 Z6.15
(creationPoint) X85.436 Y216.26 Z6.15
(creationPoint) X85.962 Y217.76 Z6.15
(creationPoint) X86.5 Y219.26 Z6.15
(creationPoint) X87.026 Y220.76 Z6.15
(creationPoint) X87.552 Y222.26 Z6.15
(creationPoint) X88.078 Y223.76 Z6.15
(creationPoint) X88.604 Y225.26 Z6.15
(creationPoint) X89.13 Y226.76 Z6.15
(creationPoint) X89.656 Y228.26 Z6.15
(creationPoint) X90.182 Y229.76 Z6.15
(creationPoint) X90.708 Y231.26 Z6.15
(creationPoint) X91.234 Y232.76 Z6.15
(creationPoint) X91.76 Y234.26 Z6.15
(creationPoint) X92.286 Y235.76 Z6.15
(creationPoint) X92.812 Y237.26 Z6.15
(creationPoint) X93.338 Y238.76 Z6.15
(creationPoint) X93.864 Y240.26 Z6.15
(creationPoint) X94.39 Y241.76 Z6.15
(creationPoint) X94.916 Y243.26 Z6.15
(creationPoint) X95.442 Y244.76 Z6.15
(creationPoint) X95.968 Y246.26 Z6.15
(creationPoint) X96.494 Y247.76 Z6.15
(creationPoint) X97.02 Y249.26 Z6.15
(creationPoint) X97.546 Y250.76 Z6.15
(creationPoint) X98.072 Y252.26 Z6.15
(creationPoint) X98.598 Y253.76 Z6.15
(creationPoint) X99.124 Y255.26 Z6.15
(creationPoint) X99.65 Y256.76 Z6.15
(creationPoint) X100.176 Y258.26 Z6.15
(creationPoint) X100.702 Y259.76 Z6.15
(creationPoint) X101.228 Y261.26 Z6.15
(creationPoint) X101.754 Y262.76 Z6.15
(creationPoint) X102.28 Y264.26 Z6.15
(creationPoint) X102.806 Y265.76 Z6.15
(creationPoint) X103.332 Y267.26 Z6.15
(creationPoint) X103.858 Y268.76 Z6.15
(creationPoint) X104.384 Y270.26 Z6.15
(creationPoint) X104.91 Y271.76 Z6.15
(creationPoint) X105.436 Y273.26 Z6.15
(creationPoint) X105.962 Y274.76 Z6.15
(creationPoint) X106.5 Y276.26 Z6.15
(creationPoint) X107.026 Y277.76 Z6.15
(creationPoint) X107.552 Y279.26 Z6.15
(creationPoint) X108.078 Y280.76 Z6.15
(creationPoint) X108.604 Y282.26 Z6.15
(creationPoint) X109.13 Y283.76 Z6.15
(creationPoint) X109.656 Y285.26 Z6.15
(creationPoint) X110.182 Y286.76 Z6.15
(creationPoint) X110.708 Y288.26 Z6.15
(creationPoint) X111.234 Y289.76 Z6.15
(creationPoint) X111.76 Y291.26 Z6.15
(creationPoint) X112.286 Y292.76 Z6.15
(creationPoint) X112.812 Y294.26 Z6.15
(creationPoint) X113.338 Y295.76 Z6.15
(creationPoint) X113.864 Y297.26 Z6.15
(creationPoint) X114.39 Y298.76 Z6.15
(creationPoint) X114.916 Y300.26 Z6.15
(creationPoint) X115.442 Y301.76 Z6.15
(creationPoint) X115.968 Y303.26 Z6.15
(creationPoint) X116.494 Y304.76 Z6.15
(creationPoint) X117.02 Y306.26 Z6.15
(creationPoint) X117.546 Y307.76 Z6.15
(creationPoint) X118.072 Y309.26 Z6.15
(creationPoint) X118.598 Y310.76 Z6.15
(creationPoint) X119.124 Y312.26 Z6.15
(creationPoint) X119.65 Y313.76 Z6.15
(creationPoint) X120.176 Y315.26 Z6.15
(creationPoint) X120.702 Y316.76 Z6.15
(creationPoint) X121.228 Y318.26 Z6.15
(creationPoint) X121.754 Y319.76 Z6.15
(creationPoint) X122.28 Y321.26 Z6.15
(creationPoint) X122.806 Y322.76 Z6.15
(creationPoint) X123.332 Y324.26 Z6.15
(creationPoint) X123.858 Y325.76 Z6.15
(creationPoint) X124.384 Y327.26 Z6.15
(creationPoint) X124.91 Y328.76 Z6.15
(creationPoint) X125.436 Y330.26 Z6.15
(creationPoint) X125.962 Y331.76 Z6.15
(creationPoint) X126.5 Y333.26 Z6.15
(creationPoint) X127.026 Y334.76 Z6.15
(creationPoint) X127.552 Y336.26 Z6.15
(creationPoint) X128.078 Y337.76 Z6.15
(creationPoint) X128.604 Y339.26 Z6.15
(creationPoint) X129.13 Y340.76 Z6.15
(creationPoint) X129.656 Y342.26 Z6.15
(creationPoint) X130.182 Y343.76 Z6.15
(creationPoint) X130.708 Y345.26 Z6.15
(creationPoint) X131.234 Y346.76 Z6.15
(creationPoint) X131.76 Y348.26 Z6.15
(creationPoint) X132.286 Y349.76 Z6.15
(creationPoint) X132.812 Y351.26 Z6.15
(creationPoint) X133.338 Y352.76 Z6.15
(creationPoint) X133.864 Y354.26 Z6.15
(creationPoint) X134.39 Y355.76 Z6.15
(creationPoint) X134.916 Y357.26 Z6.15
(creationPoint) X135.442 Y358.76 Z6.15
(creationPoint) X135.968 Y360.26 Z6.15
(creationPoint) X136.494 Y361.76 Z6.15
(creationPoint) X137.02 Y363.26 Z6.15
(creationPoint) X137.546 Y364.76 Z6.15
(creationPoint) X138.072 Y366.26 Z6.15
(creationPoint) X138.598 Y367.76 Z6.15
(creationPoint) X139.124 Y369.26 Z6.15
(creationPoint) X139.65 Y370.76 Z6.15
(creationPoint) X140.176 Y372.26 Z6.15
(creationPoint) X140.702 Y373.76 Z6.15
(creationPoint) X141.228 Y375.26 Z6.15
(creationPoint) X141.754 Y376.76 Z6.15
(creationPoint) X142.28 Y378.26 Z6.15
(creationPoint) X142.806 Y379.76 Z6.15
(creationPoint) X143.332 Y381.26 Z6.15
(creationPoint) X143.858 Y382.76 Z6.15
(creationPoint) X144.384 Y384.26 Z6.15
(creationPoint) X144.91 Y385.76 Z6.15
(creationPoint) X145.436 Y387.26 Z6.15
(creationPoint) X145.962 Y388.76 Z6.15
(creationPoint) X146.5 Y390.26 Z6.15
(creationPoint) X147.026 Y391.76 Z6.15
(creationPoint) X147.552 Y393.26 Z6.15
(creationPoint) X148.078 Y394.76 Z6.15
(creationPoint) X148.604 Y396.26 Z6.15
(creationPoint) X149.13 Y397.76 Z6.15
(creationPoint) X149.656 Y399.26 Z6.15
(creationPoint) X150.182 Y400.76 Z6.15
(creationPoint) X150.708 Y402.26 Z6.15
(creationPoint) X151.234 Y403.76 Z6.15
(creationPoint) X151.76 Y405.26 Z6.15
(creationPoint) X152.286 Y406.76 Z6.15
(creationPoint) X152.812 Y408.26 Z6.15
(creationPoint) X153.338 Y409.76 Z6.15
(creationPoint) X153.864 Y411.26 Z6.15
(creationPoint) X154.39 Y412.76 Z6.15
(creationPoint) X154.916 Y414.26 Z6.15
(creationPoint) X155.442 Y415.76 Z6.15
(creationPoint) X155.968 Y417.26 Z6.15
(creationPoint) X156.494 Y418.76 Z6.15
(creationPoint) X157.02 Y420.26 Z6.15
(creationPoint) X157.546 Y421.76 Z6.15
(creationPoint) X158.072 Y423.26 Z6.15
(creationPoint) X158.598 Y424.76 Z6.15
(creationPoint) X159.124 Y426.26 Z6.15
(creationPoint) X159.65 Y427.76 Z6.15
(creationPoint) X160.176 Y429.26 Z6.15
(creationPoint) X160.702 Y430.76 Z6.15
(creationPoint) X161.228 Y432.26 Z6.15
(creationPoint) X161.754 Y433.76 Z6.15
(creationPoint) X162.28 Y435.26 Z6.15
(creationPoint) X162.806 Y436.76 Z6.15
(creationPoint) X163.332 Y438.26 Z6.15
(creationPoint) X163.858 Y439.76 Z6.15
(creationPoint) X164.384 Y441.26 Z6.15
(creationPoint) X164.91 Y442.76 Z6.15
(creationPoint) X165.436 Y444.26 Z6.15
(creationPoint) X165.962 Y445.76 Z6.15
(creationPoint) X166.5 Y447.26 Z6.15
(creationPoint) X167.026 Y448.76 Z6.15
(creationPoint) X167.552 Y450.26 Z6.15
(creationPoint) X168.078 Y451.76 Z6.15
(creationPoint) X168.604 Y453.26 Z6.15
(creationPoint) X169.13 Y454.76 Z6.15
(creationPoint) X169.656 Y456.26 Z6.15
(creationPoint) X170.182 Y457.76 Z6.15
(creationPoint) X170.708 Y459.26 Z6.15
(creationPoint) X171.234 Y460.76 Z6.15
(creationPoint) X171.76 Y462.26 Z6.15
(creationPoint) X172.286 Y463.76 Z6.15
(creationPoint) X172.812 Y465.26 Z6.15
(creationPoint) X173.338 Y466.76 Z6.15
(creationPoint) X173.864 Y468.26 Z6.15
(creationPoint) X174.39 Y469.76 Z6.15
(creationPoint) X174.916 Y471.26 Z6.15
(creationPoint) X175.442 Y472.76 Z6.15
(creationPoint) X175.968 Y474.26 Z6.15
(creationPoint) X176.494 Y475.76 Z6.15
(creationPoint) X177.02 Y477.26 Z6.15
(creationPoint) X177.546 Y478.76 Z6.15
(creationPoint) X178.072 Y480.26 Z6.15
(creationPoint) X178.598 Y481.76 Z6.15
(creationPoint) X179.124 Y483.26 Z6.15
(creationPoint) X179.65 Y484.76 Z6.15
(creationPoint) X180.176 Y486.26 Z6.15
(creationPoint) X180.702 Y487.76 Z6.15
(creationPoint) X181.228 Y489.26 Z6.15
(creationPoint) X181.754 Y490.76 Z6.15
(creationPoint) X182.28 Y492.26 Z6.15
(creationPoint) X182.806 Y493.76 Z6.15
(creationPoint) X183.332 Y495.26 Z6.15
(creationPoint) X183.858 Y496.76 Z6.15
(creationPoint) X184.384 Y498.26 Z6.15
(creationPoint) X184.91 Y499.76 Z6.15
(creationPoint) X185.436 Y501.26 Z6.15
(creationPoint) X185.962 Y502.76 Z6.15
(creationPoint) X186.5 Y504.26 Z6.15
(creationPoint) X187.026 Y505.76 Z6.15
(creationPoint) X187.552 Y507.26 Z6.15
(creationPoint) X188.078 Y508.76 Z6.15
(creationPoint) X188.604 Y510.26 Z6.15
(creationPoint) X189.13 Y511.76 Z6.15
(creationPoint) X189.656 Y513.26 Z6.15
(creationPoint) X190.182 Y514.76 Z6.15
(creationPoint) X190.708 Y516.26 Z6.15
(creationPoint) X191.234 Y517.76 Z6.15
(creationPoint) X191.76 Y519.26 Z6.15
(creationPoint) X192.286 Y520.76 Z6.15
(creationPoint) X192.812 Y522.26 Z6.15
(creationPoint) X193.338 Y523.76 Z6.15
(creationPoint) X193.864 Y525.26 Z6.15
(creationPoint) X194.39 Y526.76 Z6.15
(creationPoint) X194.916 Y528.26 Z6.15
(creationPoint) X195.442 Y529.76 Z6.15
(creationPoint) X195.968 Y531.26 Z6.15
(creationPoint) X196.494 Y532.76 Z6.15
(creationPoint) X197.02 Y534.26 Z6.15
(creationPoint) X197.546 Y535.76 Z6.15
(creationPoint) X198.072 Y537.26 Z6.15
(creationPoint) X198.598 Y538.76 Z6.15
(creationPoint) X199.124 Y540.26 Z6.15
(creationPoint) X199.65 Y541.76 Z6.15
(creationPoint) X200.176 Y543.26 Z6.15
(creationPoint) X200.702 Y544.76 Z6.15
(creationPoint) X201.228 Y546.26 Z6.15
(creationPoint) X201.754 Y547.76 Z6.15
(creationPoint) X202.28 Y549.26 Z6.15
(creationPoint) X202.806 Y550.76 Z6.15
(creationPoint) X203.332 Y552.26 Z6.15
(creationPoint) X203.858 Y553.76 Z6.15
(creationPoint) X204.384 Y555.26 Z6.15
(creationPoint) X204.91 Y556.76 Z6.15
(creationPoint) X205.436 Y558.26 Z6.15
(creationPoint) X205.962 Y559.76 Z6.15
(creationPoint) X206.5 Y561.26 Z6.15
(creationPoint) X207.026 Y562.76 Z6.15
(creationPoint) X207.552 Y564.26 Z6.15
(creationPoint) X208.078 Y565.76 Z6.15
(creationPoint) X208.604 Y567.26 Z6.15
(creationPoint) X209.13 Y568.76 Z6.15
(creationPoint) X209.656 Y570.26 Z6.15
(creationPoint) X210.182 Y571.76 Z6.15
(creationPoint) X210.708 Y573.26 Z6.15
(creationPoint) X211.234 Y574.76 Z6.15
(creationPoint) X211.76 Y576.26 Z6.15
(creationPoint) X212.286 Y577.76 Z6.15
(creationPoint) X212.812 Y579.26 Z6.15
(creationPoint) X213.338 Y580.76 Z6.15
(creationPoint) X213.864 Y582.26 Z6.15
(creationPoint) X214.39 Y583.76 Z6.15
(creationPoint) X214.916 Y585.26 Z6.15
(creationPoint) X215.442 Y586.76 Z6.15
(creationPoint) X215.968 Y588.26 Z6.15
(creationPoint) X216.494 Y589.76 Z6.15
(creationPoint) X217.02 Y591.26 Z6.15
(creationPoint) X217.546 Y592.76 Z6.15
(creationPoint) X218.072 Y594.26 Z6.15
(creationPoint) X218.598 Y595.76 Z6.15
(creationPoint) X219.124 Y597.26 Z6.15
(creationPoint) X219.65 Y598.76 Z6.15
(creationPoint) X220.176 Y600.26 Z6.15
(creationPoint) X220.702 Y601.76 Z6.15
(creationPoint) X221.228 Y603.26 Z6.15
(creationPoint) X221.754 Y604.76 Z6.15
(creationPoint) X222.28 Y606.26 Z6.15
(creationPoint) X222.806 Y607.76 Z6.15
(creationPoint) X223.332 Y609.26 Z6.15
(creationPoint) X223.858 Y610.76 Z6.15
(creationPoint) X224.384 Y612.26 Z6.15
(creationPoint) X224.91 Y613.76 Z6.15
(creationPoint) X225.436 Y615.26 Z6.15
(creationPoint) X225.962 Y616.76 Z6.15
(creationPoint) X226.5 Y618.26 Z6.15
(creationPoint) X227.026 Y619.76 Z6.15
(creationPoint) X227.552 Y621.26 Z6.15
(creationPoint) X228.078 Y622.76 Z6.15
(creationPoint) X228.604 Y624.26 Z6.15
(creationPoint) X229.13 Y625.76 Z6.15
(creationPoint) X229.656 Y627.26 Z6.15
(creationPoint) X230.182 Y628.76 Z6.15
(creationPoint) X230.708 Y630.26 Z6.15
(creationPoint) X231.234 Y631.76 Z6.15
(creationPoint) X231.76 Y633.26 Z6.15
(creationPoint) X232.286 Y634.76 Z6.15
(creationPoint) X232.812 Y636.26 Z6.15
(creationPoint) X233.338 Y637.76 Z6.15
(creationPoint) X233.864 Y639.26 Z6.15
(creationPoint) X234.39 Y640.76 Z6.15
(creationPoint) X234.916 Y642.26 Z6.15
(creationPoint) X235.442 Y643.76 Z6.15
(creationPoint) X235.968 Y645.26 Z6.15
(creationPoint) X236.494 Y646.76 Z6.15
(creationPoint) X237.02 Y648.26 Z6.15
(creationPoint) X237.546 Y649.76 Z6.15
(creationPoint) X238.072 Y651.26 Z6.15
(creationPoint) X238.598 Y652.76 Z6.15
(creationPoint) X239.124 Y654.26 Z6.15
(creationPoint) X239.65 Y655.76 Z6.15
(creationPoint) X240.176 Y657.26 Z6.15
(creationPoint) X240.702 Y658.76 Z6.15
(creationPoint) X241.228 Y660.26 Z6.15
(creationPoint) X241.754 Y661.76 Z6.15
(creationPoint) X242.28 Y663.26 Z6.15
(creationPoint) X242.806 Y664.76 Z6.15
(creationPoint) X243.332 Y666.26 Z6.15
(creationPoint) X243.858 Y667.76 Z6.15
(creationPoint) X244.384 Y669.26 Z6.15
(creationPoint) X244.91 Y670.76 Z6.15
(creationPoint) X245.436 Y672.26 Z6.15
(creationPoint) X245.962 Y673.76 Z6.15
(creationPoint) X246.5 Y675.26 Z6.15
(creationPoint) X247.026 Y676.76 Z6.15
(creationPoint) X247.552 Y678.26 Z6.15
(creationPoint) X248.078 Y679.76 Z6.15
(creationPoint) X248.604 Y681.26 Z6.15
(creationPoint) X249.13 Y682.76 Z6.15
(creationPoint) X249.656 Y684.26 Z6.15
(creationPoint) X250.182 Y685.76 Z6.15
(creationPoint) X250.708 Y687.26 Z6.15
(creationPoint) X251.234 Y688.76 Z6.15
(creationPoint) X251.76 Y690.26 Z6.15
(creationPoint) X252.286 Y691.76 Z6.15
(creationPoint) X252.812 Y693.26 Z6.15
(creationPoint) X253.338 Y694.76 Z6.15
(creationPoint) X253.864 Y696.26 Z6.15
(creationPoint) X254.39 Y697.76 Z6.15
(creationPoint) X254.916 Y699.26 Z6.15
(creationPoint) X255.442 Y700.76 Z6.15
(creationPoint) X255.968 Y702.26 Z6.15
(creationPoint) X256.494 Y703.76 Z6.15
(creationPoint) X257.02 Y705.26 Z6.15
(creationPoint) X257.546 Y706.76 Z6.15
(creationPoint) X258.072 Y708.26 Z6.15
(creationPoint) X258.598 Y709.76 Z6.15
(creationPoint) X259.124 Y711.26 Z6.15
(creationPoint) X259.65 Y712.76 Z6.15
(creationPoint) X260.176 Y714.26 Z6.15
(creationPoint) X260.702 Y715.76 Z6.15
(creationPoint) X261.228 Y717.26 Z6.15
(creationPoint) X261.754 Y718.76 Z6.15
(creationPoint) X262.28 Y720.26 Z6.15
(creationPoint) X262.806 Y721.76 Z6.15
(creationPoint) X263.332 Y723.26 Z6.15
(creationPoint) X263.858 Y724.76 Z6.15
(creationPoint) X264.384 Y726.26 Z6.15
(creationPoint) X264.91 Y727.76 Z6.15
(creationPoint) X265.436 Y729.26 Z6.15
(creationPoint) X265.962 Y730.76 Z6.15
(creationPoint) X266.5 Y732.26 Z6.15
(creationPoint) X267.026 Y733.76 Z6.15
(creationPoint) X267.552 Y735.26 Z6.15
(creationPoint) X268.078 Y736.76 Z6.15
(























## **Appendix F: BME Learning Outcomes**

An ability to design a system, component, or process to meet desired needs within realistic constraints such as economic, environmental, social, political, ethical, health and safety, manufacturability, and sustainability (ABET 3c) while incorporating appropriate engineering standards (ABET Criterion 5) (need to assess each of these separately, but since ‘or’ and “such as” not all need to be met separately).

Multiple realistic constraints (economic, environmental, social, political, ethical, health and safety, manufacturability) – **page(s) 30-31**

Appropriate engineering standards - **page(s) 27-34**

4. An ability to function on multidisciplinary teams (3d). **page(s) 33-34**

6. An understanding of professional and ethical responsibilities (3f)

Professional – **page(s) 61-63**

Ethical – **page(s) 63-65**

7. An ability to communicate effectively (3g). **pages 28-33**

8. The broad education necessary to understand the impact of engineering solutions in a global, economic, environmental, and societal context (3h). (Both economic AND environmental need to be addressed)

Economic – **page(s) 63**

Environmental – **page(s) 63**

10. A knowledge of contemporary issues (3j). **page(s) 64-65**